Bone marrow transplantation of CD117+ (c-Kit) stem cells and investigation of the bile acid transporter regulation in *Abcb4*$^{-/-}$ mice, a model of sclerosing cholangitis

Inauguraldissertation

zur Erlangung des Grades eines Doktors der Humanbiologie
des Fachbereichs Medizin
der Justus-Liebig-Universität Gießen

Vorgelegt von

Sravanthi Pasupuleti

aus Machilipatnam, India

Gießen 2014

Aus dem Medizinischen Zentrum fur Innere Medizin

Medizinischen Klinik II und Poliklinik

Schwerpunkt Gasteroenterologie

Leiterin: Univ.Prof. Dr. med. Elke Roeb MA

der Universitätsklinikum Gießen und Marburg GmbH

Standort Gießen

Supervisor: Prof. Dr. E. Roeb

Referee: Prof. Dr. S. Wenisch

Unterstützer betreuer: PD. Dr. M. Roderfeld

Date of defence: 25.03.2015

Dedicated

to my grandmother and parents

Table of Contents

Summary

Abcb4 (ATP-binding cassette sub family-b) or *Mdr2* (multidrug resistance protein 2) is a gene which encodes for ABCB4 protein that mediates the transportation of phospholipids across the canalicular membrane of hepatocytes into the bile. Functional loss of the ABCB4 transporter disturbs the excretion of phospholipids into bile, leading to toxic bile composition, bile duct alterations, and damaged bile duct epithelia resembling sclerosing cholangitis (1). Long term consequences are biliary cirrhosis, cholangiocarcinoma and liver failure (2).

In *Abcb4*$^{-/-}$ mice, a model of sclerosing cholangitis, we aimed to investigate the regenerative potential of bone marrow transplantation (BM-Tx) and especially BM-Tx of desialylated CD117+ (c-Kit) stem cells. CD117 receptor expressing cells are hematopoietic progenitors, which bear the potential to differentiate into specialized cell types depending upon tissue environment. Based on these characteristics we analysed whether CD117+ cells differentiated into hepatocytes, e.g. by by cell fusion (3).

Successfully isolated mouse (BALB/c-GFP) hematopoietic stem cells were sorted with the help of hematopoietic (Lin- CD117+) cell surface markers. Neuraminidase treated CD117+ progenitor cells were transplanted into lethally irradiated *Abcb4*$^{-/-}$ (BALB/c-GFP → BALB/c-*Abcb4*$^{-/-}$ allogenic transplantation) mice at the age of 6-7 weeks. At respective time points (*i.e* 2 and 20 weeks after transplantation, actually 8 and 26 weeks of age) mice were sacrificed and underlying immunomodulatory and matrix remodelling processes were analyzed. In addition, we elucidated molecular and biochemical analysis of hepatic bile acid transport in *Abcb4*$^{-/-}$ mice during the course of the disease.

The present studies demonstrated a reduced temporary graft versus host disease and unaltered liver integrity. Fusion of transplanted (GFP+) cells with host (*Abcb4*$^{-/-}$) hepatocytes was a rare event. Whereas lots of GFP+ cells, including T-cells infiltrated around portal fields could be detected. Significant upregulation of proinflammatory (Th1) and profibrogenic (Th2) cytokines revealed enhanced fibrosis in the longterm observation. Furthermore, bile acid transporter data revealed an altered gene regulation at basolateral and canalicular membrane in chronically injured liver of *Abcb4*$^{-/-}$ mice.

The present work suggests that transcriptional changes of bile acid transporters may open new molecular targets for therapy of liver fibrosis in *Abcb4*$^{-/-}$ mice. These data from fibrogenesis in *Abcb4*$^{-/-}$ mice are of great interest for translational antifibrotic strategies.

Zusammenfassung

Abcb4 (ATP-Bindungs-Cassette-Unterfamilie-b) auch bekannt als *Mdr2* (multidrug resistance protein 2) ist ein Gen, das für das ABCB4 Protein, das den Transport von Phospholipiden für die kanalikuläre Membran der Hepatocyten in die Galle vermittelt, codiert. Ein Funktionsverlust der ABCB4 Transporter stört die Ausscheidung von Phospholipiden in die Galle und führt zu einer toxischen Zusammensetzung der Galle, Gallengangsveränderungen und beschädigtem Gallengangsepithel, was einer sklerosierenden Cholangitis ähnelt (1). Langfristige Folgen sind biliäre Leberzirrhose, Gallengangskarzinom und Leberversagen (2). In *Abbc4*$^{-/-}$ Mäusen, einem Modell der sklerosierenden Cholangitis, wollten das regenerative Potenzial der Knochenmarkstransplantation (BM-Tx) und vor allem BM-Tx desialylierten CD117+(c-Kit) Stammzellen zu untersuchen. CD117-Rezeptor exprimierende Zellen sind hämatopoetische Vorläuferzellen, die das Potenzial in spezialisierte Zelltypen je nach Gewebeumgebung unterscheiden zu tragen. Basierend auf diesen Eigenschaftenhaben wir untersucht, ob CD117+ Zellen in Hepatozyten differenzieren können, z. B. durch Zellfusion (3). Erfolgreich aus einer Maus (BALB/c-GFP) isolierte hämatopoetische Stammzellen wurden mit Hilfe von hämatopoetischen (Lin- CD117+) Zelloberflächenmarker aussortiert. (BALB/c-GFP → BALB/c-*Abcb4*$^{-/-}$ allogene Transplantation) Mäuse im Alter von 6-7 Wochen - Neuraminidase CD117+ Vorläuferzellen wurden in letal bestrahlten *Abcb4*$^{-/-}$ transplantiert. An den jeweiligen Zeitpunkten (2 und 20 Wochen nach der Transplantation, eigentlich 8 und 26 Wochen alt) wurden die Mäuse getötet und die zugrunde liegenden immunmodulatorischen und Matrix-Umbauprozesse wurden analysiert. Darüber hinaus führten wir molekulare und biochemische Analysen von Leber-Gallensäure -Transport in *Abcb4*$^{-/-}$ Mäusen im Verlauf der Erkrankung durch. Die vorliegenden Studien zeigten eine reduzierte temporäre Graft-versus-Host-Krankheit und unveränderte Leberintegrität. Die Fusion von transplantierten (GFP+) Zellen mit Host (*Abcb4*$^{-/-}$) Hepatozyten war ein seltenes Ereignis. Während könnten viele GFP+ Zellen, einschließlich T-Zellen um Portalfeldern infiltriert erkannt werden. Bedeutende Hochregulation proinflammatorischer (Th1) und profibrogenen (Th2) Zytokine zeigte verbesserte Fibrose in der langfristigen Beobachtung. Darüber hinaus offenbaren die Gallensäure-Transporter-Daten eine veränderte Genregulation der basolateralen Membran und kanalikulären bei chronisch verletzte Leber *Abcb4*$^{-/-}$ Mäusen.Die vorliegende Arbeit zeigt, dass Transkriptionsänderungen von Gallensäure- Transportern neue molekulare Ziele für die Therapie von Leberfibrose in *Abcb4*$^{-/-}$ öffnen Mäusen sein können. Diese Daten aus Fibrose in *Abcb4*$^{-/-}$ Mäuse sind von großem Interesse für translationale antifibrotischen Strategien.

1. Introduction

Liver fibrosis is a consequence of chronic damage to the liver. It arises via a complex network of signaling pathways that regulates the accumulation of extracellular matrix proteins and fibrogenesis, a characteristic feature of many types of chronic liver disease. Fibrosis is a common outcome of chronic hepatic diseases including viral hepatitis, alcohol abuse and metabolic diseases and can ultimately lead to liver cirrhosis and hepatic failure. Primary sclerosing cholangitis is a chronic cholestatic liver disease, which impairs the biliary system often associated with inflammation and fibrosis.

1.1 Primary sclerosing cholangitis (PSC):

PSC is characterized by progressive obliteration of extrahepatic and intrahepatic bile ducts and systemic accumulation of bile acids (4). It is often accompanied with inflammatory bowel disease and high risk for hepatobiliary tree heading to final stage of liver fibrosis requiring liver transplantation (5). The incidence of PSC is estimated to be 13.9 per 100,000 individuals across the USA and 10 per 10,000 in northern Europe. The prevalence of PSC seems to be increasing steadily. Occurrence of disease takes place at any age, but is more common in people aged around 40 years. It is twice more common in men than in women (6) (7).

PSC is characterised by inflammation of the bile ducts, scar formation and narrowing of bile ducts. As scaring increases, bile builds up in the liver and damages parenchyma which eventually leads to biliary cirrhosis, cholangio carcinoma and liver failure (8). The cellular mechanism involved in the development of PSC is transdifferentiation of hepatic stellate cells (HSC) into myofibroblasts expressing α-smooth muscle actin (α-SMA) and subsequent accumulation of extra cellular matrix (ECM) (9). Recent studies on mice (10) and human (11) reported the contribution of bone marrow derived fibrocytes and portal myofibroblasts (12) and their involvement in the hepatic fibrogenesis. Accumulated portal myofibroblasts in PSC are shown to be activated by epithelial cells in order to secrete collagen and its deposition around damaged bile ducts (13).

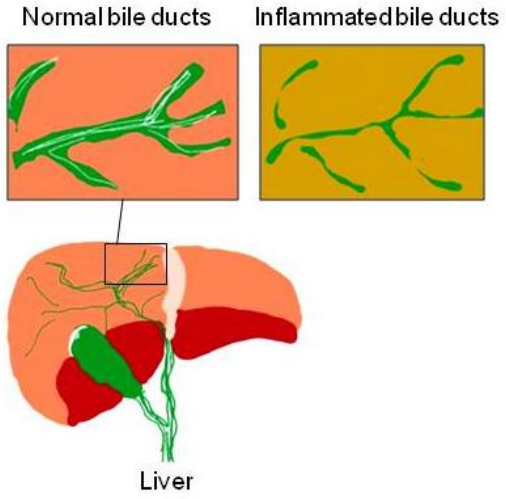

Figure 1: Depiction of a normal liver with hepatic biliary tree showing normal bile duct as well as ducts destroyed by inflammation and scarring (Resource - Modified from http://www.liver.ca/liver-disease/types/primary-sclerosing-cholangitis.aspx).

At the molecular level, matrix metalloproteinases (MMPs) and tissue inhibitor of metalloproteinases (TIMPs) play a pivotal role to balance the homeostasis of ECM. Juran and colleagues comprehensively assessed the influence of genetic variation in MMP-3 on risk of PSC development as well as disease progression (14). While transient up-regulation of MMP-2, MMP-7, MMP-9, and MMP-13 expression demonstrated improved hepatic fibrosis in *Abcb4*$^{-/-}$ mice (15). In mice the development of sclerosing cholangitis is spontaneous due to the disruption of multidrug resistance gene (*Mdr2/Abcb4*), which is a member of ATP binding cassette sub family.

1.2 ATP binding cassette sub family B member 4 (*Abcb4*$^{-/-}$) knockout:

The multidrug resistance protein 2 (MDR2/ABCB4) flops phospholipids from interior to exterior bile leaflet of the canalicular membrane. These phospholipids bind to bile acids and forms mixed micelles with cholesterol. *Abcb4* (an ortholog of human MDR3/ABCB4) knockout mice represent a well-studied and highly reproducible non-surgical *in-vivo* (mouse) model system for cholangiopathy, clearly showing the macroscopic (bile duct structures and dilatations of the large bile ducts) and microscopic features (onion skin-type like pericholangitis and periductal fibrosis) of sclerosing cholangitis in humans (16, 17). Deletion of multidrug resistance protein2 (MDR2) results in no excretion of Phosphatidyl choline (PC) into bile leading to sclerosing cholangitis,

biliary fibrosis and hepatocellular carcinomas (18). Mutations of the human *Abcb4* gene result in phenotypes of chronic liver disease like progressive familial intrahepatic cholestasis (PFIC type 3) or biliary liver cirrhosis (19). Whereas in mice *Abcb4*$^{-/-}$ represents a murine model of chronic cholestasis, which spontaneously develops biliary fibrosis, proliferation of bile ducts and sclerosing cholangitis (9). Furthermore this model provides the possibility to study mechanisms of inflammation driven fibrosis (20). There are some evidences that norUDCA (side chain-modified bile acid 24-norursodeoxycholic acid) reverses liver fibrosis in *Abcb4*$^{-/-}$ and Insulin like growth factor 1 (IGF1) effectively blocks fibrosis in acute models of liver damage in mice. IGF1 over-expression, however, failed to inhibit liver fibrogenesis in *Abcb4*$^{-/-}$ mice, a model of chronic cholangiopathy (21, 22). In spite of current medical therapies, PSC still needs a lot of attention because PSC is considered to be a potential fatal disorder with poor prognosis. Stem cell transplantation remains the only conventional treatment, hence stem cells and its lineages become a promising new approach and might be able to address mostly unmet medical needs. Over a decade, intensive research has focused on stem cell transplantation, which has an enormous capability of becoming an alternate therapy for liver transplantation.

1.3 Stem cells:

Stem cells can be defined as a class of undifferentiated cells that are able to differentiate into specialized cell types. The hot topic in stem cell biology is the transdifferentiation potential or so called plasticity of adult stem cells. The concept of transdifferentiation stands for cellular reprogramming in response to external stimuli leading to phenotypically differentiated cells towards lineages different from the tissue of their origin (23). Ability of stem cells to differentiate in to any kind of cell depends on surrounding environment is known as potency. Totipotency, is to form any kind of tissue in the body and pluripotency is the capability of the cell to generate almost any type of cells in the organism. Multipotent stem cells are those that can only give rise to a few number of cell types (24). Basically two types of stem cells are exist, they are

Embryonic stem cells (ES) and

Adult stem cells

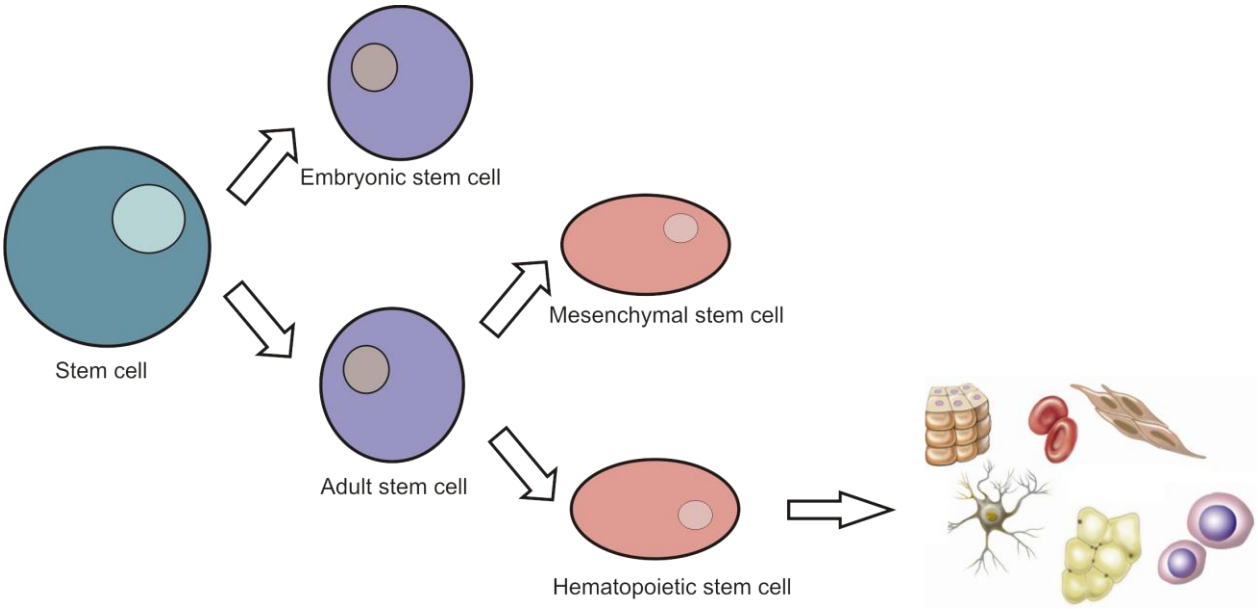

Figure 2: Hierarchy of stem cells

Both (embryonic and adult) stem cells have their own advantages and limitations. Ethical issues are a major aspect for embryonic stem cells, whereas adult stem cells are multipotent and able to differentiate only a limited number of cell types. Adult stem cells exist in two fractions of cell populations a) Hematopoietic stem cells (HSC) and b) Mesenchymal stem cells (MSC). The adult stem cells can be derived from bone marrow, peripheral blood and umbilical cord (25). The main source of tissue specific stem cells is bone marrow (both MSC and HSC), having the potential for differentiation into cells of different lineages. MSCs are stromal cells, which give rise to adipocytes, chondrocytes and osteoblast cells. HSCs are the most studied adult stem cells over the last years (26)

1.3.1 Hematopoietic stem cells (HSC):

HSCs are rare cells that reside in adult bone marrow where hematopoiesis is continuously taking place. These cells are self-renewing and have the capacity to differentiate into all types of mature blood cells that comprises the blood forming system (27). These are multipotent precursors that can differentiate into any hematogenous cell types. Easy accessibility of HSC provides an attractive cell population for cell regeneration therapy. Isolation of HSC can be performed by different cell surface markers. Mouse HSCs are characterized by expression of the c-Kit tyrosine kinase receptor (CD117), stem cell antigen-1 (sca-1), and low levels of the Thy-1.1

cell surface antigens found on differentiated cells of various lineages (28). HSCs are classified into two types:

a) Myeloid progenitor cells and b) Lymphoid progenitor cells

These HSC cells were carefully sorted to enrich the CD117+ progenitor cells and were treated with 2U/ml of neuraminidase (N5254, Sigma Aldrich) enzyme to enhance the stem cell fusion to the existing healthy hepatocytes (Misawa et al 2006). Neuraminidase removes terminal sialic acid residues from cell surface glycoproteins and helps to bind the hepatic asialoglycoprotein receptor (ASGPR).

1.3.2 Plasticity / Transdifferentiation of stem cells:

Plasticity and the self-renewal ability of stem cells attracted a tremendous attention towards stem cell therapy transplantation and regeneration medicine. BMCs as a potential source of hepatocytes (29-31) and purified HSCs differentiation towards functional hepatocytes were shown in recent studies (32). Similarly, these progenitor cells were also found to partially regenerate myocardium and vascular structure (33) as well as other organs (34-36). In contrast, Wagers and his colleagues showed that transdifferentiation of bone marrow stem cells (BMCs) into non hematopoietic tissue is a rare event (37). In *Fah*$^{-/-}$ (fumarylacetoacetate hydrolase) mice hepatocytes are derived from hematopoietic stem cells (HSC), where “cell fusion is the principal mechanism’’ of hepatocyte regeneration (38, 39). Hence, the hematopoietic system is currently under extensive investigation with respect to their potential for transdifferentiation into hepatocytes. The aim of the current study is to investigate the therapeutic potential of transplantation of bone marrow derived hematopoietic stem cells (BM-Tx) in *Abcb4* knockout mice, a model system of sclerosing cholangitis. Several studies demonstrated that Lin^{-} (Lineage^{-}), c-Kit^{+}(CD117^{+}), and sca-1^{+} cells display characteristic features of HSCs. The other name of c-Kit is CD117 (stem cell factor receptor) or tyrosine-protein kinase. Lin^{-}, sca-1^{+} and CD117 expressing cells are hematopoietic progenitors (32, 40).

1.4 Liver physiology:

The liver is the central organ for metabolic processes. The major functions of the liver are gluconeogenesis, glycogenesis, detoxification, bile acid synthesis, and lipid metabolism. It performs many essential functions such as biosynthesis and the breakdown of important proteins (e.g lipoproteins, acute phase proteins, complement system proteins). Another

important role of the liver is excretion of waste substances through bile. In addition, the liver performs the production of albumin protein, which processes of hemoglobin and maintains the homeostasis of chemicals in blood.

1.4.1 Immunity and inflammation:

The liver receives two thirds of its blood supply from the intestine. This blood enriched with nutrients contains many antigenes, that are filtered through the hepatic sinusoids by cells of the innate immunity system. The liver contains cells of the innate immune system including Kupffer cells (KCs), dendritic cells (DCs) and natural killer (NK) cells (41). Liver sinusoidal endothelial cells (LSEC's), DC's and KC's represent as antigen-presenting cells (APCs). Kupffer cells are resident macrophages that play a major role in liver inflammation by releasing reactive oxygen species (ROS) and cytokines (42). Fibrocytes (CD34+) can be mobilized upon inflammatory signals and infiltrate damaged tissue where, they are involved in wound healing, antigen presentation, and cytokine production. While CD34+ fibrocytes were derived from hematopoietic bone marrow cells (43). In chronic cholestatic models it has been observed that portal inflammation was associated with infiltrating macrophages and lymphocytes specifically near to the biliary epithelium (44). In addition, Fickert and his colleagues proved that changing of CD11b (integrin αM) rich niche to a CD4/CD8 rich infiltration results in pronounced periductal inflammation and enhanced KCs with induced intrahepatic production of proinflammatory and profibrogenic cytokines (e.g TNF-α, IL-1β, TGFβ-1) in *Abcb4*$^{-/-}$ mice (1). Due to the enhanced inflammation after BM-Tx, we analyzed microarray data to get an overview of genes, which are mainly involved in inflammatory signaling milieu. Interestingly, our attention was attracted by bile acid transporting genes with higher (NTCP ≥ 4 OATP≥ 100,000) fold change. Hence we further focussed on bile acid transportation since ABCB4 is also a member of the hepatobiliary transport system.

1.4.2 Bile acids:

Bile is an alkaline solution and bile salts (the ionized from of bile acids) are major organic components that include phospholipids and cholesterol (45). Bile acids (BAs) are 24-carbon steroids and are end products of cholesterol catabolism. They are synthesized in the liver, stored in the gall bladder, and discharged in the duodenum during digestion allowing the absorption of dietary lipids. In the liver *de novo* synthesized primary bile acids (cholic acid and chenodeoxycholic acid) result from hydroxylation of cholesterol with help of the key rate limiting enzyme CYP7A1 (cholesterol 7 alpha hydroxylase) (46). All bile acids secreted by the liver are

conjugated with an amino acid, either with glycine or with taurine making them hydrophilic. Thereby conjugated bile acids are converted to secondary (deoxycholic acid) and tertiary bile salts as a result of bacterial catabolism in the gut (47). The conjugated bile acids form further complexes with sodium to become bile salts. Two major functions of biliary phospholipids are emulsification of fats and reduction of detergent activity of the bile acids (48). Bile acids affects glucose and lipid metabolism and can also influence the energy homeostasis, drug metabolism via activation of FXR (49). Since BAs are identified as natural endogenous ligands of FXR and various number of membrane-bound transporters and nuclear receptors are involved in secretion and uptake of bile salts.

1.4.3 Phospholipids and cholesterol:

The Mdr2/MDR3 designates the canalicular flippase translocating PCs from the inner to the outer leaflet of the canalicular membrane. The transport of cholesterol into bile is enabled by the hemi transporters ABCG5/8. Indeed an accurate secretion of PC is essential to reduce the toxicity on the canalicular membrane by forming mixed micelles along with cholesterol and bile acids (BA). Apart from binding of bile acids with micelles it is necessary to undergo bile hydration, alkalinisation, mucin formation and bile flow to avoid the damage of bile ducts via the detergent nature. In *Abcb4*$^{-/-}$ knockout mice, PC secretion is virtually absent and spontaneously develops sclerosing cholangitis (20, 50). PC deficiency also leads to periductular fibrosis via massive dysregulation of pro and anti-fibrotic genes in *Abcb4*$^{-/-}$ mice (9). Elimination of cholesterol from the body is essential and excreted via feces either directly or after the conversion into BAs. Release of phospholipids into bile prevents the formation of gall stones by solubilizing cholesterol. Thereby, phospholipids reflect themost important elimination pathway of cholesterol and a large part of these lipids are reabsorbed in the intestine (51).

1.4.4 Hepatobiliary transport system:

Uniquely bile acids undergo enterohepatic circulation under the control of corresponding transporters and their nuclear receptors in order to perform normal physiological functions. The transport of bile acid (about 90%) from portal blood into the hepatocyte cytoplasm is mediated by sodium taurocholate co-transporting peptide (NTCP). The sodium independent translocation of unconjugated bile salts and other lipophilic albumin bound molecules are transported by organic anion transporting peptide (OATP). Both NTCP and OATP are located on the basolateral side of hepatocytes (52). Bile salt export pump (BSEP), located on the canalicular membrane, mediates excretion of conjugated bile acids into bile. Intestinal recycling of bile acids occurs via a Na^+

dependent carrier (apical sodium bile acid transporter ASBT) located on the apical side of enterocytes in the terminal ilium as well as on the apical side of hepatocytes and cholangiocytes. Organic solute and steroid transporters (Ostα/Ostβ) have been shown to be essential transporters on the basolateral side of enterocytes and cholangiocytes. Under normal physiological conditions expression of basolateral transporters is low, but can be upregulated under cholestatic conditions (53, 54).

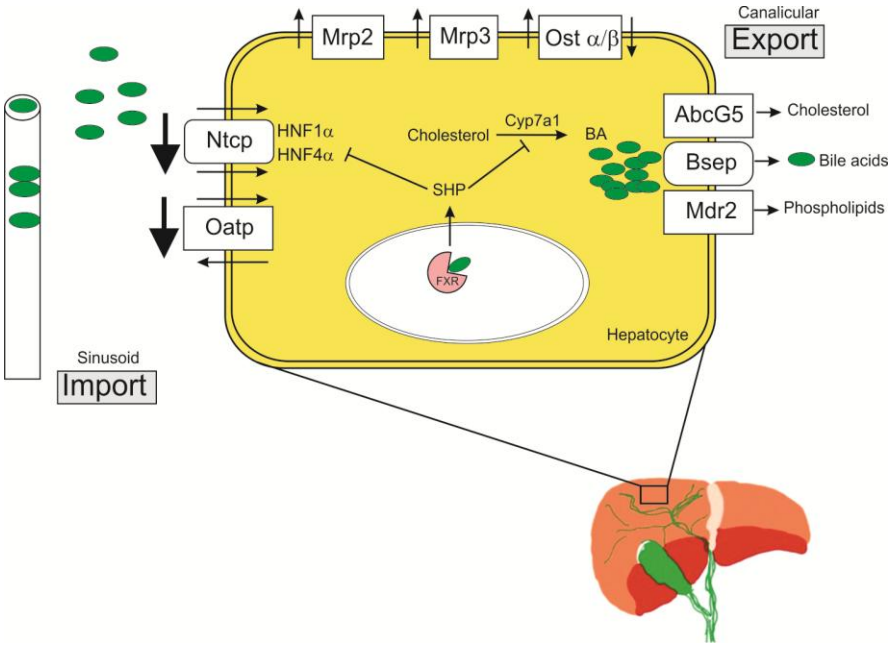

Figure 3: Diagram representing the mechanism of the hepatobiliary transport system

At the canalicular membrane, the Bsep (bile salt export pump) secretes bile, which is almost reabsorbed into the small intestine and transported back to the liver via the portal circulation at the sinusoidal membrane (via Ntcp) of hepatocytes to complete a cycle (55, 56). Alterations or mutations in the hepatobiliary transport system cause a spectrum of liver diseases. The rodent models of hereditary and acquired cholestasis have been proven very useful to study the role of transport system in the pathogenesis of cholestasis (57). Denson and his co-workers showed Ntcp feedback regulation via shp (small heterodimer partner) induction by bile acid activated FXR. This FXR serves as a coordinated down regulation of bile acid synthesis and import, thereby protecting bile acid induced damage in rats. Regulation at the transcription and post-transcription levels of these transporters are under tight regulation by the nuclear receptor (NR) to limit the bile synthesis (58).

1.4.5 Nuclear receptors:

Nuclear receptors (NRs) are transcription factors typically under the control of small lipophilic molecules, which easily pass through biological membranes. The ligand activated NRs thereby regulate expression of target genes by binding to cis-acting DNA sequences (59). Historically nuclear receptors are classified into three types:

a) Classical receptors: Extensively regulated by endocrine ligands

b) Adopted orphan receptors: either natural or synthetic ligands

c) Orphan receptors: Have no natural ligands and act as transcription factors (small heterodimer partner (shp)

1.4.5.1 FXR nuclear receptor:

FXR (farnesoid X receptor) belongs to the group of nuclear hormone receptors and functions as a transcription factor for which bile acids are naturally endogenous ligands (60). Activated FXR in the liver can induce the expression of BSEP and MDR3/Mdr2 for the secretion of BAs and phosphatidylcholine, respectively, into the canalicular lumen (61-63). In liver and gut gene expression can be altered by bile acids via activation of FXR (Nr1H4 nuclear receptor subfamily 1 group H, member4), Vitamin D receptor (VDR, Nr1l1), G protein coupled receptor TGR5, and other signaling cascades (JNK 1/2, AKT and ERK1/2) (64). In feedback mechanism FXR inhibits Cyp7a1 and Cyp8b1 expression via small heterodimer partner (shp) hindering the accumulation of bile acids and thereby preventing toxic damage to the liver (65, 66). Evidence has shown that mutations as well as polymorphisms in FXR lead to cholestasis. Studies with bile duct ligated (BDL) and α-naphthylisothiocyanate rat models of acute intrahepatic and extrahepatic cholestasis showed improved liver injury after treatment with GW4064 a synthetic agonist for FXR. Hence they suggest FXR agonists may be the best suitable treatment of cholestatic liver diseases (67). Also in a chronic cholestatic model induced by 17α-ethinylestradiol, the FXR agonist 6-ethyl chenodeoxycholic acid (6-ECDCA) protected cholestasis by enhanced shp and reduced cyp7a1, cyp8b1 and NTCP, thus proving its pivotal role in *in-vivo* (67). In *Abcb4*$^{-/-}$ mice, transgenic expression of activated FXR in the intestine protected against liver damage, and absence of FXR promoted progression of liver disease (68). Recent evidence showed that *FXR*$^{-/-}$ mice develop a pronounced inflammation with high expression of inflammatory genes in the liver. Activation of FXR in animal models of non-alcoholic fatty liver diseases demonstrated

inhibition of inflammation and fibrosis (69). Growing evidence suggests that, miRNA expression is regulated by nuclear receptor (NR) either by directly binding to the promoter region or by transcriptional regulation of miRNA expression via NR target genes and interacting with regulation of miRNA biogenesis (70-72). Therefore we aimed to elucidate miRNA expression at transcriptional level and their involvement in underlying mechanisms that might have major roles in liver fibrosis and tumerogenesis. Taken together, nuclear receptors are actively investigated because of therapeutic options for cholestatic liver diseases (73).

1.6 MicroRNAs (miRNAs):

miRNAs are small non-coding RNA transcripts of about 22–24 nucleotides, which are capable of interacting with the 3' untranslated region of coding RNAs (mRNAs), leading to a blockage of protein translation and/or mRNA degradation. miRNAs interfere with transcriptional and post-transcriptional regulation of gene expression. They affect various signalling pathways by acting as regulators of gene expression at the translational and transcriptional level (74-77). miRNAs play a central role in diverse cellular processes including development, immunity, cell-cycle control, metabolism, viral or bacterial disease, stem-cell differentiation, and oncogenesis (77-79). In general, miRNAs are transcribed from RNA polymerase II or III in the nucleus and transported to the cytoplasm, where they are processed into mature miRNAs. Mature miRNAs can target hundreds of genes by either binding to the 3′ or 5′ untranslated (UTR) regions of mRNA.

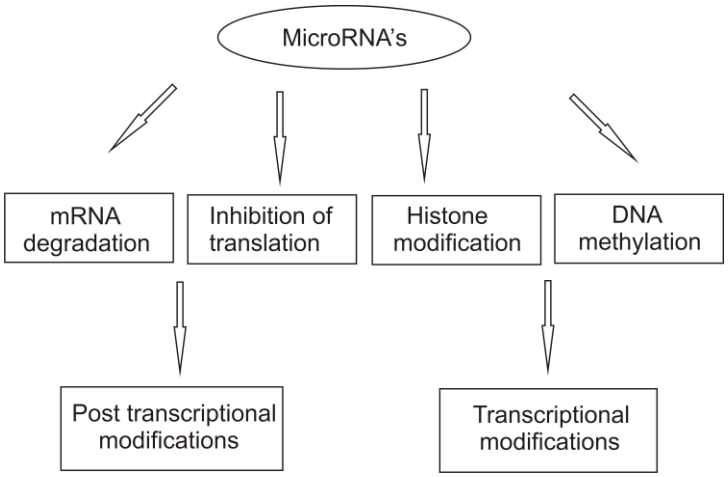

Figure 4: This diagram depicts miRNA involvment in various molecular mechanisms (modified according to Shashi Bala et al. World Journal of Gastroenterology 2009)

Emerging evidence suggests that miRNAs are also capable of modulating transcription and methylation processes (80, 81). In a short time, miRNA research has received tremendous attention due to their fine-tuning roles in almost all biological pathways. Thus, miRNAs regulate diverse physiological and developmental processes by controlling levels of specific mRNAs and their own expression and processing must be tightly regulated for normal cell function (82, 83). Each miRNA could be transcribed and regulated independently, at the transcriptional levels by activators and repressors, or at the epigenetic level through DNA methylation (84, 85). The expression levels of processing components are also specifically controlled to regulate the abundance of mature miRNAs. Variances in any of these processes could lead to tumorigenesis or development of other diseases (86).

miRNA	**Regulation**	**Note**	**Target**
miR 122	HNF-4α	HNF4α binds to the miR122 promoter	Hfe; Hvj; CPEB; HCV; CAT-1; smarcd1/baf60α
miR-34a	FXR, SHP	P^{53} binds to miR-34a promoter, FXR interacts with p53 via sHP to regulate miR-34a	FoxP1
miR-29a	FXR	FXR responsive element in the miR-29a promoter, regulated by TGF-β, c-Myc, Nf-kB or hedgehog	ski; MCT1; PTEN; CDK6
miR-146a	ER, AR	Repressed by estradiol, androgen and LPS; LPS induces Nf-kB binding to the miR-146a promoter	ROCK1; TRAF6; IRAK1; BRCA1; CD40L; STAT1
miR-221/222	ER, AR	Nf-kB, c-JUN, ER and AR bind to the miR-221/222 promoter	P27; kip1; PTEN; ERα;PUMA
miR-26a	ER, AR	Esterdiol induces miR-26a, which reduces PR at mRNA level	EZH2; MTDH
miR-17-92 cluster	ER	c-Myc, adiol, binds to the miR-17-92 promoter induced by estrogen ; p53 and sTAT3 bind to the miR-17-92 promoter	Myc; E2F; HNF1; PTEN; B IM; ER; AIB1; cyclin D1

Table 1. Showing miRNA expression regulated by nuclear receptors (Modified according to Yang and Wang Cell & Bioscience 2011)

1.6.1 miRNA's in liver and disease:

Disease-specific tissue miRNA signatures have been identified in various etiologies such as hepatocellular carcinoma (HCC), hepatitis C virus (HCV), hepatitis B virus (HBV), cardiac disease, neuro inflammation, rheumatic arthritis (RA), and various cancers (79-81, 87, 88). Expression of miR-122 is liver specific and inhibition of miR-122 expression in mice leads to a down-regulation of cholesterol and lipid-metabolizing enzymes (89). miR-122 was first identified as liver-specific cellular miRNA and is associated with the enhanced replication of HCV by targeting the viral 5' non-coding region (90). Down-regulation of hepatocyte-specific miR-122, promoted growth of HCCs in mice, regulated expression of cell cycle components, and increased migration of HCC cells and their invasive activities. miR-122 might therefore be a suppressor of HCC metastasis (91).

Endoplasmic reticulum (ER) stress is associated with pathogenesis of many liver diseases. The potential role of miRNAs in the hepatic ER stress responses to bile acid and other agents just beginns to emerge. Recently, miR-199a has also been proven to regulate ER stress in cancer cells (92). Studies have implicated an overexpression of the miR-199 with progression of liver fibrosis (93). In general, down-regulation of miRNAs was observed in a feedback mechanism that develops during the early phases of liver regeneration (94). miR-199a-5p is believed to be a multifunctional miRNA involved in the regulation of many diseases like angiogenesis, cell proliferation and autophagy. Dai et al. (92) observed that miR-199a-5p is necessary for the modulation of hepatic ER stress progression and may reduce hepatic ER stress by targeting ER, chaperones and signal transducers, which may protect the liver from injury.

2. AIM OF THE STUDY

Mutations of the *Abcb4* gene can cause a wide clinical spectrum of liver diseases ranging from neonatal cholestasis to adult liver diseases (95). In spite of our growing knowledge of the pathogenesis of liver fibrosis, this subject still requires a lot of attention due to ineffective medical therapies. In this situation, bone marrow transplantation (BM-Tx) emerged a better alternative for the treatment of hepatic fibrogenesis. In the current study, our intentions were:

1) reconstitution of *Abcb4*$^{-/-}$transporter function.
2) isolation and purification of CD117+ (c-kit) expressing hematopoietic stem cells from whole bone marrow population
3) investigation of the regenerative potential of desialylated CD117+ stem cells by means of cell fusion with recipient mouse hepatocytes in *Abcb4*$^{-/-}$ mice
4) the analysis of microarray data to get an overview about the transcriptome with focus on hepatobiliary transport
5) analysis of miRNA data to perceive the underlying molecular mechanism leading to hepatic fibrogenesis and tumorigenesis.

MATERIALS AND METHODS:

3. Materials:

3.1 Chemicals:

All standard chemicals and reagents were purchased from VWR chemicals (France), Sigma Aldrich (Steinheim), Merck (Darmstadt), Roth (Karlsruhe) and Fluka (Steinheim), J.T Backer (Netherlands) unless otherwise stated.

3.1.1 Chemicals for Histology:

3.1.1.1 Hematoxylin and Eosin (H&E staining):

- Haematoxylin (Mayers' acidic, Fa Waldeck)
- Eosin (Thermo Scientific, Heraeus)

3.1.1.2 Sirius red staining

- 0.1% Sirius red (0.1 g of Sirius red in 100 ml of picric acid)
- 1 % Acetic acid (1 ml of 100% Acetic acid in 99 ml of distilled water)

3.1.1.3 Masson goldner staining

- Weigert's Hematoxylin solution:

  Solution A: 1 g - hematoxylin, 100 ml - 95% alcohol

  Solution B: 4 ml - 29% Ferric chloride, 1 ml - Hydrochloric acid (HCl) in dd H_2O

- Ponceau de Xylidine: 0.5 g - ponceau de xylidine, 250 mg - Acid fuchsin, 100 ml - acetic acid, 50 ml - distilled water
- Orange G: 200 mg - Phospho tungstic acid, 50 ml distilled water
- Light green: 0.1 g - light green, 100 µl - acetic acid, 50 ml - distilled water
- Methanol (JLU pharmacy)

- Isopropanol
- Xylene
- Ethanol

3.1.2 Chemicals for peroxidase / microwave method: (paraffin sections)

- Stock Solution A: 0.1 M Citric acid ($C_6H_80_7$) = 21.01g (fill up to 1 liter; pH=2.1)
- Stock Solution B: 0.1 M tri-Na-Citrate dihydrate ($C_6H_5Na_3O_7$ X $2H_20$) =29.41 g (fill up to 1 liter; pH=6.0)

  Use: 9 ml of buffer A + 41 ml of buffer B and 500ml of distilled water (pH=6.0)

3.2 Buffers and solutions used for MACS (magnetic activated cell sorting):

Common laboratory solutions and buffers were prepared according to the standard lab protocols. The buffer solutions required for performing the experiments are listed below.

3.2.1 MACS buffer for bone marrow cells:

- 0.5% - BSA, 2 mM - EDTA in 1 X PBS - pH 7.2; Sterile filtered and maintained at 4-8°C
- Biotin-Antibody: biotin-conjugated monoclonal antibodies CD5, CD45R (B220), Cd11b, Anti-Gr1 and Ter-119.
- Anti-Biotin Micro beads: Micro beads conjugated to monoclonal Anti-biotin antibodies.
- Micro beads conjugated to monoclonal anti-mouse CD117 antibodies (PE conjugated) (Miltenyi Biotec)

Column	Max. number of labeled cells	Separator
MS	10^7	Mini MACS
LS	10^8	Midi MACS
XS	10^9	Super MACS

Table 2. Columns used for magnetic cell sorting

3.2.2 FACS buffer:

0.5% - BSA, 1 X PBS - pH 7.2

Sterile filtered and maintained the buffer at 4-8°C

3.3 Hydorxyproline (HYP) assay:

- Glass tubes Schott Duran
- Ultra Turrax T18 homogenizer, IKA-Works, USA
- Sterile needle (B. Braun, Germany)
- Filter Millex HP (Merck Millipore, Cat. No. SLHP033RS)
- Syringe, 1 ml (B.Braun, Germany)

Solutions Used:

- 6N HCL

Standards used in HYP assay

Concentration	Dilution
640 µg/50 µl (12.8 µg /ml)	1:2
320 µg/50 µl (6.4 µg/ml)	1:2
160 µg/50 µl (3.2 µg/ml)	1:2
80 µg/50 µl (1.6 µg/ml)	1:2
40 µg/50 µl (0.8 µg/ml)	1:2

Table 3. Standards for hydroxyproline assay

87.2 µl of 50% isopropanol + 12.8 µl of 100 µg/ml of Hydroxyproline were mixed to obtain a concentration of 640 ng/50 µl.

3.4 Buffers for Western blot and gel electrophoresis:

- Resolving buffer: 2 M Tris (pH 8.8), 20% SDS in dd H_2O
- Stacking gel buffer: 2 M Tris (pH 6.8), 20% SDS in dd H_2O
- Western blotting buffers:

Anode buffer 1	Anode buffer 2	Cathode buffer
0.3 M Tris, 20% Methanol pH (10.4)	25 mM Tris, 20% Methanol pH (10.4)	40 mM Aminocaproic acid 20% SDS, 20% methanol

Table 4. Buffers used in Western blot

- 10 X Electrophoresis buffer: 10 g - SDS, 30 g - Tris, 144 g - Glycine in 1 liter of dd H_2O.
- TBS buffer: 20 mM - Tris and 137mM- NaCl were dissolved in dd water. pH was adjusted to 7.5 with concentrated HCl.
- TBST buffer/wash buffer: 20 mM - Tris and 137 mM - NaCl were dissolved in dd water. pH was adjusted to 7.5 with concentrated HCl then 0.1 % tween 20 was added.
- 5% milk powder in TBST: 5% milk was prepared by dissolving 5 g of milk powder in 100ml of TBST buffer (w/v) and used for blocking, also for primary and secondary antibodies.
- Stripping Buffer: 15 g - Glycine, 1 g - SDS, 10 ml – Tween 20 in 1 liter of dd H_2O and pH was adjusted to 2.2

- Resolving gel components

Concentration of the resolving gel	**8%**	**10 %**	**12 %**	**15 %**
dd H_2O	7.025 ml	6.025 ml	5.025 ml	3.525ml
30 % Acrylamide	4 ml	5 ml	6 ml	7.5 ml
4 X Resolving buffer	3.75 ml	3.75 ml	3.75 ml	3.75 ml
15 % Ammonium per sulphate (APS)	75 µl	75 µl	75 µl	75 µl
Temed	7.5 µl	7.5 µl	7.5 µl	µl
Optimum Separation for	> 100 kDa	30-100 kDa	20-30 kDa	< 20 kDa

Table 5. Resolving gel components

- Stacking gel components

Concentration of the stacking gel	**Volume**
dd H_2O	2.6 ml
30 % Acrylamide	625 µl
4 X stacking buffer	1,25 ml
15 % Ammonium per sulphate (APS)	25 µl
Temed	3.75 µl

Table 6. Stacking gel components

3.4.1 Buffers used to check protein concentration:

- Amido black stain:

  0.25% - Amido black, 45% - MeOH, 45% - dd H_2O, 10% - glacial acetic acid

- Amido black destain:

  45% - MeOH , 10% - glacial acetic acid , 45% - dd H2O

- Cellulose acetate dissolving solution:

  80 ml formic acid, 10 ml glacial acetic acid and 1 ml 100% trichloric acid

Standards used in amido black assay

Concentration	Dilution
25 µg/µl	1:2
12,5 µg/µl	1:2
6,25 µg/µl	1:2
3,125 µg/µl	1:2
1,56 µg/µl	1:2
0,78 µg/µl	1:2

Table 7. Amido black standards

3.6 Antibodies

Primary antibodies

Antibodies	Dilution/Isotype	Manufacturer
Goat anti mouse GFP+	1:50/Goat IgG	Bio legend
Rabbit anti CD3	1:50/Rabbit IgG	Abcam
Rat anti CD34	Rat IgG/1:50	Abcam
Rat anti mouse CD8a	1:50/Rat IgG2a	Bio legend
Rabbit anti CD4	1:50/ Rabbit IgG	Abcam
Goat anti-mouse GFP+	1:200/goat IgG	Rockland

Rabbit anti-mouse NTCP & OATP	1:200/Rabbit IgG	Provided by Dr. B. Stieger (Zurich)
Armenian hamster anti-mouse CD11c	1:50/Armenian hamster IgG	Bio legend

Secondary antibodies

Antibodies	Dilution/Isotype	Manufacturer
Donkey anti goat Alexa568	1:1000	eBio science
Goat anti rat Alexa568	1:1000	Invitrogen
Goat anti Rabbit Alexa488	1:1000	Invitrogen

Table 8. Antibodies used in the experiments

3.7 Primers list:

Primer Name	Company	Catalog number
CD 8a	**Qiagen**	**QT00244433**
CD 11c	**Qiagen**	**QT00113715**
CD45	**Qiagen**	**QT00139405**
F4-80	**Qiagen**	**QT00099617**
Ifg	**Qiagen**	**QT01038821**
IL-10	**Qiagen**	**QT00106169**
IL-13	**Qiagen**	**QT00099554**
MMP-9	**Qiagen**	**QT00108815**

Myeloperoxidase	**Qiagen**	**QT01065687**
Tnf-α	**Qiagen**	**QT00104006**
Abcc3	**Qiagen**	**QT00251006**
Abcc4	**Qiagen**	**QT01199226**
Bsep	**Qiagen**	**QT00157752**
Cyp7a1	**Qiagen**	**QT00121569**
Cyp7b	**Qiagen**	**QT01168944**
Fxr(nr1h4)	**Qiagen**	**QT00105336**
c-Met	**Qiagen**	**QT00126616**
Hnf-1a	**Qiagen**	**QT00170975**
Hnf-4a	**Qiagen**	**QT00144739**
Ntcp	**Qiagen**	**QT01045177**
Oatp	**Qiagen**	**QT01065239**
Ostb	**Qiagen**	**QT00171717**
Shp	**Qiagen**	**QT00319333**

Table 9. Primers used in PCRs

3.8 miRNA list

miRNA	Catalog number	ID number
SnoRNA 202 (as control)	4427975	001232
miRNA199-5p	4427975	002304

Table 10. miRNAs used in PCRs

- Components and volume used in reverse transcription (RT) miRNA assay

Component	Master mix volume per 15-µl reaction
10mM dNTPs (with dttp)	0.15 µL
Multiscribe Reverse Transcriptase 50U/µl	1.00 µL
10X Reverse Transcription buffer	1.50 µL
RNase Inhibitor, 20 U/µl	0.19µL
Nuclease-free water	4.16 µL
Total volume	7.00 µL

Table 11. Components used in reverse transcription (RT) of miRNA assay

- Components used in qRT-PCR of miRNA

Components	Volume per 20 - µL reaction (for single reaction)
TaqmanR small RNA Assay (20X)	1.00 µL
Product from RT reaction	1.33 µL
TaqmanR universal PCR master mix II (2X)	10.00 µL
Nuclease – free water	7.67 µL
Total volume	20.00 µL

Table 12. Components used in reverse transcription (RT) of miRNA assay

3.9 Kits

Kit Name	Company
Bile acid kit	Diazyme
RNA isolation kit	Qiagen
cDNA synthesis kit	Bio-Rad
Micro RNA isolation kit	Qiagen

RT (reverse transcription) kit	Applied biosystems
Micro RNA PCR kit	Applied biosystems

3.10 General equipment:

Laminar flow hood	Heraeus
Mega centrifuge	Beckman
Mini centrifuge	Hettich
Microscope	Leica
Microtome	Leica
Weighing machine	Sartorius
Thermo cycler	Biometra
Western blotting chambers (protein gel)	Biometra
Nano drop machine	Pecalab
Spectrophotometer	Thermo
Gel imager	Camag
X-ray film developing machine	Curix 60
RT-PCR machine	Applied biosystems/stratagene
pH meter	Metrohm
Incubator	Heraeus
FACS canto	BD (Becton Dickinson) biosciences

4. METHODS

4.1 Animals:

The current study was performed with permission of the state of Hessen, Regierungspräsidium Giessen, according to section 8 of the German Law for the Protection of Animals and confirms to the NIH guide for the care and use of laboratory animals. The BALB/c-GFP+ transgenic mice were raised from C57BL/6-TgN (ACTbEGFP+) 1 Osb (Jackson laboratories, Bar Harbor, Maine, USA) and crossed back on BALB/c for 10 generations which were kindly provided by Dr. M. Heil (Max-Planck Institute, Bad Nauheim, Germany). The BALB/c- *Abcb4*$^{-/-}$ mice were raised by breeding FVB/N knockout mice (Jackson laboratories, Bar Harbor, Maine, USA) with BALB/c over 10 generations.

4.2 Isolation of bone marrow stem cells:

BALB/c-GFP+ transgenic mice were sacrificed by isoflurane inhalation. Tibia and femur bones were collected into RPMI 1640 medium (PAN biotech, Aidenbach, Germany) with 0.01 % FCS (Fetal calf serum) and 1 % PS (penicillin streptomycin). The bone ends were tarred and the cells were flushed out with a 21G needle (BD Microlance, Spain) and syringe (B. Braun, Melsungen, Germany). Single cell suspension was produced by repeated gentle pipetting and then transferred into a new falcon tube through 100 µm sterile nylon cell strainer (BD Falcon, USA). Cells were centrifuged at 400 x g for 5 min at 4°C. After discarding the supernatant cells were resuspended in 1 ml of RPMI 1640 medium. Single cell suspension was produced by repeated gentle pipetting and transferred into the new falcon tube through 40 µm sterile nylon cell strainer. Cells were centrifuged at 400 x g for 5min at 4°C and resuspended in 1 ml of MACS buffer (PBS, pH 7.2, 0.5% BSA, 2 mM EDTA and maintained at 4-8°C). Cell viability was checked with trypan blue solution (Life Technologies, Darmstadt) and cells were counted by Neubauer chamber (Brandt, Mannheim). Thus isolated bone marrow stem cells were sorted by MACS using antibodies against cell surface markers Lin^- and $CD117^+$.

Medium: RPMI 1640

1% of pencillin streptomycin (PS)

0.1% of fetal calf serum (FCs) were added and maintained at 4-8°C

4.2.1 Lineage depletion by Magnetic Activated Cell Sorting (MACS):

To enrich CD117+ pluripotent stem cells, mature hematopoietic cells, such as T cells, B cells, monocytes/macrophages, granulocytes and erythrocytes and their committed precursors were depleted from bone marrow of BALB/c GFP+ transgenic mice. Depletion was performed by magnetic labeling of cells with a cocktail of biotinylated antibodies against a panel of "lineage" antigens and anti-biotin micro beads (clone: Bio3-18E7.2; mouse IgG1). Cells were centrifuged at 300 x g for 10 min and the supernatant was completely aspirated. After washing the cell pellet was resuspended in 40 µl of MACs buffer and blocked with the FCR reagent to avoid unspecific binding. Cells (10 µl per 10^7 cells) were incubated with biotin-antibody cocktail and incubated at 4-8°C for 10 min. Then 20 µl of anti-biotin micro beads (30 µl MACS buffer per 10^7 cells) were added and the cell suspension was incubated for 15 min at 4-8°C. Later cells were washed by MACS buffer (1 - 2 ml) and centrifuged at 300 x g for 10 min. Then supernatant was aspirated completely and the pellet was resuspended into MACS buffer (up to 10^8 cells in 500 µl). Washed and resuspended cell suspension was loaded onto a MACS column for cell separation. Magnetically labeled cells were retained in the column while the unlabeled lineage negative cells passed through the column and were collected for further separation.

CD117+ cell sorting: After depletion of Lin- cells, CD117+ cell sorting was continued. Cells were counted to determine the cell number. Once the counting was performed, cells were centrifuged at 300 x g for 10 min and the supernatant was aspirated completely. The cell pellet was resuspended in buffer (80µl to 10^7 cells) and anti-mouse CD117 micro beads 20 µl (PE conjugated) to 10^7 cells were added. Cells were mixed by gently tapping in between the incubation time (10 min at 4-8°C). Later cells were washed (1 ml of buffer per 10^7 cells) and centrifuged at 300 x g for 10 min. The supernatant was aspirated completely and resuspend in 500 µl of the MACS buffer up to 10^8 cells. Separation was performed by loading cell suspension onto MACS column according to the number of cells obtained. The magnetically labeled CD117+ stem cells retained within the column, which is placed in a magnetic field of MACS separator. Thus the cell fraction retained in MACs column was flushed out and the effluent was collected as positive (CD117 cells) fraction, after removal from the separator.

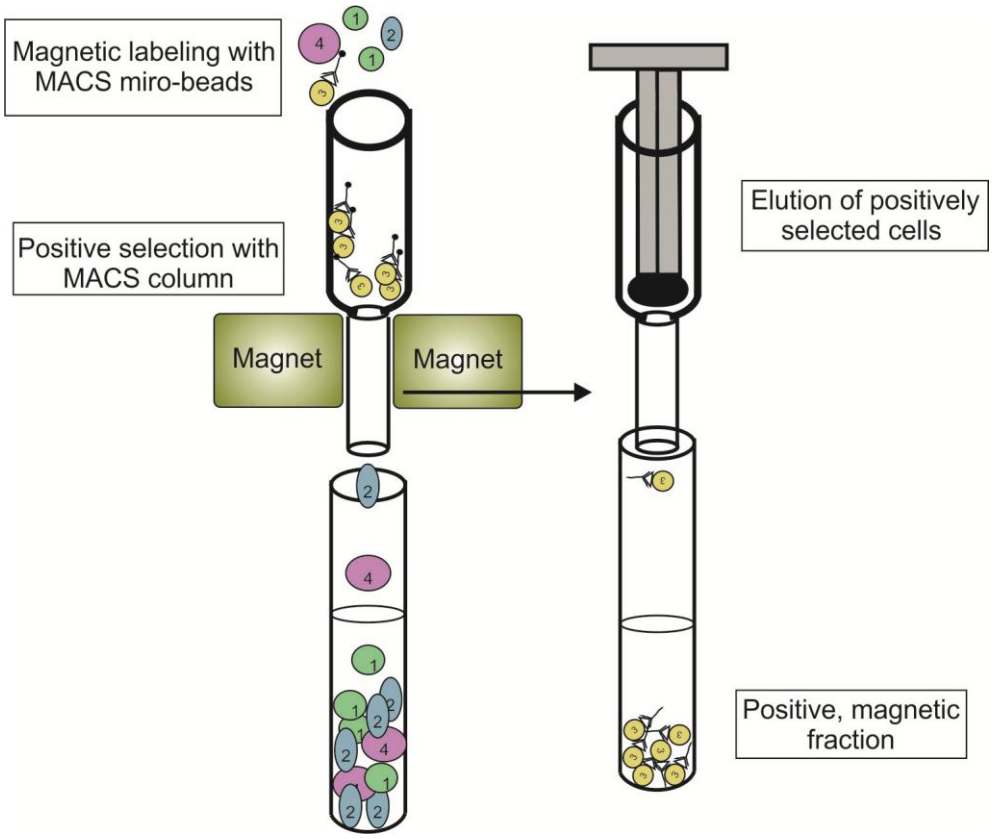

Figure 5: Magnetic activated cell sorting (modified from http://edoc.hu-berlin.de/dissertationen/hajkova-petra-2002-09-16/HTML/chapter3.html)

4.2.2 Desialylating of bone marrow cells by neuraminidase:

Cells were treated with 2U/ml of neuraminidase (N5254, Sigma Aldrich) enzyme to enhance the stem cell fusion to the existing healthy hepatocytes (96). This enzyme removes terminal sialic acid residues from cell glycoprotein surface and helps to bind with asialoglycoprotein receptor (ASGPR) of hepatocytes. To determine the enrichment of CD117+ cells, a suspension of positive and negative aliquots was collected and analyzed by flow cytometry.

4.2.3 Fluorescence activated cell sorting (FACS):

Cells were washed with FACS buffer (0.5% BSA in 1 X PBS maintained at 4-8°C) and then cells were stained with PE (Phycoerythrin) conjugated (10 µl per 10^6 cells) antibodies, which were specific for CD117+ cells. The basic principle involved is an antigen - antibody interaction where, PE labelled CD117+ cells were stimulated and recognized by laser light of FACS Canto (Becton

Dickinson, Heidelberg). Once sorting was finished cells were ready to transplant into the irradiated mice.

4.3 Transplantation of Hematopoietic (CD117+) progenitor cells:

At the age of 6 weeks, *Abcb4*$^{-/-}$ mice were lethally irradiated with (11 Gy, $_{60}$Co) in order to weaken the immune system and to avoid the immune reactions as well as graft rejections. Subsequently CD117+ (4 X 10^5) stem cells were transplanted into *Abcb4*$^{-/-}$ mice via tail vein injection under aseptic conditions. After transplanting successfully, mice were housed in sterile cages and kept under supervision. Body weight and food intake were observed each day. One week later, weight was observed every alternate day. Till the date of killing all mice were monitored to avoid infections or any other contaminations. On completion of time points that is 2 and 20 weeks after transplantation, mice were sacrificed to assess liver staging and gading by means of histological and serological examinations.

4.4 Serum transaminases measurement:

Serum biochemistry was analyzed by measuring the transaminases such as Alanine transaminase (ALT), Aspartate transaminase (AST) and Alkaline phosphatase (AP). Blood was collected from the vena cava of transplanted mice kept 10 min at room temperature, which allowed blood to clot and 20 min on ice. Following incubation on ice, blood was centrifuged at 2510 xg for 10 min. Then 50 µl of the supernatant was collected into new 1.5 ml Eppendorf tube and stored at -80°C for further use. On the day of measurement probes were thawed on ice and 30 µl of serum taken on to Reflotron (Roche, Mannheim, Germany) strips and measured at 567 nm after 124 seconds. In case of ALT and AST, the sample was diluted in 1:100, whereas no dilution was performed for AP.

4.5 Liver histology and preparing paraffin sections:

The livers were harvested and fixed in 1% paraformaldehyde (PFA) at 4° C for overnight, then washed for 5 times with 1 x PBS for 20 min. Then the tissue was processed to exclude water and the tissue was paraffin embedded (Leica EG 1140H). Sections of 3-5 µm thickness were cut on a microtome (Leica RM2165) and left overnight at 37°C. Later sections were kept in dark at room temperature and the rest of the paraffin embedded probes was stored at 4°C for future evaluations. All the stainings (H&E, Sirius red and Masson Goldner) were performed according to standard procedures.

4.5.1 Hematoxylin and Eosin (H&E) staining:

HE staining is most popular because of its usage to diagnose abnormalities in morphology of organ tissues. Paraffin embedded sections were incubated for 40-60 min at 60°C and were washed in alcoholic solutions like 2 x 10 min and 1 x 5 min Xylol, 2 x 5 min 99.6% Ethanol, 1 x 5 min 96 % Ethanol, 1 x 2 min 70% Ethanol and 1 x 5 min under tap water. Then the sections were incubated in HE (Mayers' acidic, Fa Waldeck, Germany) solution for 2-4 min and washed under tap water for 5 min. Following HE staining the sections were incubated for 15 min in Eosin (Thermo scientific, Heraeus,Germany) solution and followed by washing in row of chemical reagents such as 2 min in 96% ethanol, 2 x 5 min in isopropanol, 3 x 5 min in xylene. Subsequently the tissue sections were covered with glass cover slips with mounting (Medite, Pertex, Burgdorf) solution and allowed them to dry.

4.5.2 Sirius red staining:

Sirius red staining is specific for collagens. These collagens were highlighted by sirius red and make the stain particularly suitable for quantification by image analysis. Sections of liver tissue of 3 µm thickness were stained with sirius red in order to analyze collagen fibril deposition in Abcb4 knockout mice. Firstly sections were incubated at 60°C for an hour and hydrated using a series of alcohol solutions. Xylol - 10 min; 10 min; 5 min, 99, 6%; 90%; 70% - ethanol 5 min in each solution, 5min under running tap water. Then probes were left in 0.1% Sirius red (Sigma Aldrich, Steinheim) solution for 1 hour and dipped in freshly prepared 1% acetic acid. Thus stained sections were treated with a row of ethanol solutions for 1 x 2 min 96% ethanol, 2 x 5 min Isopropanol, 3 x 5 min Xylene and mount with Pertex. The sections were investigated under polarized light microscopy (Leica) and for image acquisition Mirax software was used.

4.6 Immunohistochemistry*:*

Liver tissue was embedded in tissue tec and frozen at -80°C. Prior to cutting sections the probes were placed at -20°C overnight. The following day tissue sections were cut with microtome (3 µm thick) and picked up on microscopic glass slides. Slides were used either directly or stored at -20°C until further use. It was ensured that the sections were neither thawed until final processing, nor dried up during the pre-treatment and dyeing. Nonspecific, purified IgG Isotype was used as controls, which were immunized from the same host of antibody purified.

4.6.1 Immunostaining of cryosections:

In order to quantify the expression, 3 µm frozen tissue sections were fixed in acetone/methanol for 2 minutes at -20°C min and washed with PBS buffer. Unspecific binding sites were blocked for 30 min with 5% bovine serum albumin and 0.1% cold fish skin gelatin (Sigma-Aldrich, Munich, Germany) in PBS with 0.1% Triton (Roth, Karlsruhe, Germany) and 0.05% Tween 20 (Serva, Heidelberg, Germany). The antibodies used in immunohistological staining are shown (in table 8) and fluorescent conjugated secondary antibodies Alexa fluor 488 and Alexa 588 were purchased from Molecular Probes (Eugene, OR, USA). Nucleus staining was performed with DAPI (4´,6-diamidino-2-phenylindole dihydrochloride, Sigma Aldrich, Munich, Germany). Specificity of all immunofluorescence staining was proved using equally concentrated unspecific Isotype IgG instead of primary antibodies. In case primary antibodies are of mouse origin, we have utilized a specific blocking reagent called mouse on mouse (Vector Biolabs) to prevent unwanted background.

4.6.2 Immunostaining of paraffin sections: (peroxidase/microwave method)

As in histology liver tissue sections were deparaffinized at 60°C for 1 h and plunged in descending order of alcohol row 2 x 10 min 1 x 5 min Xylol, 2 x 5 min in 99.6% ethanol, 1 x 5 min in 96% ethanol, 1 x 2 min 70% ethanol and 1 x 5 min under running tap water. Slides were allowed to cook with citrate buffer for 1 min for 10 times and colled at room temperature about an hour. The sections were washed with 2 x 5 min PBS; 1 x 5 min tap water. By heat treatment with citrate buffer antigens were unmasked that have been masked by formalin fixation. This was followed by 10 min blocking with a 1:10 diluted H_2O_2: methanol mixture and washed 2 x 5 min PBS; 1x 5 min tap water with gentle agitation. Then tissue sections were blocked with 2.5% normal horse serum for 20 min (prevents excessive background) and subsequently washed briefly with PBS and incubated with primary antibody for overnight at 4°C (in humid chamber). Immunostaining was performed against membrane proteins Ntcp and Oatp using rabbit anti Ntcp (1:200 Zurich, Switzerland) rabbit anti Oatp (1:150 Zurich, Switzerland). The antibodies were kindly provided by Dr. B. Stieger (Zurich).

After primary antibody incubation, slides were washed again 4 x 5 min with PBS, and then incubated with secondary antibody for 1 h at room temperature under humid conditions. Later slides were decanted, washed and gently swiped. Followed by vector VIP (catalog number SK-4600) incubation 2-3 min to achieve optimum colour, observed under microscope and washed

under tap water for 5 min subsequently counterstained with methylene green/hematoxylin. After counterstaining tissue sections were washed in a series of alcohols such as 96% Ethanol - 2 min, Isopropanol - 2 x 5 min, Xylene 3 x 5 min. At the end slides were mounted with cover slips with the help of Pertex solution.

4.7 Hydroxyproline assay:

Hydroxyproline is a cyclic amino acid and a key component of collagen. By acid hydrolysis it is possible to determine the hydroxyproline content of the liver sample (quantified and to calculate there from the total collagen content (10). Increased hydroxyproline content in tissue samples is thus an indicator of increased collagen deposition.

4.7.1 Sample preparation:

Liver tissue (50 mg) was weighed and put on dry ice until further processing. Added 1 ml of 6N HCl, homogenized and incubated for 16 h at 110°C in an incubator. Taken out the content with a sterile needle and syringe and transferred into 1.5 ml Eppendorf tube throughthe filterr and centrifuge for 5 min at 14000RPMm and transferred 15 µl 2 x (double value) in 1.5 ml of Eppendorf tube. 15 µl of methanol added to each sample and mixed well before keeping on to theheatert block. Then the samples were heated about 20 min at 40°C and gassed simultaneously with nitrogen. The resulting pellet was either used directly or stored at -20°C for further use. In the meantime, standards (table 3) were prepared and later the pellet was dissolved in 50 µl of 50% isopropanol. 100 µl of 0.6% chloramine T solution was added to the sample (50 µl) and to the standards, vortexed immediately and incubated at room temperature for 10 min. It was Mixed shortly after adding 100 µl of freshly prepared Ehrlich's reagent and incubated at 50°C for 45 min. At the end samples were measured at 570 nm (Fusion, Packard) and concentration was calculated in parallel with the standards (µg/g liver).

4.8 Semi quantitative polymerase chain reaction (PCR):

4.8.1 RNA isolation:

Mouse liver tissue of 20-30µg was homogenized with 600 µl of the RLT buffer to which mercaptoethanol (10 µl/ml) was added. The homogenate was centrifuged at maximum speed for 3 min and carefully extracted the supernatant. 1 volume of 70% ethanol was added to the lysate, and then mixed gently. Up to 700 µl of the sample was transferred (including any precipitate) to RNeasy mini spin column and placed in a 2 ml collection tube and centrifuged at ≥ 8000xg for 15

sec and discarded the flow through. Then 700 µl of 2 x RW1 buffer was added (pink columns) and centrifuged at ≥ 8000xg for 15 sec and discarded the flow through. Later 500µl of RPE buffer was added to the RNeasy spin column and centrifuged at ≥ 8000xg for (1 x 15 sec and 1 x 2 min). The RNeasy spin columns were placed in a new 1.5 ml collection tube and added 30 µl of RNase free water directly on to the spin column membrane and centrifuged at ≥ 8000xg for 1 min to elute the RNA. After elution the DNA digestion was performed.

4.8.2 DNA digestion:

Genomic DNA contamination was eliminated by TURBO Dnase digestion. One µl of 10X TURBO Dnase buffer and one µl of TURBO DNase was added to the RNA. The reaction mixture was incubated at 37°C for 20-30 min. Then the reaction mixture was resuspended well in Dnase inactivation reagent and incubated 5 minutes at room temperature by mixing occationally. The total reaction was centrifuged at 10,000 x g for 1.5 min and transferred to a fresh tube. Thus obtained RNA was measured for concentration and purity by Nano drop at 260/280 nm and the quality of the RNA was evaluated by agarose gel electrophoresis.

4.8.3 cDNA synthesis:

For reverse transcription (RT), extracted RNA (1 µg) was converted to cDNA using the iScript cDNA synthesis kit as of end reaction volume 20µl (5 X iScript reaction mix-4µl; iScript reverse transcriptase-1µl; Nuclease free water + RNA (1 µg) template - 15 µl). Total reagents were then incubated in thermo mixer at 25°C for 5 min followed by 30 min at 42^0C where reverse transcription takes place and for 5 min at 85°C to inactivate reverse transcriptase. Using r18s as the housekeeping gene quality of cDNA was checked by qRT-PCR.

4.8.4 Quantitative real time PCR (qRT-PCR):

Real time PCR was performed with stratagene and quantification of Cts (threshold cycle) was done by Maxpro software. For PCR amplification 6.3 µl of SYBR ROX (12.5 ml Syber green+100 µl of Rox), 4.45 µl of water, 1.25 µl of Qiagen primers and 0, 5 µl of cDNA were used. Samples were taken as duplicates and PCR conditions were as follows.

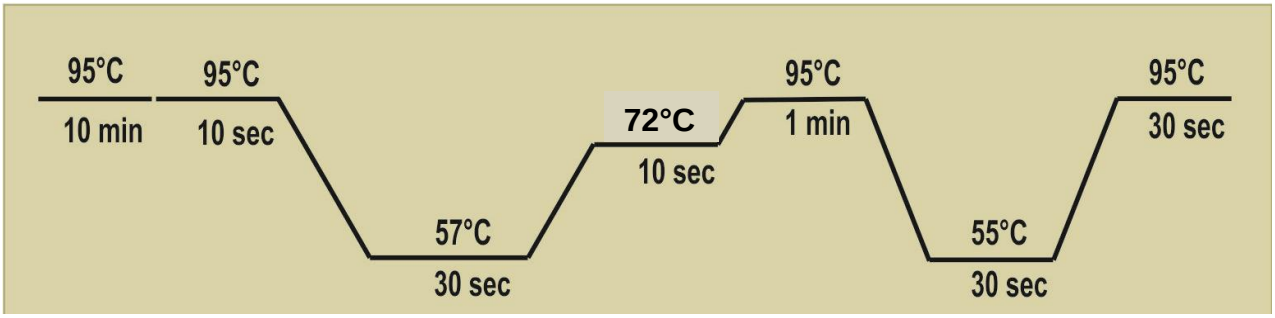

Chosen an appropriate annealing temperature according to primers used (table 9). The expression of all genes was normalized to r18s to determine the relative mRNA expression (Δ CT). The fold change ($2^{\Delta\Delta CT}$) was calculated. Among all genes, expression of few genes was analysed at protein level by Western blot.

4.9 Western Blot:

4.9.1 Liver lysates preparation:

Liver tissue of 10 mg wasweighed on dry ice and was mixed in 400 µl of Laemmli buffer (1:4 dilutions) by short vortexing. The tissue was, incubated for 10 min in thermo mixer at 99 ^{o}C following centrifugtion for 10 min at ≥ 8000 x g. The supernatant was transferred into a new 1.5 ml eppendorf and loaded immediately on the gel. The liver tissue was normalized by adding Laemmili buffer according to weight (W/V). Protein concentration was measured by Amido black stain method. Starting with 5 mg/ml BSA in Laemmli series of 1:2 dilutions in Laemmli (100µl BSA+100µl of Laemmli) were made. One µl of each standard (as shown in figure 7) and the samples to be estimated were added to a strip of cellulose acetate membrane and the spots were allowed to air dry. Dried membrane was stained with amido black reagent for 10 minutes under shaking condition. Then the membrane was de-stained in destaining buffer until the background is nearly white. Thus obtained membrane was utilized to examine the intensities of the test protein by comparing the standard spot intensities. Each spot was carefully punched out and dissolved in 400µl of cellulose acetate dissolving solution and the protein concentration was measured at 630nm and the concentration was calculated according to the standard curve. Carefully punched out the each spot and dissolved in 400µl of cellulose acetate dissolving solution. According to the obtained concentration, 20 µg/µl of protein was loaded on to gel to perform SDS PAGE for Western blot analysis.

4.9.2 SDS-polyacrylamide gel electrophoresis (SDS-PAGE) and Western blot:

Sodium dodecyl sulphate-polyacrylamide gel electrophoresis was prepared according to Laemmli (1970). It is particularly useful for separation of proteins according to size (molecular weight), the method can also be used to determine the relative molecular mass of proteins. According to molecular weight of the protein, gels were prepared (table 5,6). Then proteins were transferred onto the polyvinylidene fluoride membrane (PVDF) membrane by semi-dry method. Unspecific binding sites were blocked with 5% milk powder by dissolved in 1x TBS-T buffer for 1 h at room temperature. Incubation with respective primary antibody was performed at 4°C for overnight. Next day blots were washed with 1xTBS-T buffer and incubated with horse radish peroxidase (HRP) conjugated secondary antibody. After washing with 1x TBS-t, blot was placed in ECL reagent for a short time to detect HRP signal by enhanced chemoluminescence. Then the blots were exposed on to the X-ray film (CL-xposure^{Tm} film Thermo scientific, Belgium) in a dark room. Later blots were reprobed for housekeeping gene α-tubulin as internal control. The antibodies used for immunobloting were mentioned in table 8.

4.10 Measurement of serum total bile acids:

Bile acids are metabolized in the liver; hence they act as a marker for the normal liver function. Serum total bile acids (TBA) were measured with the help of TBA assay kit (DIAZYME DZ042A-K, Dresden). Firstly 4 µl of sample and standard was pipetted into two different cuvettes, to this 270 µl of R1 buffer was added. Similarly 4 µl of water and 270 µl of R1 buffer were added into another cuvette which was used as blank. Then all the samples were incubated at 37° C for 3 min. After the incubation, 90 µl of R2 buffer was pipetted into the cuvettes and mixed well. Immediately measured the absorbance at 405 nm for 2 min (made autozero of the blank at same absorbance). Optical density (OD) values obtained by (ΔA405 = O.D at 120 sec – O.D at 60 sec). Using the following formula total amount of bile acids concentrations were determined.

$$\text{Sample (TBA, µ mole/L)} = \frac{\text{Sample } \Delta A405\text{nm/min} - \text{Blank } \Delta A405\text{nm/min}}{\text{Standard } \Delta A405\text{nm/min} - \text{Blank } \Delta A405\text{nm/min}} \times \text{Standard}$$

The following equation represents the principle of the assay

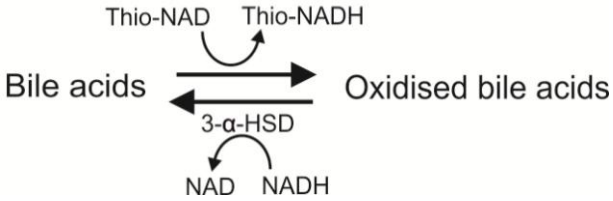

4.11 miRNA Analysis:

4.11.1 miRNA isolation:

For isolation of miRNA, 20-30 mg of mouse liver tissue was used and miRNeasy mini Kit (Qiagen, Cat. no. 217004, Hilden, Germany) was used for extraction. To disrupt the tissue 700µl of QIAzol lysis buffer was added and homogenized. Homogenate was incubated at 15-25°C, for 5 min. To the lysate 140 µl of chloroform was added and mixed vigorously for 15 sec. Following 2-3 min of incubation at room temperature the lysates were centrifuged for 15 min at 12,000 X g at 4°C. The upper aqueous phase was gently collected in to a new tube avoiding the interphase contamination. To this 525 µl of 100 % ethanol was added and mixed thoroughly by pipetting up and down. Thus obtained 700 µl of the sample was transferred into RNeasy mini column which is attached to collection tube. Then the sample was centrifuged at 8000 X g for 15 sec at room temperature. Flow through was discarded and 700 µl of RWT buffer was added to the column and centrifuged for 15 sec at 8000 X g and discarded the flow through. To the column 500 µl of RPE buffer was pipetted and centrifuged again at 8000 X g for 15 sec. This step was repeated for 2 times and the RNeasy mini column was placed into new 2 ml collection tube to centrifuge at full speed for 1 minute to allow to dry the column membrane. Finally 30-50 µl of Rnase free water was pipetted directly onto the RNeasy mini column membrane and centrifuges for 1 minute at 8000 X g to elute the RNA. Thus eluted RNA was measured on Nano drop to check the concentration and stored at -80°C for future use.

4.12.2 Reverse transcription of miRNA:

Reverse Transcription (RT) was performed with extracted RNA (1 µg/µl) by using TaqMan® MicroRNA Reverse Transcription Kit (Applied Biosystems, Cat.No. 4366596, Germany). The components required for preparation RT master mix were given (table 11). For amplification 7 µl master mix, 3 µl of 5 X RT primer, and 5 µl of RNA were used. Samples were mixed gently and briefly centrifuged. The thermal cycler conditions were 30 min 16 °C, 30 min 42°C, 5 min 85°C and hold at 4°C.

4.12.3 miRNA quantitative real time PCR (qRT-PCR):

The expression of different mature miRNAs was verified by real-time PCR analysis, using a TaqMan® Micro RNA Assays (Applied Biosystems, Cat.No.4427975, ID 002304 Germany). The components used to prepare the qRT-PCR mix were as follows (table 12). In each case specific RT primers were used to each miRNAs which were listed in table 6. The real-Time PCR reactions were performed in duplicate in a total volume of 15 µl. The following temperatures were used to program the PCR machine 50°C for 2 min, an initial step at 95°C for 10 min followed by 40 cycles each of 15 s at 95°C and then 60 s at 60 °C (Applied Biosystems StepOne Plus). The expression of all miRNAs was normalized to RT-001232 (life technologies, cat.no 4427975, Darmstadt) as a control miRNA to determine the relative miRNA expression (Δ CT) and the fold change (2 Δ ΔCT) was calculated.

5. Results:

Bone marrow transplantation (BM-Tx) demonstrated both, enhanced and reduced effects on liver fibrogenesis (97). In our previous studies, we could demonstrate that whole bone marrow transplantation (BM-Tx) improves liver fibrosis via induction of Th1 switch as the underlying mechanism of the fibrolytic effects and upregulated MMP-9 (Matrix metalloproteinase-9) activity (15).

In the present study, our aim was the reconstitution of Abcb4 transporter. Therefore, we sorted and transplanted desialylated CD117+ hematopoietic progenitor cells in *Abcb4*$^{-/-}$ mice by via tail vein injection. Allogenic BM-Tx (*i.e* BALB/c-GFP+ to BALB/c-*Abcb4*$^{-/-}$) was performed for two time periods to understand the short and longterm effects of BM-Tx on liver physiology.

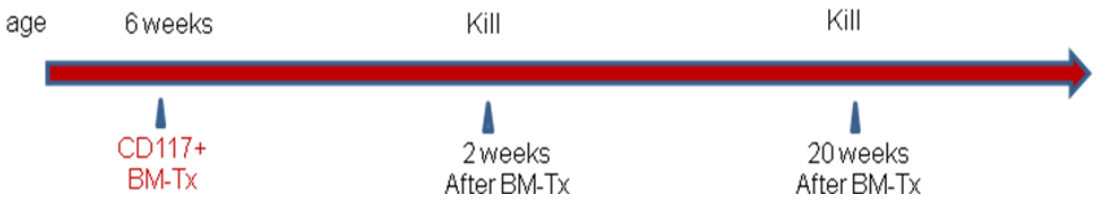

In addition, we investigated the regenerative potential of CD117+ cells and to get an insight of the genes that were involved in inflammatory signaling and cytokine production in *Abcb4*$^{-/-}$ mice. Microarray data from BM-Tx of liver tissue revealed a set of genes (e.g *Ntcp* and *Oatp*), which play a pivotal role in the hepatobiliary transport system at transcriptional level (98). ABCB4 transport phospholipids across the hepatocyte canalicular membrane. Thereby, demonstrating that defects in transporter expression and function can cause cholestasis (57). Therefore, we further evaluated the expression analysis of hepatobiliary transporter genes during the course of disease.

5.1 Transplantation of CD117+ hematopoietic stem cells in *Abcb4*$^{-/-}$ mice

5.1.1 Isolation, purification and transplantation of CD117+ hematopoietic stem cells:

CD117+ stem cells were isolated and purified from the tibia and femur of BALB/c-GFP+ transgenic murine bone. The lineage depleted cells were counted and further sorted for CD117+ stem cells with the help of cell surface markers. Sorted cells were counted and treated with 7AAD (7 aminoactinomycin-D) to analyse the dead cell amount and purity by FACS (figure 6).

We tried to increase the accumulation of bone marrow cells (BMCs) directly into the liver through the interaction between hepatic asialoglycoprotein receptor and desialyted BMCs. Desialylated BMCs were obtained by treating with neuraminidase, which removes the terminal sialic acid from glycoprotein located on the cell surface. These desialyted BMCs were transplanted into 6 weeks old BALB/-c *Abcb4*$^{-/-}$ (allogeneic) mice.

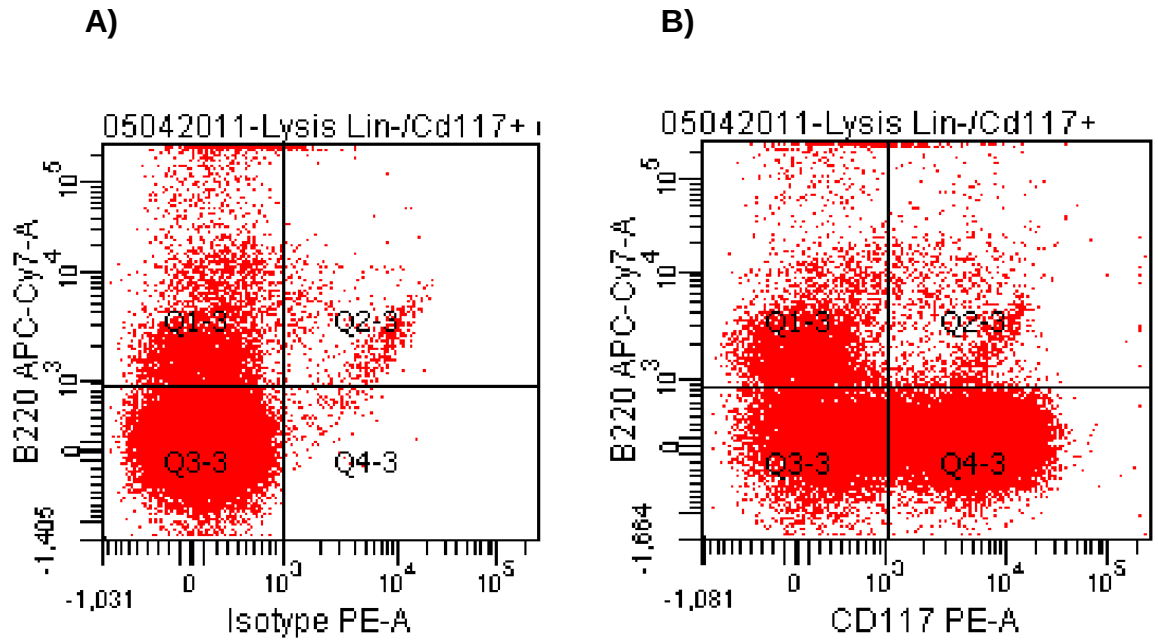

Figure 6: **Cell purity assessed by flow cytometry**. The above pictures show CD117+ stem cell with A) Isotype control. B) CD117+ bone marrow stem cells, which are labeled with Phycoerythrine-A conjugated antibodies. In quarter Q 4-3 of panel B indicates 70% cells positive for CD117+.

5.1.2 Infiltration of GFP+ cells into BALB/c-*Abcb4*$^{-/-}$ mice:

In order to identify whether transplanted GFP+ cells are recruited into recipient *Abcb4*$^{-/-}$ mice, immunostaining for GFP antigen was performed and the staining revealed that lot of GFP+ cells were infiltrated around portal fields (figure 7B). Sham control means non-transplanted *Abcb4*$^{-/-}$ mice, whereas BM-Tx means CD117+ BMC transplanted *Abcb4*$^{-/-}$ mice.

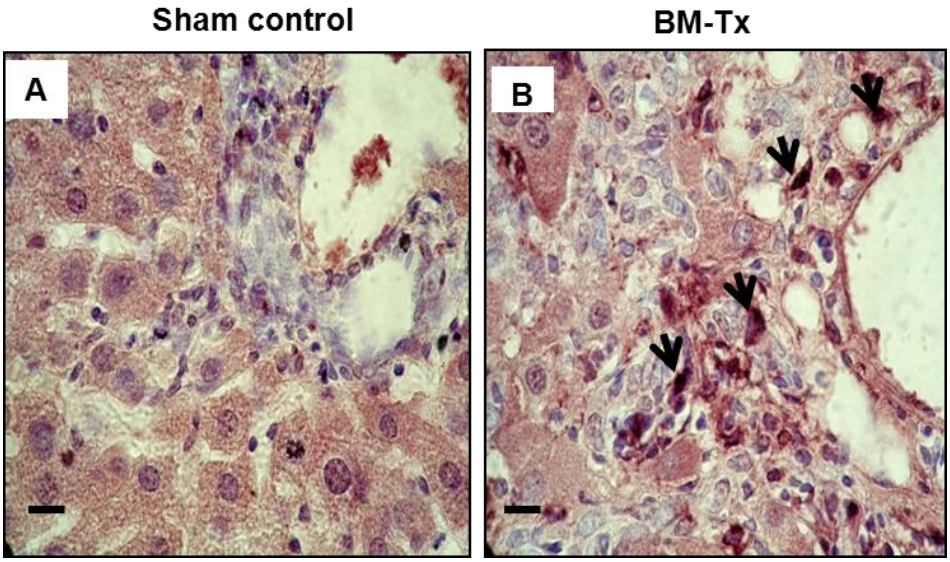

Figure 7: **Immunostaining of transplanted GFP+ bone marrow cells:** The staining provides BM engraftment of transplanted cells. A) Sham control showing no infiltration of cells B) BM-Tx mice showing infiltration of GFP+ cells, which were dark brown in colour marked by black arrows. (Original magnification - 400 x, scale bar=25µm).

5.1.3 Cell fusion of GFP+ stem cells of donor mice and host hepatocytes:

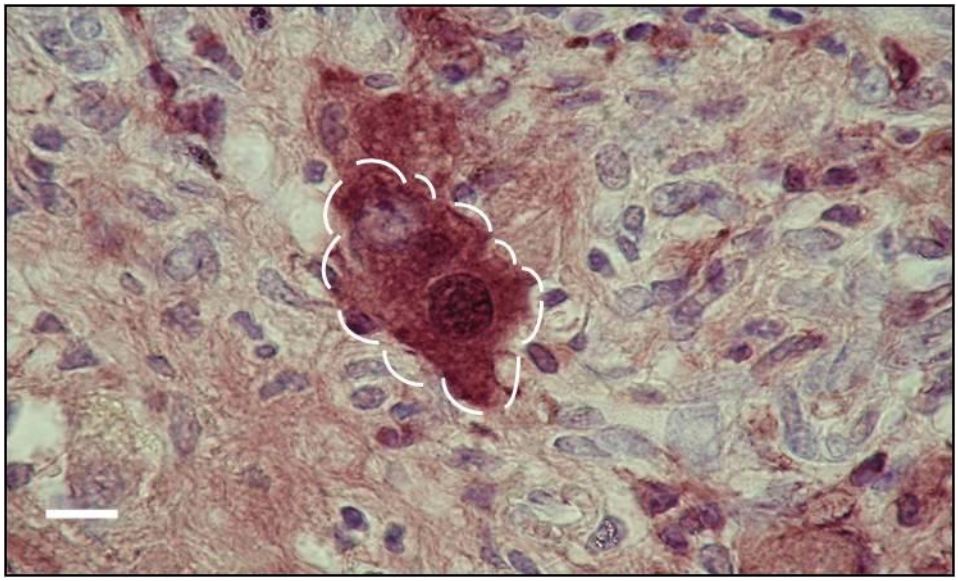

Figure 8: **Cell fusion of transplanted GFP+ BM cells with hepatocytes from recipient mouse**: The staining shows hepatocytes from recipient mouse fused with GFP+ cells, which were of purple colour. The fusioned cell is surrounded by a white dashed line (Original magnification-1000 x, scale bar=10µm).

Cell fusion is the principal mechanism by which hematopoietic stem cell (HSC)-derived hepatocytes arise (37, 38). We performed immunohistology to identify whether cell fusion occurred between transplanted GFP+ CD117+ stem cells and recipient *Abcb4*$^{-/-}$ mouse hepatocytes. The staining revealed that, fusion of transplanted cells with host hepatocytes was a rare event. Lots of GFP+ cells infiltrated portal fields (figure 8).

5.1.4 Serum biochemistry:

Under normal physiological conditions, serum transaminases were released into the bloodstream, and elevated transaminases indicate liver damage. Routine serum biochemistry was performed to assess the liver function. In 2 (8) weeks group, after BM-Tx serum levels of alanine transaminase (ALT) were significantly increased, whereas aspartate transaminase (AST) was not altered. Alkaline phosphatase (AP) levels was slightly higher in sham controls, whereas aminotransferase levels were not altered in 20 (26) weeks (long term) old *Abcb4*$^{-/-}$ mice compared to sham control (figure 9).

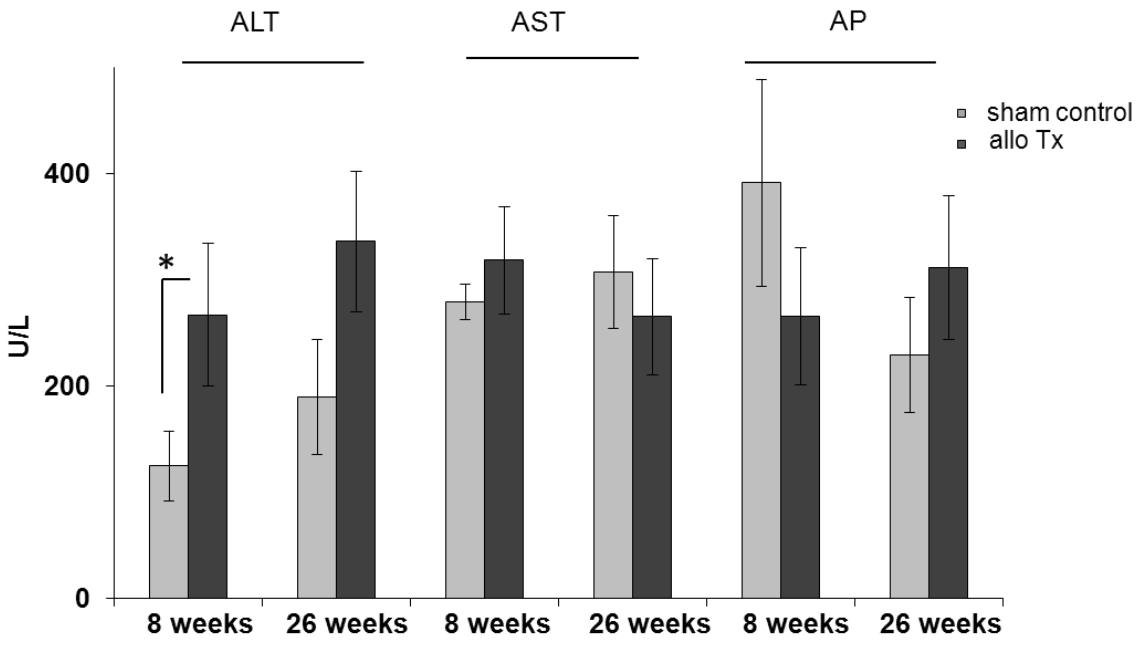

Figure 9: Serum ALT, AST, and AP levels in sham and allo Tx mice. 6 - 10 mice per group were analyzed independently; gray column: sham control; dark column: allogeneic BM-Tx.

5.2 FIBROSIS

5.2.1 Total collagen level analysis:

Unlike in previous studies (where whole bone marrow transplantation revealed reduced hepatic collagen) the current CD117+ stem cell transplantation showed significantly upregulated hepatic collagen accumulation after 2 (8) weeks of transplantation. Whereas, at 20 (26) weeks no significant enhancement was observed after allogeneic BM-Tx, which was normalized to sham (figure 10).

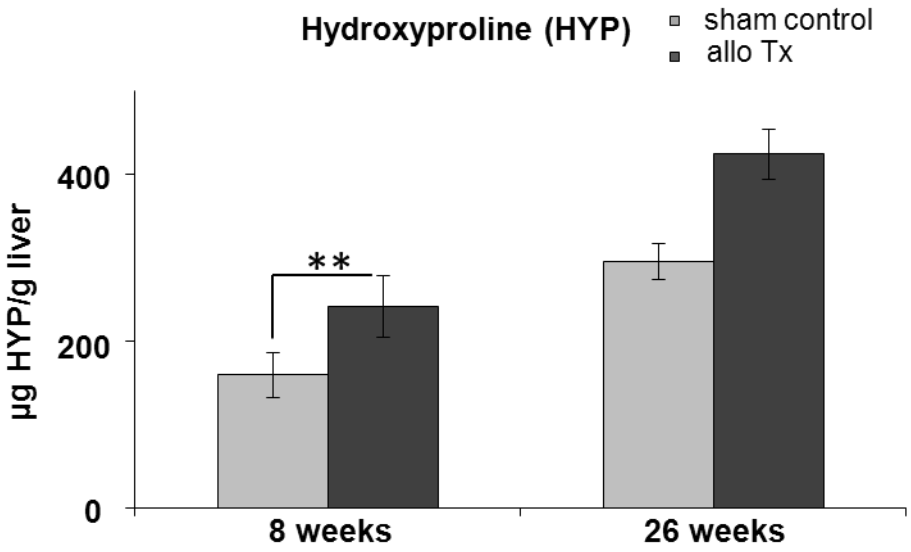

Figure 10: Hydroxyproline content for measurement of total collagen: Hydroxyproline (HYP) analysis revealed significant increases of hepatic collagen levels in 2 (8) weeks after BM-Tx (allogeneic) **p=0.002. Analysis was performed independently containing 6-10 mice per group; gray column: sham control; dark column: allogeneic BM-Tx.

5.2.2 Periductular collagen levels reflected by Sirius red staining:

Histopathological anomalies of the liver after BM-Tx was analysed by Sirius red staining, which is used to assess the accumulation of collagen levels. The stainings revealed increased fibrotic tissue content over a period of time. Presence of collagen was minimal in 8 weeks sham control, whereas, 2 (8) weeks BM-Tx increased collagen fibrils around portal fields were observed (Figure 11B). However, 20 (26) weeks after BM-Tx severe phenotype of portal field fibrosis was observed compared to 26 weeks sham control mice (Figure 11D).

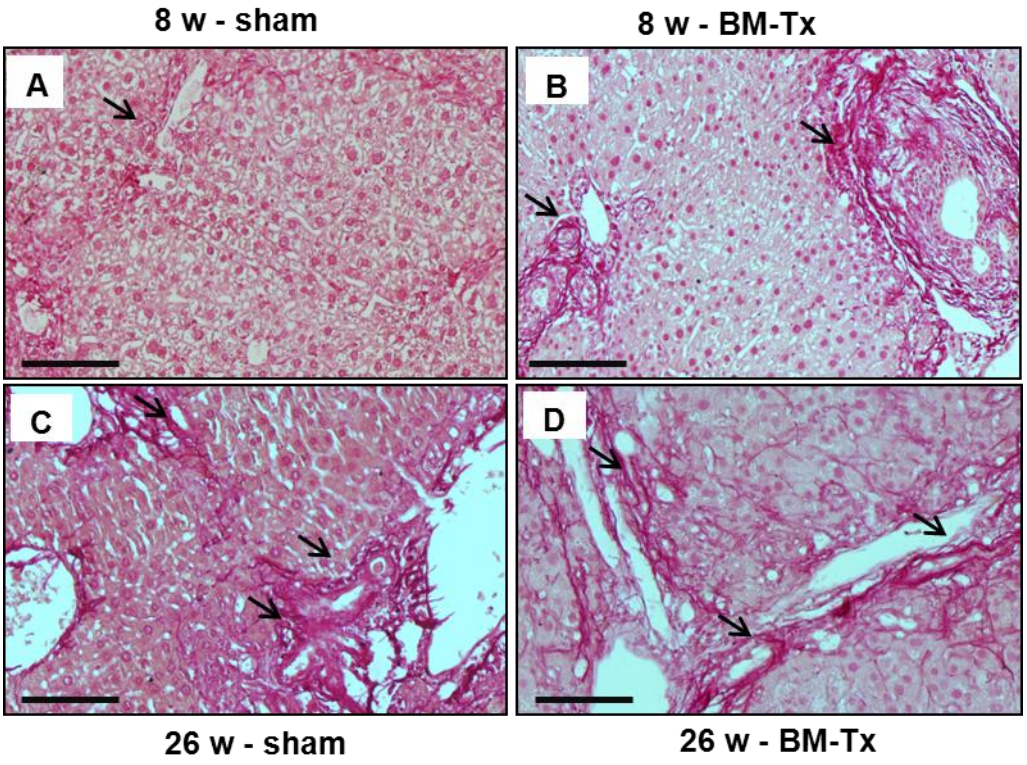

Figure 11: Long term BM-Tx induced collagen levels in *Abcb4*$^{-/-}$ liver. Sirus red staining for the liver collagen shows A) 8 weeks sham control (untreated *Abcb4*$^{-/-}$ mice) B) 2 (8) weeks BM-Tx mice (CD117+ stem cells transplanted). The lower panel shows C) 26 weeks sham control (untreated *Abcb4*$^{-/-}$ mice) D) 20 (26) weeks BM-Tx mice (CD117+ stem cells transplanted) collagen fibrils were stained in dark red colour, which were indicated by black arrows. (Original magnification -20 x, scale bar-100µm)

5.2.3 Matrix metalloproteinase-9 (MMP-9) activity after BM-Tx:

MMP-9 plays an important role in the context of hepatic fibrosis and fibrolysis. Hence, we assessed the MMP-9 activity by qRT-PCR (figure 12A) and Western blot analysis (figure 12B). At the age of 2 (8) weeks MMP-9 activity was significantly upregulated after BM-Tx at both transcriptional and protein level. Whereas, at 20 (26) weeks after transplantation no significant changes were observed.

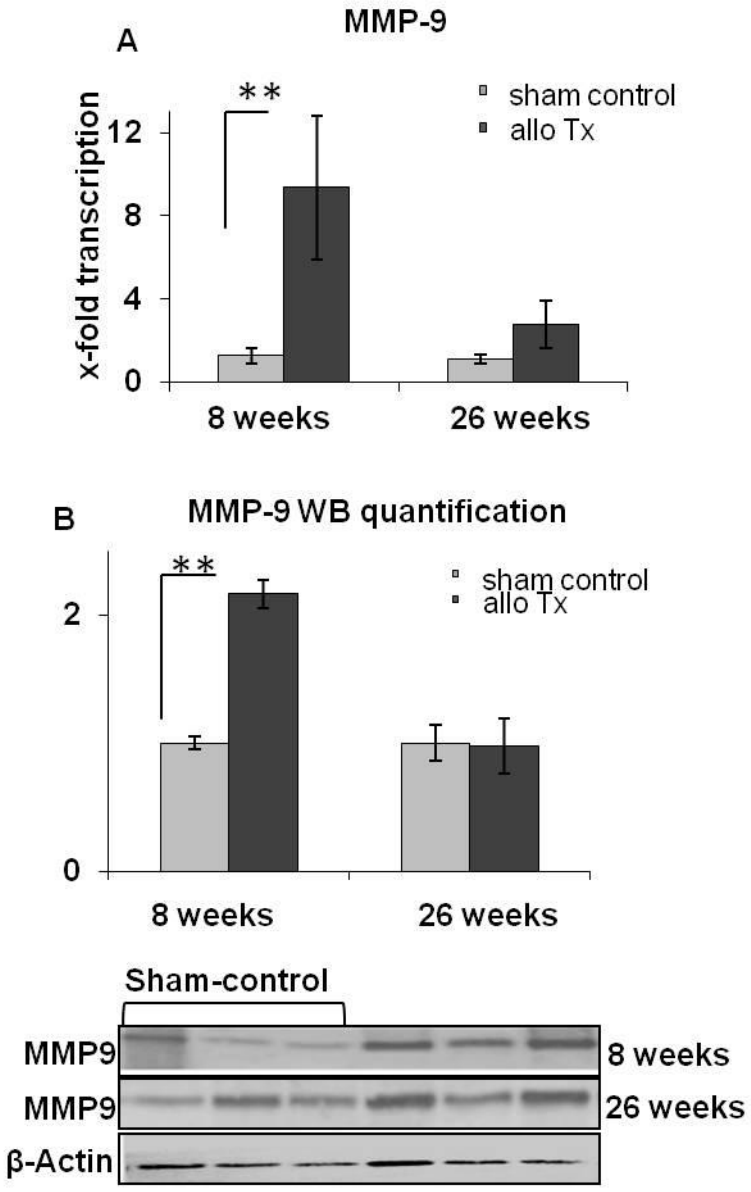

Figure 12: A) In the above picture mRNA expression of matrix metalloproteinase-9 (MMP-9) after bone marrow transplantation was indicated. Following CD117+ BM-Tx, MMP-9 transcription was significantly increased (**p=0.002) whereas, in 20 (26) weeks old mice we didn't observe any significant changes. 6-10 mice per group were analyzed independently; gray column: sham control; dark column: allogeneic BM-Tx. A) Following mRNA expression, protein level expression was revealed a transiently prolonged expression of matrix metalloproteinase-9 (MMP-9) in 2 (8) weeks after bone marrow transplantation was detected by Western blotting.

5.2.4 Acute expression of transforming growth factor (TGF-β) after BM-Tx:

TGF-β known to be a potent cytokine, which is mainly involved in liver disease progression (99). In order to analyze the TGF-β contribution in liver fibrosis and liver injury, its expression analysis was performed by qRT-PCR. Our results indicated a significant up-regulation of TGF-β 2 (8) weeks after BM-Tx (figure 13). But later, 20 (26) weeks after BM-Tx, significant changes were not observed in comparison to sham controls.

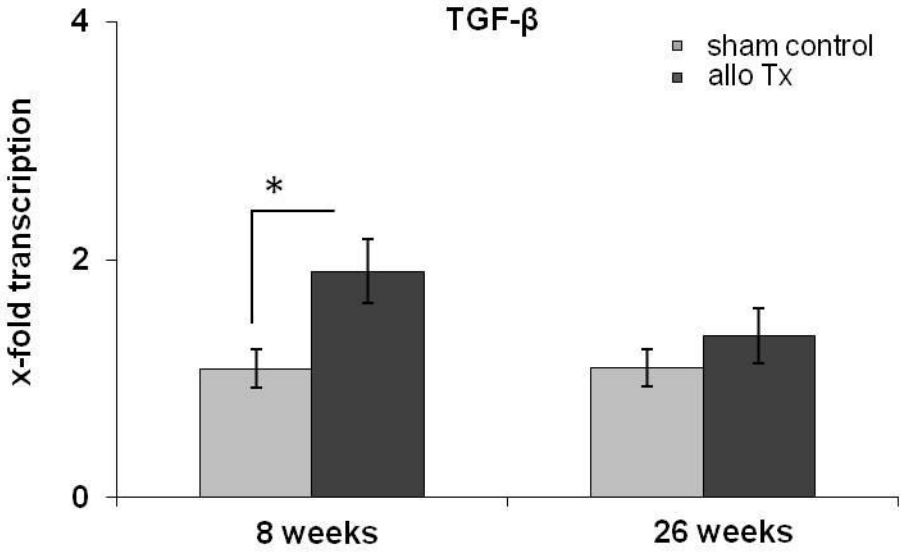

Figure 13: Transforming growth factor-β expression: Significantly increased expression (*p=0. 04) of TGF-β 2 (8) weeks after BM-Tx. whereas, in 20 (26) weeks the expression was not regulated when compared to sham control.

5.3 INFLAMMATION

5.3.1 Hepatic infiltration of inflammatory cells after BM-Tx:

Histopathological features of the liver after BM-Tx were investigated by HE stainings. 8 weeks after BM-Tx partial infiltration was observed whereas, after 26 weeks massive accumulation of infiltrated inflammatory cells appeared around periportal areas (figure 14B & 14D). These observations indicated an enhanced infiltration of inflammatory cells around periportal fields after BM-Tx compared to sham controls (8 w and 26 w).

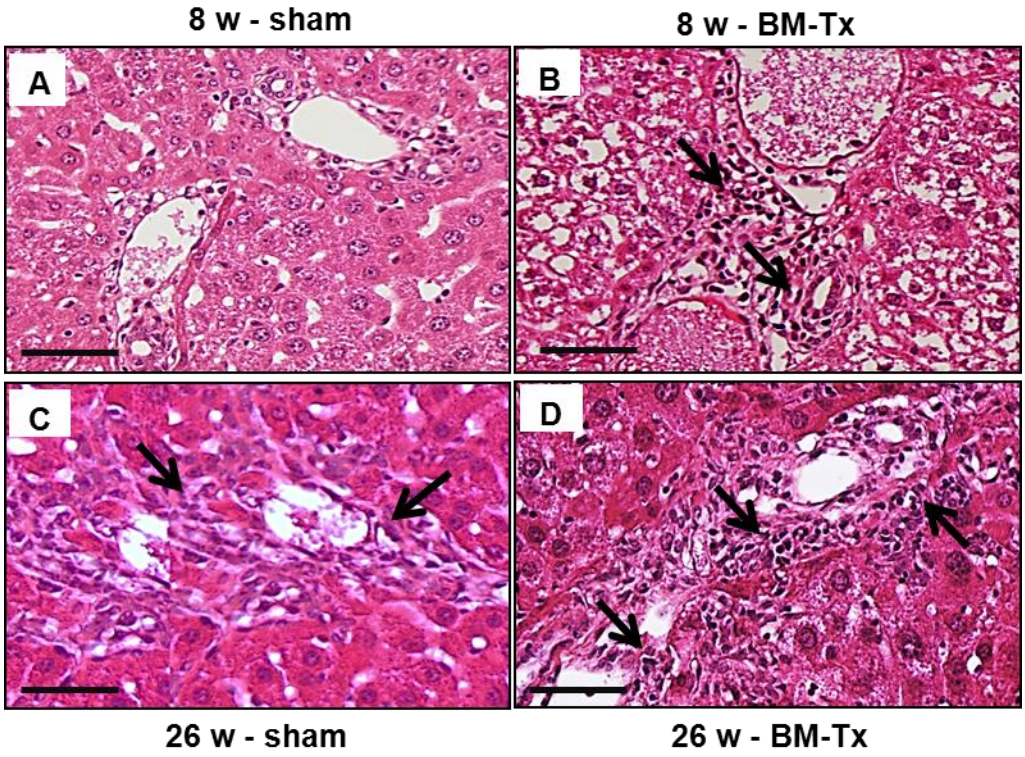

Figure 14: Infiltration of inflammatory cells around periportal fields H&E staining. The upper panel shows A) 8 weeks sham controls (untreated *Abcb4*$^{-/-}$ mice) B) 2 (8) weeks BM-Tx mice (CD117+ stem cells transplanted). The lower panel shows C) 26 weeks sham control (untreated *Abcb4*$^{-/-}$ mice) D) 20 (26) weeks BM-Tx mice (CD117+ stem cells transplanted). Clusters of infiltrating cell population around portal fields were stained in blue colour, which are indicated by black arrows. (Original magnification 20X 100µm)

5.3.2 Acute hepatic infiltration of inflammatory cells 2 weeks after BM-Tx:

In order to characterize the infiltrates of inflammatory cells, transcriptional levels of specific cellular surrogate markers of inflammation were assessed. Hepatic gene expression of myeloperoxidase (surrogate for neutrophils) was significantly enhanced at 2 (8) weeks & down regulated at 20 (26) weeks after BM-Tx. In contrast, a marker for macrophages F4/80 did not show any significant changes. CD45 (pan leucocyte surrogate marker) was increased significantly 2 weeks after BM-Tx (normalized to sham). Declined mRNA levels of all three surrogate inflammatory markers were observed in due course of 2 (8) to 20 (26) weeks of BM-Tx (figure 15).

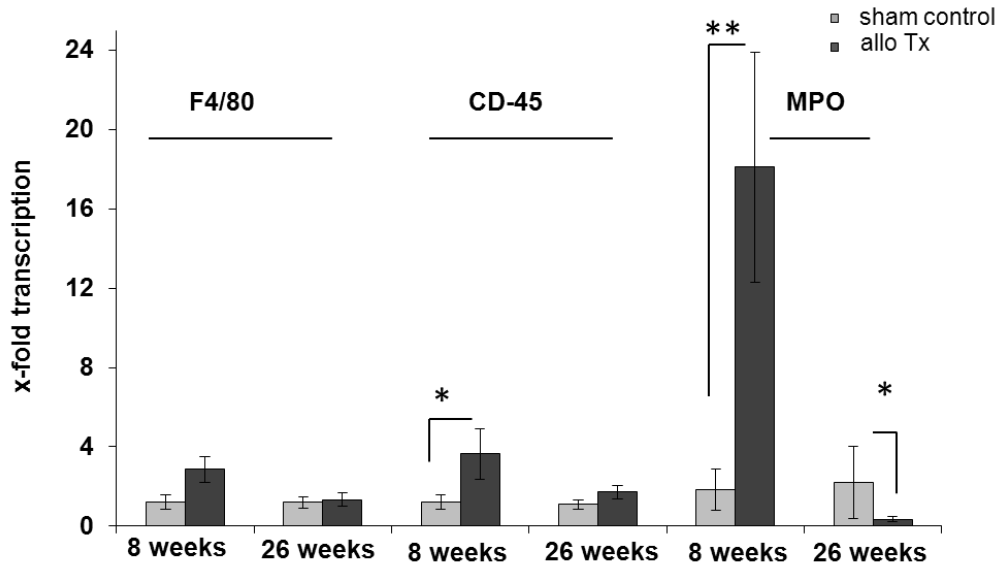

Figure 15: mRNA expression of inflammation relevant genes. This result depicts Pan leukocyte marker CD45 gene expression significantly elevated 2 (8) weeks after BM-Tx, (*p=0.02) neutrophil granulocyte marker myeloperoxidase (MPO) gene expression was significantly elevated at 2 (8) and down regulated at 20 (26) weeks after BM-Tx, (**p=0.002 and *p=0.03) compared to sham. All data were normalized to r18s (6-10 mice per group were analyzed independently). The mean SEM fold increase to sham is shown.

5.3.3 Th2 and Th1 response after CD117+ BM-Tx:

Th1 switch after bone marrow transplantation was analyzed by measuring the expression of IL-13, IFN-γ, IL-10 at transcription level by quantitative real time PCR. And the results unveiled that Th2 cytokine interleukin 13 (IL-13) and interleukin 10 (IL-10) were not altered at 2 weeks after BM-Tx. Interestingly, Th1 cytokine interferon gamma (IFN-γ) was significantly enhanced at 2 (8) and 20 (26) weeks after BM-Tx indicates a Th1 response after BM-Tx (figure 16).

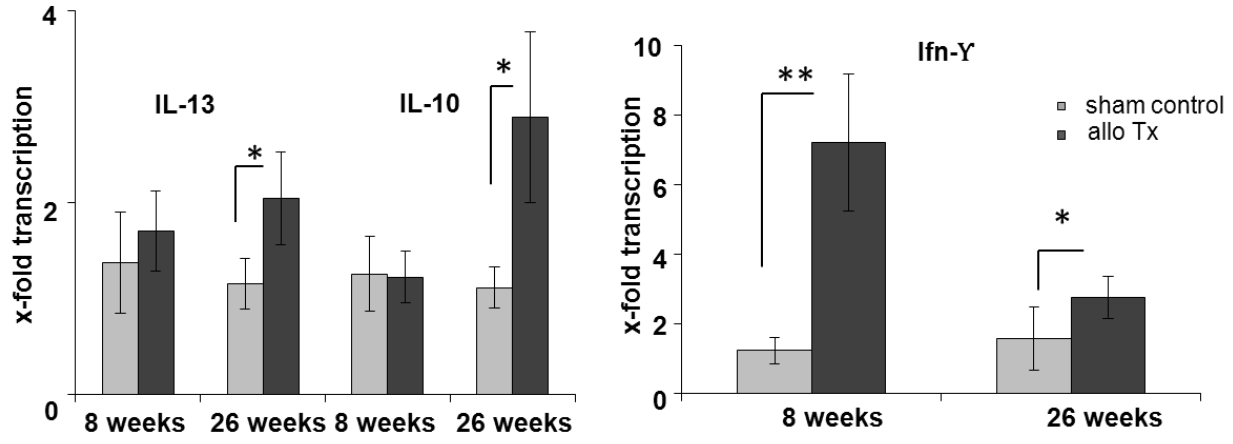

Figure 16: T-cell polarization influenced inflammation and fibrosis. The figure depicts mRNA expression of the Th2-associated interleukin 13 and 10 (IL -13 IL -10) significantly increased at 20 (26) weeks after BM-Tx (*p=0.05 and *p=0.03). Th1 cytokine IFN-γ was significantly enhanced at 2 (8) and 20 (26) weeks after BM-Tx (**p=0.001 and *p=0.02). All data were normalized to r18s. The mean SEM fold increase to sham is shown (6-10 mice per group were analyzed independently).

5.3.4 Prolonged expression of tumor necrosis factor (TNF-α) after BM-Tx:

In response to inflammation macrophages secrete TNF-α, which plays a major role in tissue inflammation. Therefore, the mRNA expression of TNF-α was measured. The results implicated a significant increase of TNF-α expression, both at 2 (8) and 20 (26) weeks after transplantation (figure 17).

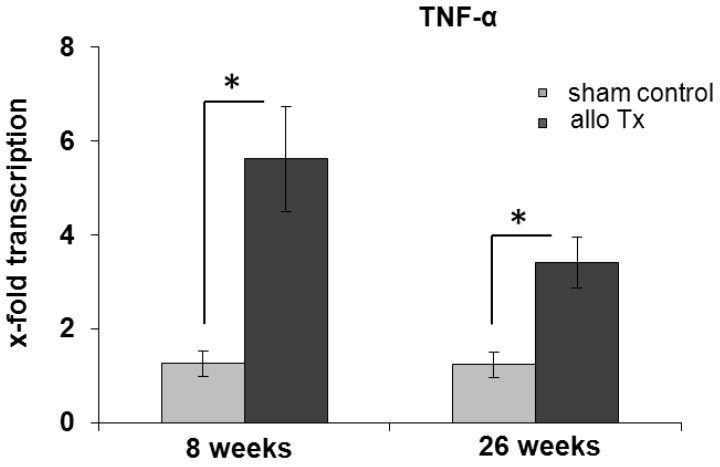

Figure 17: mRNA expression of TNF-α in tissue inflammation. This picture represents TNF-α expression, which was significantly elevated in both 2 (8) and 20 (26) weeks after BM-Tx, (*p=0.01) compared to sham control.

5.3.5 Donor derived dendritic cells (DCs):

Earlier studies indicated that the hepatic microenvironment programs hematopoietic progenitor differentiation into dendritic cells. Hence, we investigated the possibility of dendritic cell differentiation in our BM-Tx model by co-immunostaining. Our results depicted, that co-staining of dendritic cell marker CD11c and GFP+ stem cells did not occur (figure 18D). Taken together these results indicate that transplanted CD117+ progenitor stem cells did not differentiate into dendritic cells.

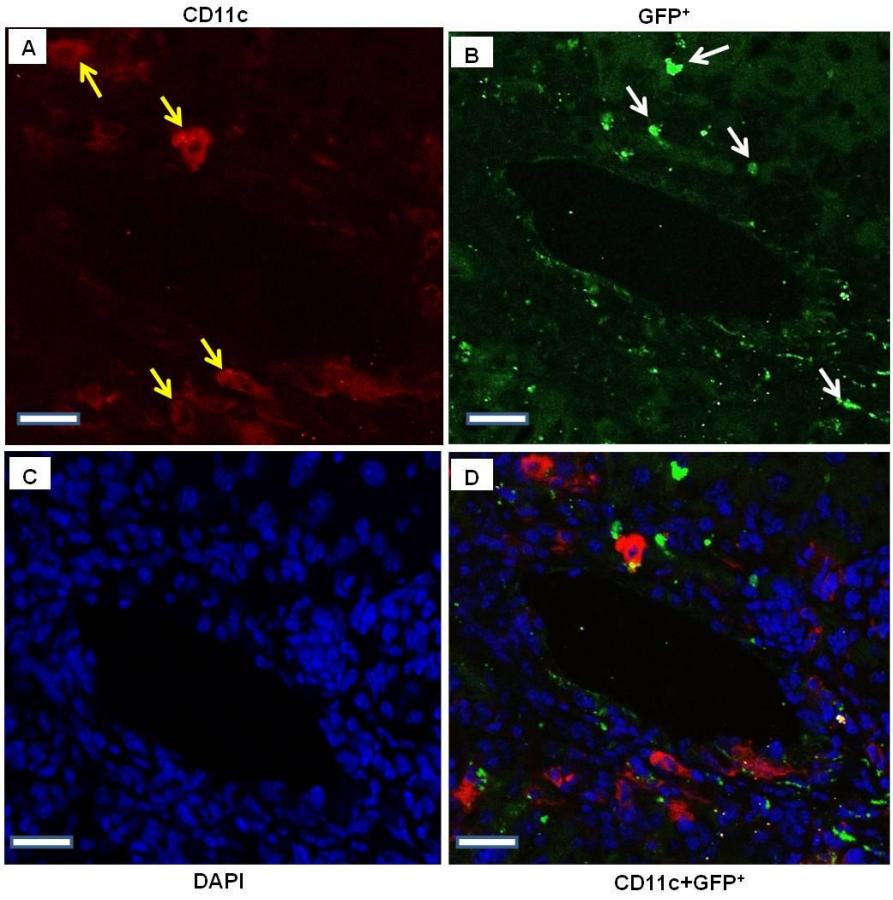

Figure 18: **Co-immunostaining of GFP+ and DCs**: The above picture shows A) CD11c (DCs marker) which was highlighted in dark red colour represented by yellow arrows; B) GFP+ cells were shown in green colour indicated by white arrows; C) DAPI staining for nuclei D) Overlay picture of GFP+ and CD11c. Scale bar-50µm.

5.3.6 Involvement of dendritic cells in tissue inflammation:

Dendritic cells (DC) are antigen presenting cells with an emerging role in hepatic inflammation inducing fibrosis. To check the involvement of DC's in inflammation of *Abcb4*$^{-/-}$ mice liver after 2(8) and 20 (26) weeks of BM-Tx, we performed Immunohistochemistry for CD11c, which is a DC marker. The obtained results indicated an increased amount of DCs observed around periportal areas after BM-Tx when compared to sham control in both age groups (figure 19a & 19b).

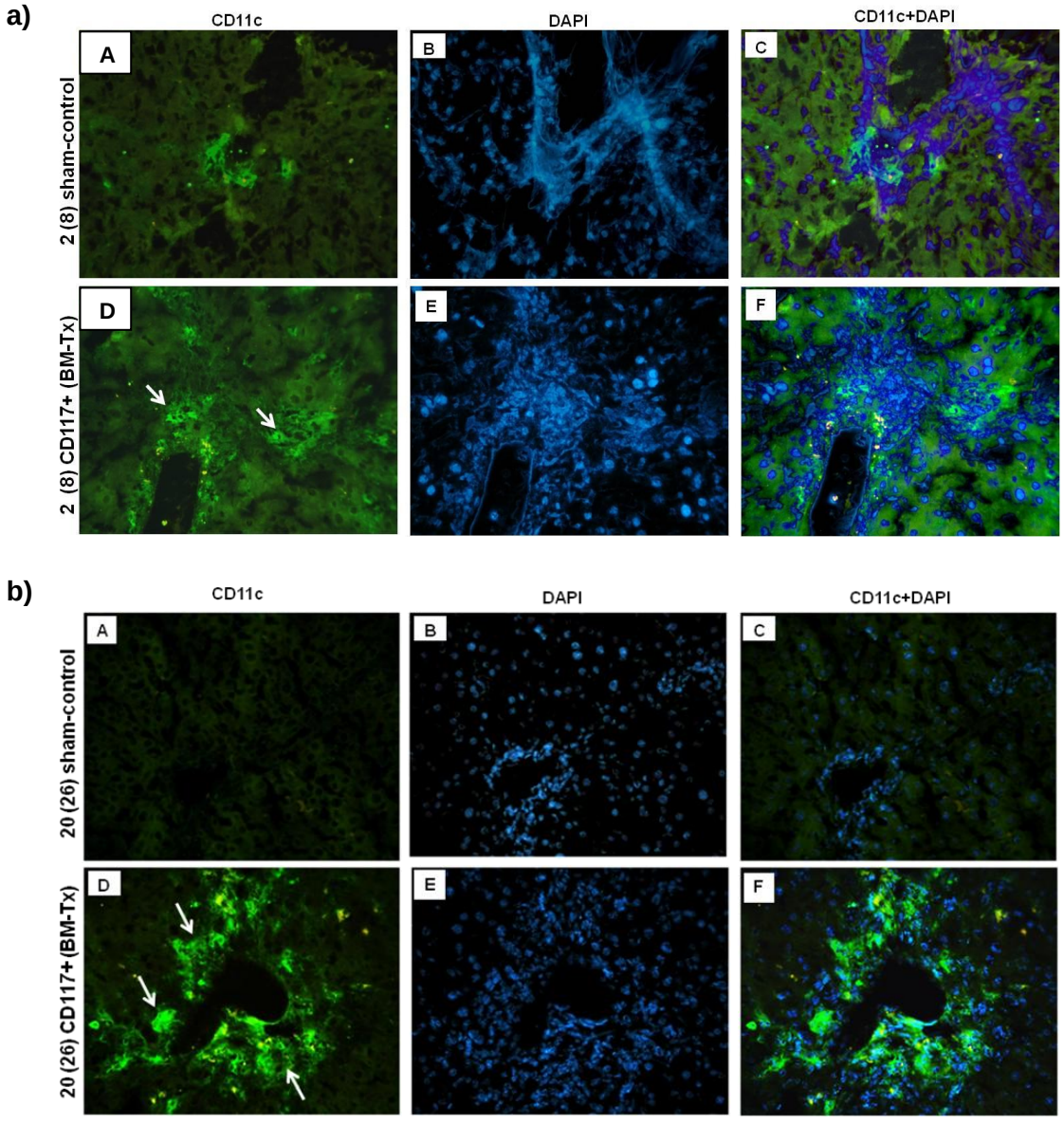

Figure 19a: DC infiltration in 2 (8) weeks after BM-TX: A) DCs (CD11c marker) in sham control B) & E) DAPI staining for nuclei C) & F) overlay of CD11c and DAPI; D) DCs in BM-Tx mice were in green colour represented by white arrows. Original magnification 40x.**Figure 19b: DC infiltration in 20 (26) weeks after BM-TX**: A) DCs (CD11c marker) in sham control B) & E) DAPI staining for nuclei C) & F) overlay of CD11c and DAPI; E) DCs in BM-Tx mice were in green colour represented by white arrows Original magnification 40 x.

5.3.7 Infiltration of inflammatory cytotoxic T (CD8+) cells:

T-cells are another important cell population mainly involved in inflammatory stimulation by profibrotic cytokines (1). Hence, we performed co-immunostaining of cytotoxic T-cells (CD8+) with T-cell receptor ($CD3^{+}$). Co-immunostaining results displayed more number of CD8+ cells around periportal areas after BM-Tx at both ages (figure 20a &20b). Additionally, with the progression of age following BM-Tx increased amounts of CD8+ staining were observed (figure 20b)

a)

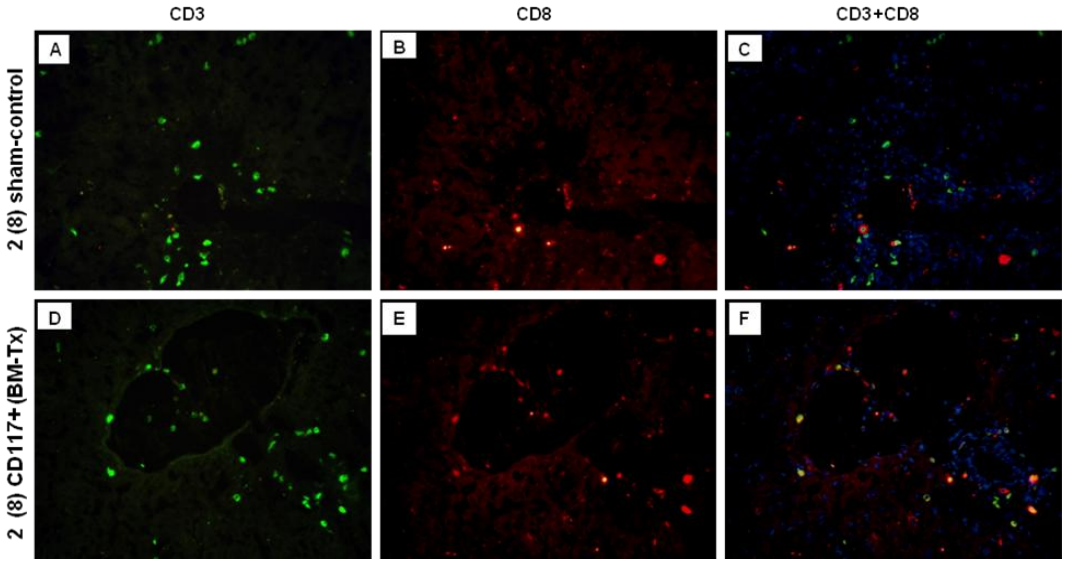

b)

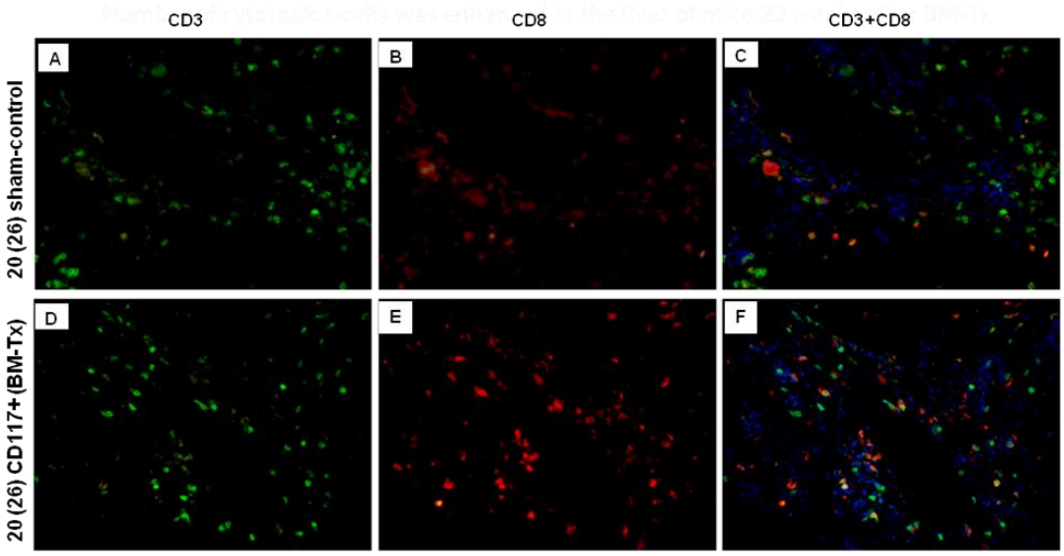

Figure 20a: CD8^{+} infiltration in 2 (8) weeks after BM-Tx: A) & D) CD3+ (T-cell receptor/TCR) in green colour (sham control & BM-Tx) B) & E) CD8+ (cytotoxic cell marker) cells in red colour (sham control & BM-Tx) C) & F) overlay of CD8+ and CD3+ in sham control and BM-Tx; Nuclei were stained with DAPI. Original magnification 40 x. **Figure 20b: CD8^{+} infiltration in 20 (26) weeks after BM-TX**: A) & D) CD3+ (T-cell receptor/TCR) in green colour (sham control and BM-Tx). B) & E) CD8+ (cytotoxic cell marker) cells in red colour (sham control & BM-TX). C) & F) overlay of CD8+ and CD3+ in sham control and BM-Tx; Nuclei were stained with DAPI. Original magnification 40 x.

5.4 Bile acid transporters in *Abcb4*$^{-/-}$ mice

5.4.1 Bile acid (BA) concentrations in serum of *Abcb4*$^{-/-}$ mice:

The toxic bile is considered to trigger the cascade of pathogenic events involved in liver damage of *Abcb4*$^{-/-}$ mice. Hence we measured concentrations of total bile acids (TBA) in serum of 8 w and 26 w old *Abcb4*$^{-/-}$ mice in comparison to wild (wt) mice. Dramatic differences were observed between wt and mutant mice such as significant elevation of total BA concentrations in both 8 w (6.88 µmol/l) and 26 w (40.33 µmol/l) mutant mice compared to wt (concentration below detection level) type mice (figure 21).

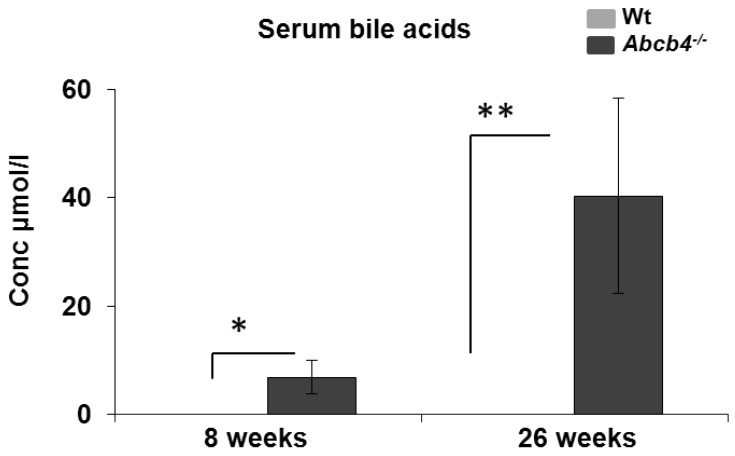

Figure 21: Bile acid concentrations in serum of *Abcb4*$^{-/-}$-mice were raised in comparison to wild type mice. Bile acid concentrations were significantly enhanced in both 8 w (*p=0.02) and 26 w (**p=0.001) compared to wt mice, where BA concentrations were below detection levels. Dark gray bars represent *Abcb4*$^{-/-}$-mice. All data are expressed as mean ± SEM for n=10 mice in each group.

5.4.2 Expression analysis of basolateral bile acid transporter Na^+ - taurocholate cotransporting polypeptide (Ntcp) in *Abcb4*$^{-/-}$ mice:

Na^+ - taurocholate cotransporting polypeptide (Ntcp) is the major BA uptake transporter in hepatobiliary system. Analysis of Ntcp mRNA transcript levels showed significant down regulation of in both 8 (2.4 fold) and 26 weeks (3.5 fold) of *Abcb4*$^{-/-}$ mice compared to wild type (figure 22A). Whereas Ntcp protein levels were unaltered at the age of 8 weeks and but significantly down regulated at the age of 26 weeks in comparison to wild type Abcb4 mice (figure 22B). Immunohistochemistry revealed lowered expression of Ntcp membrane protein both in 8 and 26 weeks *Abcb4*$^{-/-}$ mice (figure 22C,D,E&F).

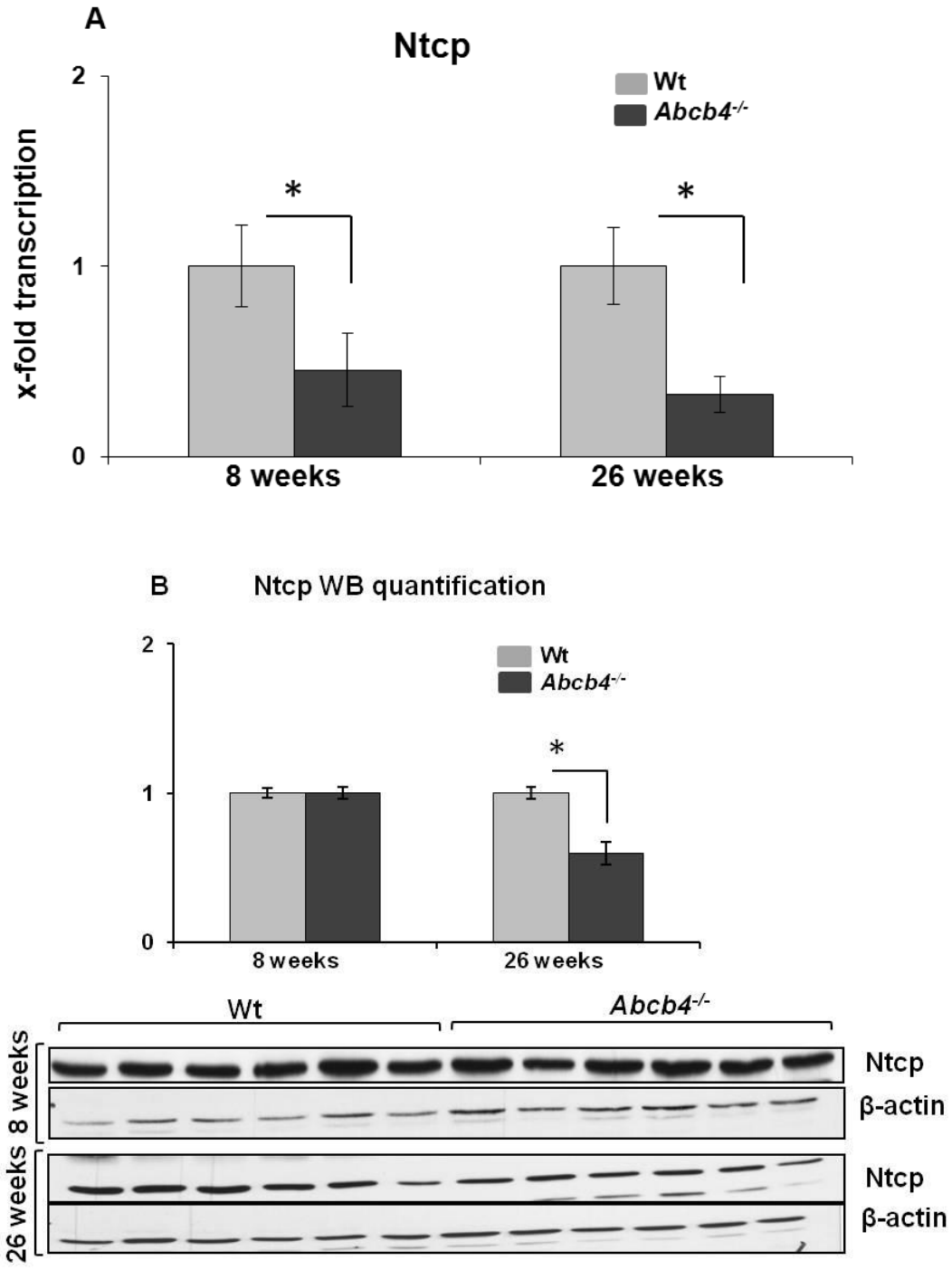
A
Ntcp
Wt
Abcb4-/-
x-fold transcription
2
1
0
*
*
8 weeks
26 weeks
B
Ntcp WB quantification
Wt
Abcb4-/-
2
1
0
*
8 weeks
26 weeks
Wt
Abcb4-/-
8 weeks
26 weeks
Ntcp
β-actin
Ntcp
β-actin

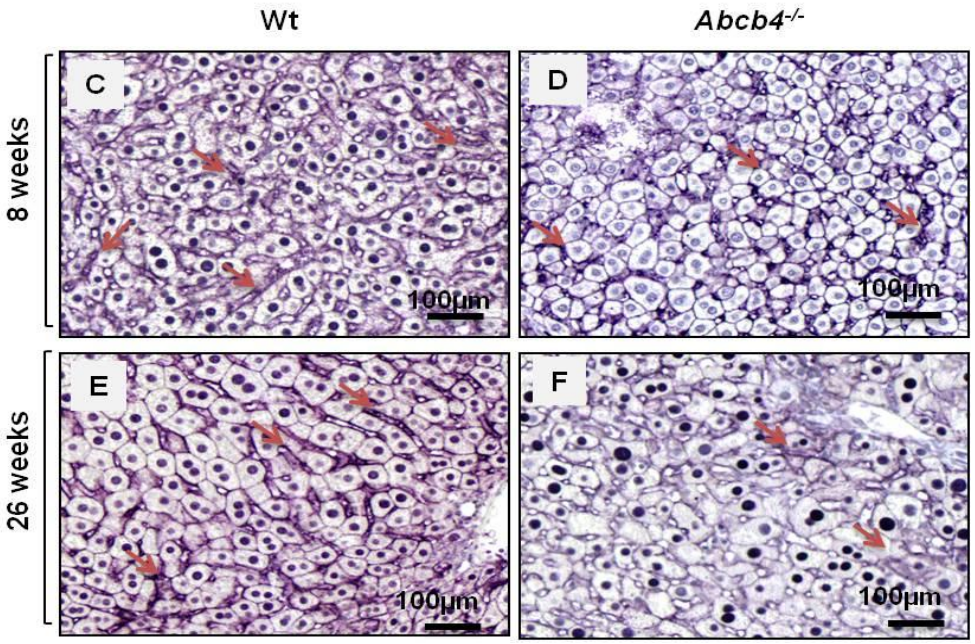

Figure 22: Reduced NTCP expression in *Abcb4*$^{-/-}$-mice: A) This picture showing significant down-regulation of Ntcp gene expression in *Abcb4*$^{-/-}$-mice at both the ages of 8 and 26 weeks (*p= 0.006) and (*p=0.009) where n = 5-10. Dark gray bars represent the wild type mice, and black bars represent *Abcb4*$^{-/-}$ mice. All the data were normalized to r18s. B) Western blot analysis of Ntcp in wt and mutant mice. The expression of Ntcp was semi-quantified by band intensity-analysis at 8 and 26 weeks. Where n = 5-10 animals per group. Dark gray bars represent the wild type mice, and black bars represent *Abcb4*$^{-/-}$ mice. C, D, E & F) Immunohistochemical analysis of Ntcp expression of liver sections of 8 and 26 weeks old wilde type and *Abcb4*$^{-/-}$-mice. Red arrows depict expression of membrane protein Ntcp (Original magnification 20 x, bars 100 µm).

5.4.3 Expression analysis of basolateral bile acid transporter organic anion transporter polypeptide Oatp1a1 (slco 1a1) in *Abcb4*$^{-/-}$ mice:

Another important basolateral bile acid transporter is organic anion transporter Oatp1a1 (slco 1a1). The uptake analysis was assessed by qRT-PCR and the results showed significantly down-regulated mRNA expression (figure 23A). While protein expression of Oatp 1a1 was not detectable in both, 8 and 26 w *Abcb4*$^{-/-}$ mice, compared to wild type (figure 23B). Histological analysis, demonstrated an elevated expression of Oatp 1 a1 membrane protein in wild type compared to *Abcb4*$^{-/-}$ mice (figure 23C,D,E&F).

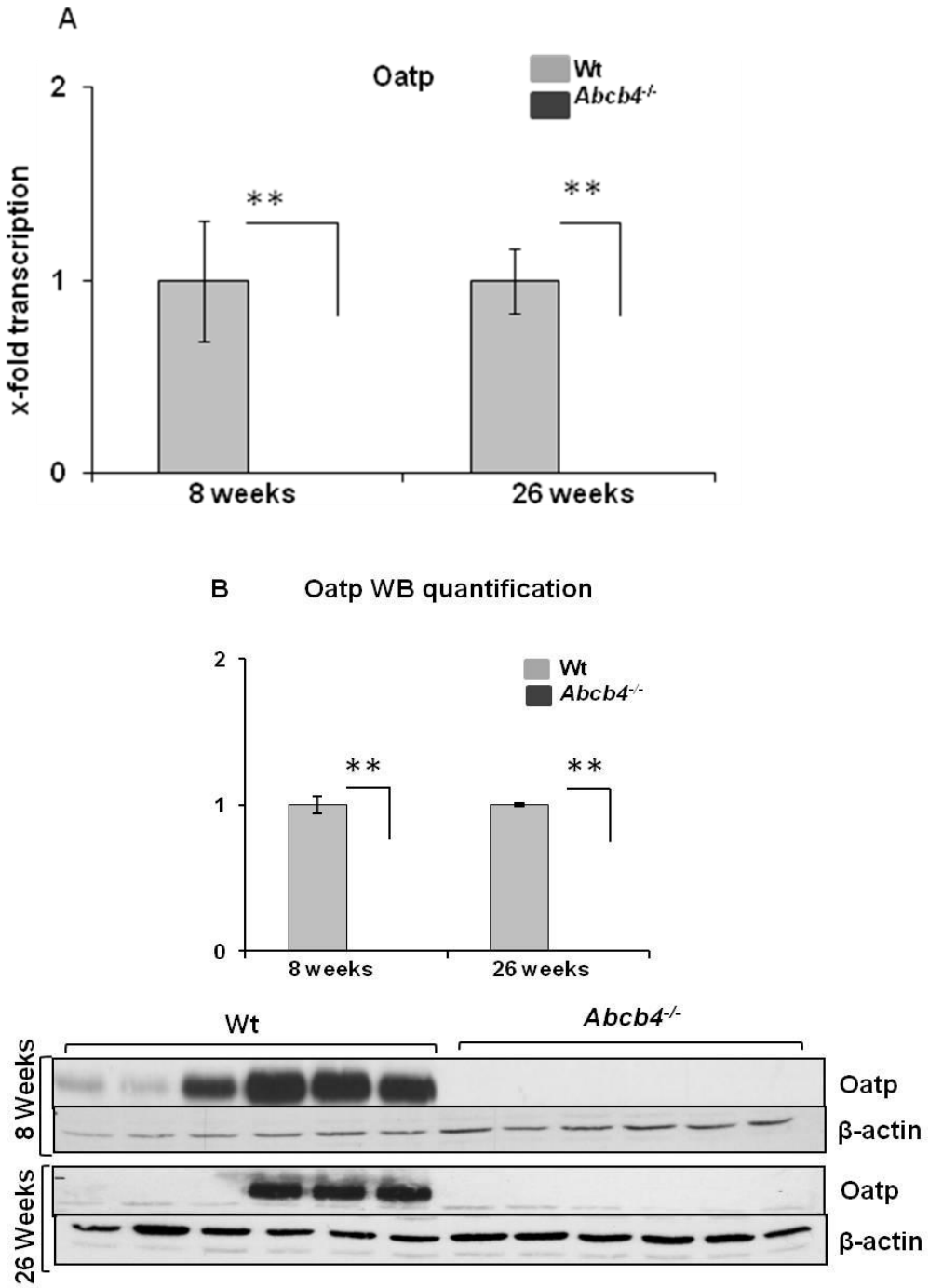
A
Oatp
Wt
Abcb4-/-
x-fold transcription
2
1
0
**
**
8 weeks
26 weeks
B
Oatp WB quantification
Wt
Abcb4-/-
2
1
0
**
**
8 weeks
26 weeks
Wt
Abcb4-/-
8 Weeks
Oatp
β-actin
26 Weeks
Oatp
β-actin

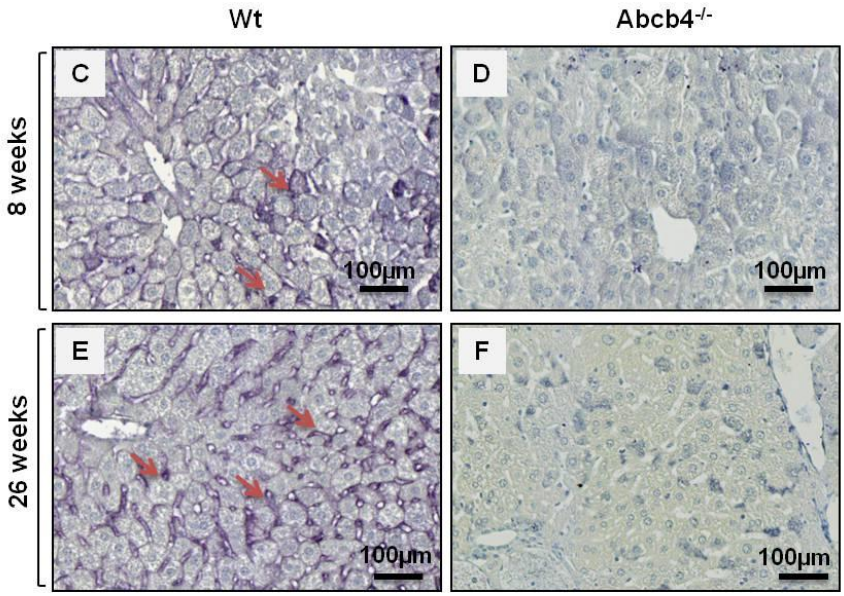

Figure 23: Complete loss of Oatp expression in *Abcb4*$^{-/-}$-mice. A) The hepatic Oatp1a1 mRNA expression at 8 weeks and 26 weeks significantly reduced in *Abcb4*$^{-/-}$ mice when compared to wild type wt mice. Dark gray bars represent the wild type mice, and black bars represent *Abcb4*$^{-/-}$ mice. All data are normalized to r18s, (**p<0.001). B) Western blot analysis of Oatp expression at 8 and 26 weeks. Dark gray bars represent the wild type mice, and black bars represent *Abcb4*$^{-/-}$-mice (**p=0.001). C, D, E, F) Immunohistochemical analysis of Oatp expression from liver sections of 8 and 26 weeks of wild type and *Abcb4*$^{-/-}$-mice. Red arrows depict expression of membrane protein Oatp. Original magnification 20x, bar=100 µm. Where n = 5-10 animals per group.

5.4.4 mRNA expression analysis of bile salt export pump (Bsep):

Bile salt export pump (Bsep; ATP-binding cassette subfamily B, member 11) functions as the major bile salt export transporter, translocating bile salts across the canalicular membranes into the bile. In order to investigate the bile acid excretion we analyzed mRNA expression of Bsep and the results revealed the significant down regulation of Bsep expression at 8 weeks (2 fold) and gradually increased by 26 weeks (0.35 fold) in *Abcb4*$^{-/-}$ mice compared to wild type mice (figure 24).

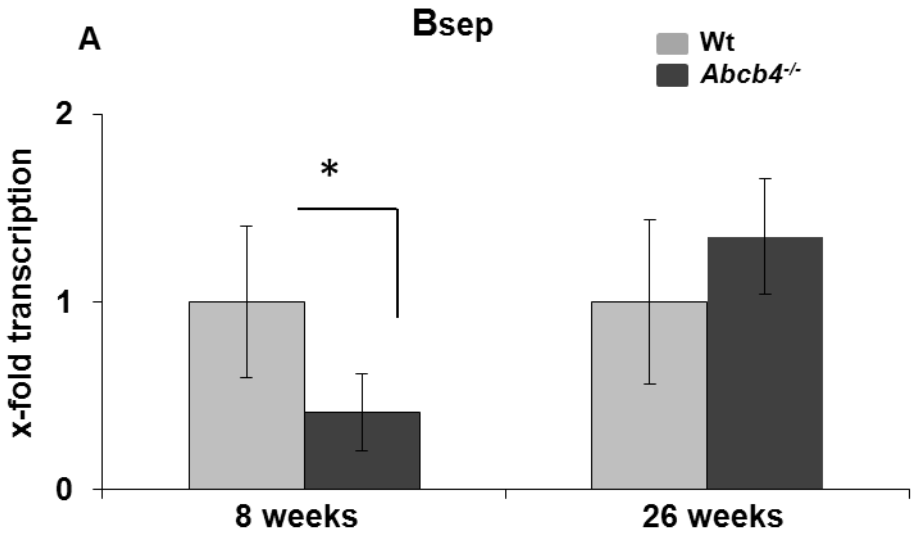

Figure 24: Canalicular membrane transporter expression: A) Hepatic mRNA expression of bile salt export pump (Bsep) in 8 (*p=0.019) weeks and 26 weeks mice of wild type and *Abcb4*$^{-/-}$ mice which was analyzed by qRT-PCR. Dark gray bars represent the wild type mice, and black bars represent *Abcb4*$^{-/-}$ mice. All data are normalized to r18s.

5.4.5 Transcript levels of alternative basolateral transporters:

mRNA expression of alternative bile acid efflux transporters such as, organic solute transporter beta (Ost-b), multidrug resistance associated protein 3 (Mrp3/Abcc3) and 4 (Mrp4/Abcc4) were measured by qRT-PCR. Transcript levels of Abcc3 expression was significantly down-regulated (2.3 fold) in *Abcb4*$^{-/-}$ compared to wild type at the age of 8 w (figure 25B). Similarly Abcc4 mRNA expression (figure 25C) was down-regulated in 26 w (3 fold) and Ost-b was reduced in 8 w (2.4 fold) and increased after 26 w in *Abcb4*$^{-/-}$ mice when compared to wild type mice (figure 25A).

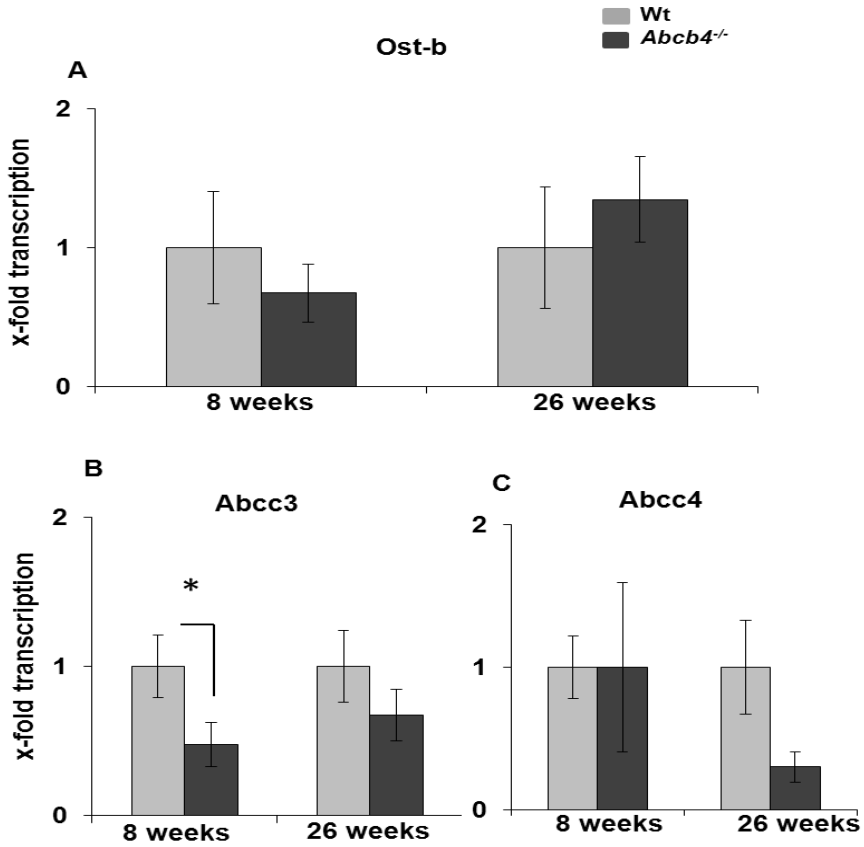

Figure 25: Alternative BA transporters are less expressed in young *Abcb4*$^{-/-}$-mice. A) Hepatic mRNA expression of organic solute transporter beta (Ost-b) in 8 weeks and 26 weeks wild type and *Abcb4* $^{-/-}$ mice, which was analyzed by qRT-PCR. B) & C) mRNA expression of multi drug resistance protein 3 and 4 (Abcc3 & Abcc4). The expression of the gene of interest was normalized against r18S RNA. Dark gray bars represent the wild type *Abcb4* mice, and black bars represent *Abcb4*$^{-/-}$ mice. Where n = 5-10 per group. All data are represented as mean ± SEM. Significance ($p < 0.05$) is indicated by *.

5.4.6 Unaltered gene expression of key bile acid transporter regulators:

To investigate the mechanism of *Abcb4*$^{-/-}$ mice induced suppression of Cyp7a1, the mRNA expression of farnesoid X receptor (FXR) and small heterodimer partner (SHP), which have been shown to regulate Cyp7a1, was quantified in livers of both wt and *Abcb4*$^{-/-}$ mice following BM-Tx. FXR gene regulation was unaltered in both 8 and 26 weeks (figure 26A). Shp mRNA level was significantly lower in 8 weeks (2 fold) and no regulation at 26 weeks was observed in *Abcb4*$^{-/-}$ mice compared to wt type (figure 26B). Whereas, the mRNA expression of Cyp7a1 was significantly upregulated (4 fold) at the age of 8 weeks and was unaltered at 26 weeks in *Abcb4*$^{-/-}$ compared to sham controls (figure 26C).

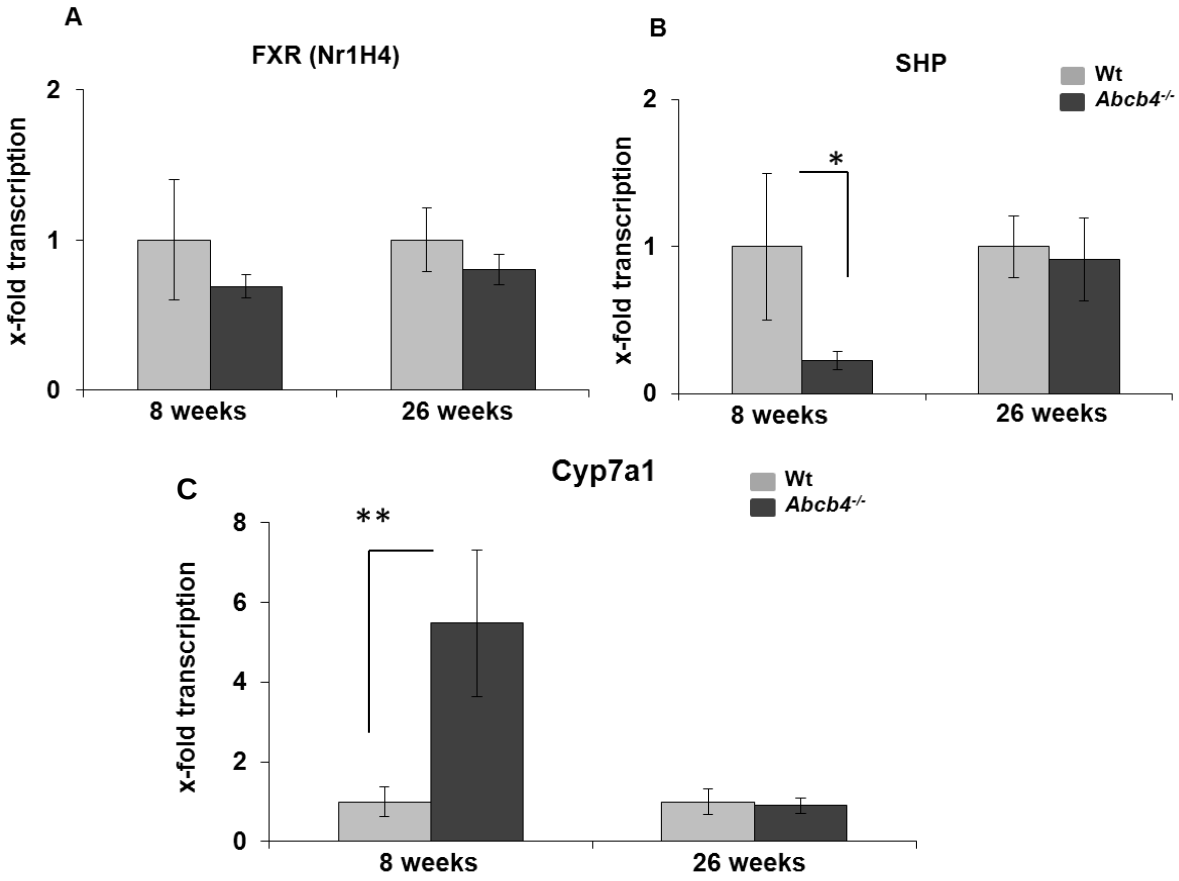

Figure 26: Key regulators of BA transporters on transcriptional level: Gene expression of bile acid (BA) regulation nuclear receptor genes farnesoid X receptor (FXR or Nr1H4), SHP were quantified using total hepatic RNA from wild type and *Abcb4*$^{-/-}$ mice of 8 and 26 weeks age. A) and B) mRNA expression of FXR and SHP. Data were normalized to against r18S RNA and presented as mean ± SEM (*n* = 5 –10 & , *p=0.015). Dark gray bars represent the wild type *Abcb4* mice, and black bars represent *Abcb4*$^{-/-}$ mice. C) Cyp7a1 gene expression is induced in young *Abcb4*$^{-/-}$-mice. The expression of the rate-limiting Cyp7a1 mRNA was significantly enhanced 2 weeks and no changes were observed 20weeks after BM-Tx in *Abcb4*$^{-/-}$ mice. Statistically significant differences (**p=0.001) compared to the control. Where n = 5-10 animals per group.

5.4.7 Transcription analysis of Hepatic nuclear factors (HNF-4α and HNF-1α):

HNF-4α gene expression was significantly down-regulated by 2.2 fold in 8 weeks and by 1.8 fold in 26 w old *Abcb4*$^{-/-}$ mice (figure 27A). Similarly, HNF-1α gene expression was significantly down-regulated 2-fold only in the 26 weeks old *Abcb4*$^{-/-}$ mice 20 weeks after BM-Tx (figure 27B). These results directly correlate with the down-regulation of Ntcp expression in the *Abcb4*$^{-/-}$ mice.

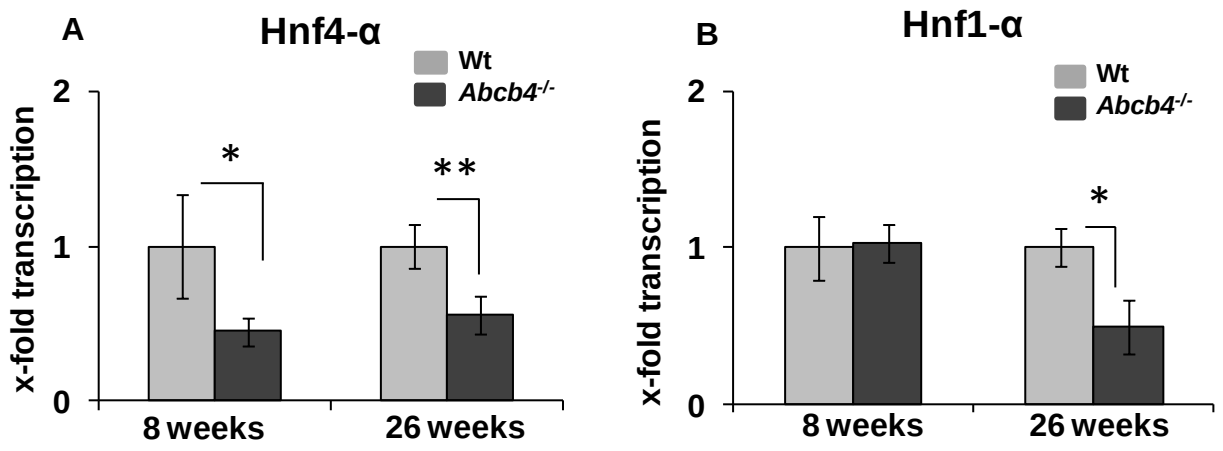

Figure 27: Gene expression of transcription factors Hnf-1α and Hnf-4α was reduced in *Abcb4*$^{-/-}$ mice. The expression of HNF-4α and HNF-1α was measured by quantitative real time PCR and normalized to 18 s RNA expression. Significant decrease of mRNA expression of HNF-4α at both 8 weeks and 26 weeks (*p=0.04 & **p=0.001) and down regulation of HNF-1α only at 26 weeks (*p=0.02) was shown. All data are expressed as mean ± SEM. Where n = 5 -10. Dark gray bars represent the wild type *Abcb4* mice, and black bars represent *Abcb4*$^{-/-}$ mice.

5.4.8 Elevated miR-199a-5P expression in *Abcb4*$^{-/-}$:

Bile acid induced hepatocellular stress was shown to be down-regulated by microRNA-199a-5p (100). Hence, we investigated the expression levels of miR-199a-5P in mice. Interestingly, the expression of miR-199a-5P was significantly up-regulated 6 fold in 8 weeks and 7 fold in 26 weeks old *Abcb4*$^{-/-}$. Hence, these results implicating that the expression of stress regulatory markers such as miR-199-5p might play a protective role in *Abcb4*$^{-/-}$ mice following BM-Tx induced hepatocellular damage (figure 28).

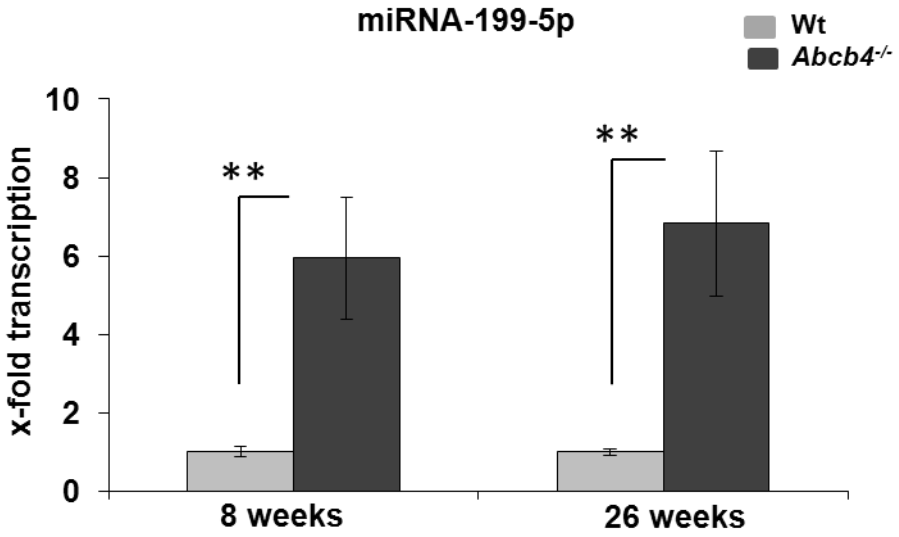

Figure 28: Hepatic miRNA-199-5p expression was analyzed by qRT-PCR and normalized to SnoRNA 202 (as a control). Dark gray bars represent the wild type mice, and black bars represent *Abcb4*$^{-/-}$ mice. All data are expressed as mean ± SE for n = 4 mice in each group. Statistically significant difference between the wild type and mutant *Abcb4*$^{-/-}$ mice was observed, **p< 0.002.

6. Discussion:

Abcb4$^{-/-}$ mice represent a well-characterized model for sclerosing cholangitis and represent several key morphological aspects of PSC (20). Since the etiology of sclerosing cholangitis remains unclear, this model represents an attractive approach to investigate potential underlying disease mechanisms. A better understanding of the basic pathogenic mechanisms of chronic immune mediated cholangiopathy is essential for developing new diagnostic, prognostic as well as therapeutic tools for these disorders. Several rodent models for chronic immune-mediated cholangiopathies such as PSC are available. Unfortunately till date, no animal model exhibits all features of PSC (102, 103). Models which are induced by bacterial cell components or colitis fill the gap of the association between IBD and cholangiopathies (101). Drugs or xenobiotics induced bile duct injury, via 3,5-diethoxycarbonyl-1,4-dihydrocollidine or litocholic acid, lead to biliary fibrosis or even cirrhosis through a direct toxic or immune mediated injury (101).

6.1 What is already known about this subject

Due to the disrupted phospholipid excretion *Abcb4*$^{-/-}$-mice develop pericholangitis, periductal fibrosis with ductular proliferation and finally sclerosing cholangitis. This defect results in an increase of free non-micellar bile acids and more hydrophobic "toxic" bile (20, 102, 103). As a consequence, mice develop histological changes resembling human PSC. This makes it the most valuable knockout-model for this type of cholestatic disorders. Since there is an urgent need for new medical treatment strategies in human PSC, this model has often been chosen as an approach for testing novel therapeutics. Furthermore, existing therapeutics (*e.g.* norUDCA) need clinical studies and a determination of the safety and efficacy of norUDCA (the principle of side chain–shortened bile acids) in the treatment of human cholangiopathies. Stem cells serve as another attractive target for liver diseases with end stage fibrosis.

Interestingly, till date, literature reporting the therapeutic benefit of stem cell transplantation to cure chronic liver disease is still controversial since both a reduction in hepatic fibrosis and an increase in BM-derived fibrogenic cell pools has been shown by different experimental approaches (96, 106). In our previous studies, we have proven that bone marrow transplantation improves hepatic fibrosis in *Abcb4*$^{-/-}$ mice via Th1 response and matrix metalloproteinase activity (10, 15) The transiently enhanced inflammation after BM-Tx described in this study reflects the enhanced expression of IFN-γ, a major Th1 cytokine, while IL-13, representing the Th2 response, remained unaltered. In agreement with others, our observation suggests that BM-Tx

induces a switch towards the anti fibrotic Th1 response which is known to restrain the pro fibrotic Th2 activity (104). Furthermore, MMP-9 expression showed a strong positive correlation with IFN-γ but not with IL -13, thereby strengthening the hypothesis that the BM-Tx-induced Th1 response was responsible for the enhanced proteolytic activity and thus for the long-term amelioration of hepatic fibrosis. Thus, the Th1 response upon BM-Tx is leading to an increased expression of anti-fibrotic IFN-γ. Prolonged MMP-9 activity from cellular infiltrates (mainly neutrophils) occured within the regions of hepatic fibrosis. This enhanced MMP activity may therefore be responsible for the long-term amelioration of hepatic fibrosis (15).

6.2 Current study findings

With the aim of further expanding the therapeutic application of specific bone marrow derived stem cells (CD117+), we evaluated whether transplantation of a specific bone marrow derived stem cell fraction CD117+ (c-Kit) might be able to regenerate healthy hepatocytes, which carries *Abcb4 genes* to regulate phospholipids transportation normally, which in turn improves the liver fibrosis in *Abcb4*$^{-/-}$ mice. CD117+ (c-Kit) is an important cell surface marker to identify hematopoietic stem cell from bone marrow. Donor derived hematopoietic stem cell are able to differentiate into hepatocytes by means of cell fusion with recipient mouse (*Fah*$^{-/-}$) hepatocytes (38, 39). Our previous results provide that whole BM-Tx is capable of improving hepatic fibrosis and inflammation on long term (*i.e.* after 20 (26) weeks). In the current study, we focused on cell fusion between the transplanted bone marrow cells with existing host hepatocytes of recipient mice (39).

The hydroxyproline content was significantly higher in 2 weeks after BM-Tx mice (Figure 10). Simultaneously sirius red staining reveals enhanced collagen fibrils over a period of time (*i.e* 20 (26) weeks after BM-Tx).

6.3 cytokines in fibrotic and inflammatory stimuli

It was well known that TGF-β stimulates the production of tissue inhibitors of metalloproteases (TIMP's) and plays a prominent role in progression of liver fibrosis through multiple molecular mechanisms (105). Transcriptinal lavels of TGF-β is significantly enhanced only after 2 (8) weeks of transplantation indicated the profibrogenic activity. But 20 (26) weeks after BM-Tx no significant changes were observed compared to sham control. Over recent years, several studies have emphasized the crucial role of hepatic infiltration of neutrophils and macrophages following hepatocyte transplantation, which is driven by cytokines and chemokines (106). The

acute infiltration of inflammatory cells such as macrophages, neutrophils and leukocyte populations were found by hepatic gene expression at transcriptional level in *Abcb4*$^{-/-}$ mice, hints the stimulation of profibrotic factors. As inflammation with leukocytes and cytokines release are known as triggers of hepatic fibrosis (107). Therefore, acute infiltration of inflammatory cells producing pro-fibrotic factors could lead to development of stronger fibrosis in the liver of transplanted *Abcb4*$^{-/-}$mice.

On the other hand, It has been shown that TNF-α plays a major role in tissue inflammation, extra cellular matrix remodelling and liver fibrosis (108, 109). Significantly increased TNF-α expression (figure 17) might be one of the major causes of infiltration of cells after BM-Tx (CD117+). Subsequently hematoxylin and eosin (HE) staining (figure 14) also showed intense accumulation of inflammatory cells around periportal fields in later stages (after 20 (26) weeks) compared to sham control. It has been discribed that the activation of neutrophils and macrophages is an initial response to TNF-α secretion after hepatocyte transplantation (106). The release of TNF-α by macrophages might have been also stimulated by neutrophils and may be capable of inducing the expression of chemokines by parenchymal cells (110). In this way, increased hepatic TNF-α expression could induce enhanced in liver inflammation following cell transplantation.

T- cell polarization known to play key role in liver fibrosis (111) and Th1 or Th2 polarization depends upon the host response to a infection or a injury (112). Earlier studies demonstrated that IL-4 and IL-13 can progress fibrocyte differentiation towards a fibrogenic phenotype (113). It has also shown that, the IL-13 is a dominant cytokine of fibrosis (114) and also large amounts IL-10 production leads to liver fibrosis (115). The mRNA expression of Th2 cytokines (IL-10 and IL-13) were significantly enhanced at 20(26) weeks (figure 16) indicating stronger fibrosis after transplantation. On the other hand several studies indicated the anti-fibrotic activity of Th1 cytokine (IFN-γ) (15, 111). Anti fibrotic acivity of Th1 (figure 16) was declined with ongoing age which correlates with Th2 cytokine response. Thus, it seems to be Th1 fibrolytic action might restrained by the significantly enhanced (figure 16) Th2 profibrotic cytokines (IL-10 and IL-13).

6.4 Matrix metalloproteinase

MMPs and TIMPs play a central role in matrix homeostasis and remodelling processes during hepatic fibrogenesis and fibrolysis. MMP-9 was expressed by CD45+ leukocytes, myeloperoxidase, neutrophil granulocytes and CD34+ fibrocytes. Apart from these cells, stellate

cells and portal fibroblasts have been described as a source of MMP-9 secretion (15). Higashiyama and co-workers observed the expression of MMP-9 and MMP-13 by BM-derived cells during fibrolysis. Sakaida et al. demonstrated MMP-9 expression by GFP+ BM derived donor cells after BM-Tx in carbon tetrachloride-induced liver fibrosis. From our observervation prolonged MMP-9 activity (figure 12) couldn't help any anti fibrotic effect. Hence, increased MMP-9 activity is not enough to resolve the fibrosis in CD117+ BM-Tx treated *Abcb4*$^{-/-}$ mice.

6.5 Dendritic and cytotoxic T-cell infiltration

As well Dendritic cells (monocyte subsets) are believed to be play a crucial role in hepatic inflammation and fibrosis (116). Based on these findings, we wondered whether grafted cells might differentiate into DCs´(dendritic cells). Since it has been shown that unique hepatic microenvironment programs Lin- CD117+ hematopoietic progenitor differentiation into regulatory DCs. These DCs are responsible for maintaining liver tolerance (117). Hence, we performed co-immunostaining of grafted (GFP+) cells and host hepatocyte. The results (figure 18) proved that our speculation was wrong, but we have observed a higher amount of DCs around the portal areas. While it is known that DCs arise either from $CD34^+$ bone marrow progenitor cells or $CD14^+$ monocytes (118). Whereas, $CD34^+$ cells were shown to be derived from bone marrow in *Abcb4*$^{-/-}$ mice (10). However, our co-immunostaining results indicate that observed DC's are not from GFP+ donar derived. The fibrotic dendritic cells have a marked capacity to induce hepatic stellate cells, NK cells and T cells to mediate inflammation, proliferation and production of potent immune responses. Importantly, these proinflammatory and immunogenic effects of fibrotic dendritic cells were contingent on their production of TNF-α (119). However, in *Abcb4*$^{-/-}$ mice DC's are not donar derived but with unknown molecular mechanisms DC's might involving in liver fibrosis.

After dendritic cells, we focused on hepatic T-cell infiltration. Most of the infiltrated cells were identified as cytotoxic (CD8) T-cells. Because, CD4/CD8 rich infiltration results in pronounced periductal inflammation. This inflammation results in enhanced kuffer cells (KCs) with induced intrahepatic production of proinflammatory and profibrogenic cytokines (e.g TNF-α, IL-1β, TGFβ-1) in *Abcb4*$^{-/-}$ mice (1). Similar effect was observed by immunohistochemistry staining of CD8 cells in our *Abcb4*$^{-/-}$ model. Stainings confirmed that accumulation of inflammatory T-cells and susequent T-cell receptors were more with ongoing age (Figure 20). Thus, the enhaced periductular inflammation is due to storonger infiltration of cytotoxic T cells around periportal fields.

In continuation of this study, we have analysed the microarray data of chemokine and cytokine receptors of inflammatory cell population. During this analysis our attention was attracted by bile acid transporter expression. Since bile acid toxicity is the major cause of sclerosing cholangitis characterized by biliary obliteration, inflammation of biliary tree and biliary cirrhosis (120)

6.6 Hepatobiliary transporters

The growing knowledge on the transcriptional regulation of hepatobiliary transport system is a key for understanding the pathophysiology and underlying molecular mechanisms of cholestasis (121). In the case of cholestasis-mediated injury, bile duct epithelial cells (BDECs) rather than hepatocytes are the primary target of damage, bile reflux being the major inducer of this type of injury (99). Therefore, in this study we used *Abcb4*$^{-/-}$ mice to investigate whether disruption of phospholipid transporter may cause transcriptional alterations at the basolateral and canalicular membrane transporters. For this reason we analyzed gene expression of BA-uptake transporters (Ntcp, Oatp), canalicular transporter (Bsep), alternative basolateral transporters (Ost-b, Abcc3/Mrp3, and Abcc4/Mrp4), bile acid synthetic enzyme (Cyp7a1), nuclear receptor (FXR), short heterodimer partner (SHP) and hepatic nuclear factor (HNF-4α, HNF-1α).

6.7 Enhanced serum BA concentration

Altered phosphatidylcholine homeostasis in the liver might lead to the accumulation of toxic bile acids in the blood and exaggerate the bile acid toxicity of the liver. From our observations, total bile acid concentrations in the serum were significantly increased at both 8 w and 26 w of age in the *Abcb4*$^{-/-}$ mice compared to wild type. Accumulation of bile acids in the serum was markedly enhanced with the disease progression in *Abcb4*$^{-/-}$ mice (figure 21). In line with this finding, 2 weeks old *Abcb4*$^{-/-}$ mice showed leaky tight junctions and concomitant regurgitation of bile acids and accumulation of bile acids in the serum (1).

6.8 Bile acid uptake at basolateral side of *Abcb4*$^{-/-}$ mice

The main hepatocellular bile acid uptake transporter is Na^+ taurocholate Co transporter (Ntcp), was shown to be down regulated in various cholestatic liver diseases and represents an important protective regulatory step to prevent further bile acid uptake by hepatocytes (123, 124). From our data, a significant down-regulation of the major hepatocellular uptake system for bile acids Ntcp in 26 w *Abcb4*$^{-/-}$ mice (figure 22) and serum BA concentrations raised in parallel, we hypothesize that hepatocellular BA uptake is reduced with progression of disease. Ntcp expression is controlled by a complex network of nuclear receptors (FXR, RXR) and hepatic

enriched transcription factors (55, 125) such as, bile acid depepromoterP induction has been shown to interfere with RXRα: RXRα activation of the *Ntcp* promotor, thus, reducing *Ntcp* gene expression (122). In addition, organic anion transporting polypeptide (Oatp a1) another bile acid up-take transporter has been shown to be down-regulated in BDL (bile duct ligated) rat model, suggesting that down-regulation of organic anion transporting polypeptide seems less pronounced than that of Na^+-dependent taurocholate co-transporting polypeptide.

Nevertheless, Oatp1a1 could contribute to a decreased uptake of potentially toxic bile acids or organic anions in this situation. Whereas our data showed that Oatp 1a1 expression (figure 23) was impaired completely in mutant *Abcb4*$^{-/-}$suggesting hepatic uptake of toxic BAs were hindered completely at Oatp1a1 system.

It is well known that *Abcb4*$^{-/}$ mice are not capable of excreting phospholipids into bile and spontaneously develop bile duct injury. Our data showed significant downregulation of Bsep (figure 24), which might be a result of spontaneous bile duct injury from potential toxic bile acid and in parallel significant up-regulation of Cyp7a1 a rate limiting enzyme in BA synthesis hints toxic BA accumulation in 8 w *Abcb4*$^{-/-}$ mice might alter the expression of Bsep. The tendency of enhanced Bsep expression supports an adaptive response, which was clearly demonstrated by the reduced Ntcp expression in 26 w *Abcb4*$^{-/-}$ mice. It is reported that Bsep expression during obstructive cholestasis is relatively well preserved compared with other membrane transporters and may lessen the extent of liver injury produced by bile acid retention, particularly when cholestasis is prolonged, thereby supporting our observation in 26 weeks old *Abcb4*$^{-/-}$ mice. In addition, induction of Bsep by bile acids via FXR seems to operate as an adaptive mechanism under these conditions by accumulating bile acids and promoting their own export into bile (123).

6.9 Alternative basolateral efflux transporters

Under normal physiological conditions alternative basolateral transporters (such as Mrp3/Abcc3, Mrp4/Abcc4, Ostα/β) are expressed at very low levels in hepatocytes (57). During obstructive cholestasis up-regulation of multi drug resistance protein 3(Mrp3) was observed in hepatocytes and cholangiocytes of rat liver (124). As we observed the tendency of Ost-b is higher in 26 w *Abcb4*$^{-/-}$ mice (figure 25) suggesting that Ost-b may play a role in the retrograde bile acid transport with increasing severity of disease. Much of our knowledge in cholestatic conditions, bile acid retention in the liver results in enhanced expression of Ostα/β at the sinusoidal membrane, where it is in position to facilitate extrusion of toxic bile acids and other sterols into

the circulation as part of the adaptive protective response to cholestatic liver injury (125, 126). Substrates for Abcc3 (MRP3/Mrp3) include sulfated and nonsulfated bile salts, bilirubin glucuronides, 17β-glucuronosyl estradiol, and leukotrienes (127-129). However, rat Mrp3 is markedly up-regulated in the liver following bile duct obstruction (124, 130). But the Abcc3 expression is found to be significantly decreased in 8w *Abcb4*$^{-/-}$ mice representing Mrp3 expression in hepatocytes, which vary between species (131, 132). Mennone *et al.* showed that serum bile acid concentrations are lower in Mrp4 knockout mice than in wt CBDL (common bile duct ligation) mice presumably owing to impaired secretion of bile acids over the basolateral hepatocyte membrane (133). However, we couldn´t find a significant change in Mrp4 expression.

6.10 Regulation role of Nucear receptor (FXR) and short hetero dimer partner (SHP)

The genes encoding for organic anion uptake, canalicular export and alternative basolateral export in liver are regulated by a complex interacting network of nuclear factors (HNF1,3,4) and nuclear receptors (FXR, SHP) (57). FXR plays a prominent role in the feedback repression of BA synthesis by reducing the expression of cholesterol 7α hydroxylase (CYP7A1) via SHP (65, 66). In our *Abcb4*$^{-/-}$ mice model, gene regulation of FXR was unaltered at both 8 and 26 weeks (figure 26A) compared to wt controls. However, SHP expression was significantly down-regulated (figure 26B) compared to wild type at the age of 8 weeks correlates with significant increase of Cyp7a1 expression (Figure 26C) in 8w *Abcb4*$^{-/-}$ mice, since *shp* is the target gene of FXR which is a key regulator in feedback mechanism of BA synthesis. It is well known that bile acids are natural ligands of farnesoid X receptor (FXR) (60), and that FXR induces the expression of short heterodimer partner (SHP) (65, 66). However, in vitro studies in primary rat hepatocytes have also demonstrated the possibility of c-JUN/AP-1 mediated activation of the SHP promoter via the JNK1 pathway, which in turn suppressed cholestrol 7α hydroxylase expression (122). In addition, activation of FXR in the liver can induce the expression of BSEP and MDR3/Mdr2 for the secretion of BAs and phosphatidylcholine, respectively, into the canalicular lumen (60-62). Loss of orphan nuclear receptor *shp* increases sensitivity to liver injury from obstructive cholestasis, which was induced by BDL (134).

6.11 Hepatic nuclear factors (HNF-4α and HNF-1α)

Bile acids have been shown to suppress HNF-4α transcription through SHP independent mechanisms (135, 136). These effects could explain reduction of HNF-1α and subsequent Ntcp expression despite low SHP levels. Our findings clearly demonstrated that transcriptional levels

of HNF-4α and HNF-1α expression (Figure 27) were significantly reduced in later stages (26-weeks), which successfully meet the SHP independent pathway in down-regulating the mRNA expression of Ntcp. Recently, an HNF4 binding site in the rat *Ntcp* promotor overlapping with the RXRα:RXRα response element has been identified, indicating that SHP may also repress rat *Ntcp* via reduced HNF4 activity (137, 138). Findings in HNF1$^{-/-}$ and conditional HNF4$^{-/-}$ mice with reduced Ntcp, Oatp1 (Oatp1a1) and Oatp2 (Oatp1a4) expression (139, 140), indicate a role of HNF1 and HNF4 as central positive regulators of these basolateral bile acid uptake systems responsible for constitutive gene expression. However, the human *OATP2* gene contains an HNF-1α binding site in its promotor region (141). Thus, HNF-1α appears to be the master regulator of basolateral Ntcp and Oatp expression. Of interest, HNF1α is also able to negatively regulate its own expression and that of HNF-4α by a negative feedback loop (142). HNF-1α expression in turn depends on HNF-4α expression and is reduced under condition HNF-4α of reduced HNF-4α activity (136, 143, 144).

6.12 miRNA-199-5p in *Abcb4*$^{-/-}$ mice

Micro RNAs role in the process of cellular pathways that attenuate hepatic ER stress induced by bile acids- and thapsigargin (TG) stimulated cultured hepatocytes, as well as in the liver of bile duct ligated mice have been the focus of recent studies. In this study it has been shown that bile acid can induce the *de novo* expression of miR-199-5p most likely through JNK/AP-1 pathway. AP-1 induced miR-199a-5P then directly targets the 3´UTRs of *GPR78*, IRE1 α (100). According to this, we also examined miR-199a-5p as one of the most abundant miRNAs in hepatocytes and found it elevated in *Abcb4* mutant mice in comparison to wild type (figure 28). This means miR-199a-5p might protecting hepatocytes from bile acid induced stress via different molecular mechanism, which needs to by elucidate in future studies.

6.13 Limitations of the study

Compared to our previous BM-Tx studies, we have come across certain limitations in the present study of CD117+ BM-Tx such as,

Intially we used to isolate a few amount of CD117+ progenitor cells. After few standardisation experiments, we had overcome this limitation. Another major drawback was after CD117+ cell transplantation some of the mice were dead due to unknown reasons. Although we had an expertise animal take carers. Due to the death of the animals our animal expeiments were

delayed for a while. In the mean time we thought of isolating liver derived CD34+ fibrocytes, but we couldn´t get any success due to lack of proper markers.

Abcb4$^{-/-}$ mice transplanted with CD117+ did not show any significant changes in liver cell integrity. Infiltrated multinucleated GFP+ hepatocytes demonstrate fusion of transplanted cells with host hepatocytes was a rare event. Hence, CD117+ BM-Tx might be not a suitable cell fraction to treat the liver fibrosis. Prolonged MMP-9 activity alone was not enough to restrain the liver fibrosis.

6.14 Conclusion

In conclusion, the results of the present study demonstrate that the fusion of transplanted BM-cells to host hepatocytes was a rare event (figure 8). The frequency of spontaneous fusion resulting in bone marrow derived hepatocytes (BMHs) is very low, but it is conceivable that induced cell fusion may achieve the efficiency necessary for the treatment of genetic diseases (145). Moreover the inflammatory effects observed in the present study were enhanced after allogeneic BM-Tx. The influx of inflammatory cells around intrahepatic bile ducts after irradiation and subsequent allogeneic BM-Tx (but not after irradiation alone) is a well-characterised phenomenon (146). Recently it was demonstrated that genetic drift in mouse inbred strains had a significant impact on the allo-reactive immune response caused by altered MHC antigens (147). This might explain the immune reactions and the enhanced effects after allogeneic BM-Tx, although GFP+ donor mice and *Abcb4*$^{-/-}$ mice bred with the same genetic background (BALB/c).

In addition, our results clearly demonstrated that the basolateral and the canalicular membrane transporter gene regulation are altered in chronically injured liver of BALB/c-*Abcb4*$^{-/-}$-mice. Hence, modulation of transporter function may represent a potential target for therapy.

Abbreviations:

Abcb4	ATP binding cassette subfamiliy B member 4
ABCG 5/8	ATP binding cassette subfamiliy G member 5/8
ALT	Alanine transaminase
AST	Aspertate transaminase
AP	Alkaline phosphatase
ATP	Adenosine triphosphate
BA	Bile acids
BM	Bone marrow
BM-Tx	Bone marrow transplantation
BSEP	Bile salt export pump
cDNA	Complementary deoxyribonucleic acid
Cyp7a1	Cholesterol 7-α hydroxylase a1
ECM	Extra cellular matrix
FACS	Flourescence activated cell sorting
FXR	Farnesoid X receptor
HSC	Hepatic stellate cells
HSC	Hematopoeitic stem cells
HNF-1α	Hepatic nuclear factor 1α
HNF-4α	Hepatic nuclear factor 4
IGF-1	Insulin like growth factor
KC	Kupffer cells

Abbreviations

MACS	Magnetic activated cell sorting
MMP	Matrix metalloproteinases
MRP3	Multidrug-resistance associated protein 3
MRP4	Multidrug-resistance associated protein 4
MSC	Mesenchymal stem cells
NR	Nuclear receptor
norUDCA	nor Ursodeoxycholic-acid
NTCP	Sodium taurocholate co-transporting polypeptide
OATP	Organic-anion transporter
Ost α/β	Organic solute transporter α/β
PC	Phosphotidyl choline
PL	Phospholipids
PSC	Primary sclerosing cholangitis
α- SMA	Alpha smooth muscle actin
TBA	Total bile acids
TIMP	Tissue inhibitor metalloproteinase
TNF-α	Tumor necrosis factor
TGF-β	Transforming growth factor
Th1&Th2	T helper cells
Wt	wild type

Index of figures

Index of figures

Index of tables

7. Reference list

Reference List

1. Fickert P, Fuchsbichler A, Wagner M, Zollner G, Kaser A, Tilg H, et al. Regurgitation of bile acids from leaky bile ducts causes sclerosing cholangitis in Mdr2 (Abcb4) knockout mice. Gastroenterology 2004 Jul;127(1):261-274.

2. Baghdasaryan A, Fickert P, Fuchsbichler A, Silbert D, Gumhold J, Horl G, et al. Role of hepatic phospholipids in development of liver injury in Mdr2 (Abcb4) knockout mice. Liver Int 2008 Aug;28(7):948-958.

3. Willenbring H, Grompe M. Embryonic versus adult stem cell pluripotency: in liver only fusion matters. J Assist Reprod Genet 2003 Oct;20(10):393-394.

4. Martin M. Primary sclerosing cholangitis. Annu Rev Med 1993;44:221-227.

5. Trauner M, Halilbasic E, Baghdasaryan A, Moustafa T, Krones E, Fickert P, et al. Primary sclerosing cholangitis: new approaches to diagnosis, surveillance and treatment. Dig Dis 2012;30 Suppl 1:39-47.

6. Molodecky NA, Kareemi H, Parab R, Barkema HW, Quan H, Myers RP, et al. Incidence of primary sclerosing cholangitis: a systematic review and meta-analysis. Hepatology 2011 May;53(5):1590-1599.

7. Bambha K, Kim WR, Talwalkar J, Torgerson H, Benson JT, Therneau TM, et al. Incidence, clinical spectrum, and outcomes of primary sclerosing cholangitis in a United States community. Gastroenterology 2003 Nov;125(5):1364-1369.

8. Eaton JE, Talwalkar JA, Lazaridis KN, Gores GJ, Lindor KD. Pathogenesis of Primary Sclerosing Cholangitis and Advances in Diagnosis and Management. Gastroenterology 2013 Jul 1.

9. Popov Y, Patsenker E, Fickert P, Trauner M, Schuppan D. Mdr2 (Abcb4)-/- mice spontaneously develop severe biliary fibrosis via massive dysregulation of pro- and antifibrogenic genes. J Hepatol 2005 Dec;43(6):1045-1054.

10. Roderfeld M, Rath T, Voswinckel R, Dierkes C, Dietrich H, Zahner D, et al. Bone marrow transplantation demonstrates medullar origin of CD34+ fibrocytes and ameliorates hepatic fibrosis in Abcb4-/- mice. Hepatology 2010 Jan;51(1):267-276.

11. Forbes SJ, Russo FP, Rey V, Burra P, Rugge M, Wright NA, et al. A significant proportion of myofibroblasts are of bone marrow origin in human liver fibrosis. Gastroenterology 2004 Apr;126(4):955-963.

12. Ramadori G, Saile B. Portal tract fibrogenesis in the liver. Lab Invest 2004 Feb;84(2):153-159.

13. Kinnman N, Housset C. Peribiliary myofibroblasts in biliary type liver fibrosis. Front Biosci 2002 Feb 1;7:d496-d503.

14. Juran BD, Atkinson EJ, Schlicht EM, Larson JJ, Ellinghaus D, Franke A, et al. Genetic polymorphisms of matrix metalloproteinase 3 in primary sclerosing cholangitis. Liver Int 2011 Jul;31(6):785-791.

15. Roderfeld M, Rath T, Pasupuleti S, Zimmermann M, Neumann C, Churin Y, et al. Bone marrow transplantation improves hepatic fibrosis in Abcb4-/- mice via Th1 response and matrix metalloproteinase activity. Gut 2012 Jun;61(6):907-916.

16. Fickert P, Fuchsbichler A, Wagner M, Zollner G, Kaser A, Tilg H, et al. Regurgitation of bile acids from leaky bile ducts causes sclerosing cholangitis in Mdr2 (Abcb4) knockout mice. Gastroenterology 2004 Jul;127(1):261-274.

17. Fickert P, Moustafa T, Trauner M. Primary sclerosing cholangitis--the arteriosclerosis of the bile duct? Lipids Health Dis 2007;6:3.

18. Baghdasaryan A, Fickert P, Fuchsbichler A, Silbert D, Gumhold J, Horl G, et al. Role of hepatic phospholipids in development of liver injury in Mdr2 (Abcb4) knockout mice. Liver Int 2008 Aug;28(7):948-958.

19. Wasmuth HE, Glantz A, Keppeler H, Simon E, Bartz C, Rath W, et al. Intrahepatic cholestasis of pregnancy: the severe form is associated with common variants of the hepatobiliary phospholipid transporter ABCB4 gene. Gut 2007 Feb;56(2):265-270.

20. Fickert P, Zollner G, Fuchsbichler A, Stumptner C, Weiglein AH, Lammert F, et al. Ursodeoxycholic acid aggravates bile infarcts in bile duct-ligated and Mdr2 knockout mice via disruption of cholangioles. Gastroenterology 2002 Oct;123(4):1238-1251.

21. Moustafa T, Fickert P, Magnes C, Guelly C, Thueringer A, Frank S, et al. Alterations in lipid metabolism mediate inflammation, fibrosis, and proliferation in a mouse model of chronic cholestatic liver injury. Gastroenterology 2012 Jan;142(1):140-151.

22. Sokolovic A, van Roomen CP, Ottenhoff R, Scheij S, Hiralall JK, Claessen N, et al. Fasting reduces liver fibrosis in a mouse model for chronic cholangiopathies. Biochim Biophys Acta 2013 Oct;1832(10):1482-1491.

23. Grove JE, Bruscia E, Krause DS. Plasticity of bone marrow-derived stem cells. Stem Cells 2004;22(4):487-500.

24. Weissman IL. Stem cells: units of development, units of regeneration, and units in evolution. Cell 2000 Jan 7;100(1):157-168.

25. Gilchrist ES, Plevris JN. Bone marrow-derived stem cells in liver repair: 10 years down the line. Liver Transpl 2010 Feb;16(2):118-129.

26. Qian H, Georges-Labouesse E, Nystrom A, Domogatskaya A, Tryggvason K, Jacobsen SE, et al. Distinct roles of integrins alpha6 and alpha4 in homing of fetal liver hematopoietic stem and progenitor cells. Blood 2007 Oct 1;110(7):2399-2407.

27. Bonnet D. Hematopoietic stem cells. Birth Defects Res C Embryo Today 2003 Aug;69(3):219-229.

28. Shizuru JA, Negrin RS, Weissman IL. Hematopoietic stem and progenitor cells: clinical and preclinical regeneration of the hematolymphoid system. Annu Rev Med 2005;56:509-538.

29. Petersen BE, Bowen WC, Patrene KD, Mars WM, Sullivan AK, Murase N, et al. Bone marrow as a potential source of hepatic oval cells. Science 1999 May 14;284(5417):1168-1170.

30. Theise ND, Badve S, Saxena R, Henegariu O, Sell S, Crawford JM, et al. Derivation of hepatocytes from bone marrow cells in mice after radiation-induced myeloablation. Hepatology 2000 Jan;31(1):235-240.

31. Alison MR, Poulsom R, Jeffery R, Dhillon AP, Quaglia A, Jacob J, et al. Hepatocytes from non-hepatic adult stem cells. Nature 2000 Jul 20;406(6793):257.

32. Lagasse E, Connors H, Al-Dhalimy M, Reitsma M, Dohse M, Osborne L, et al. Purified hematopoietic stem cells can differentiate into hepatocytes in vivo. Nat Med 2000 Nov;6(11):1229-1234.

33. Orlic D, Kajstura J, Chimenti S, Jakoniuk I, Anderson SM, Li B, et al. Bone marrow cells regenerate infarcted myocardium. Nature 2001 Apr 5;410(6829):701-705.

34. Eglitis MA, Mezey E. Hematopoietic cells differentiate into both microglia and macroglia in the brains of adult mice. Proc Natl Acad Sci U S A 1997 Apr 15;94(8):4080-4085.

35. Ferrari G, Cusella-De AG, Coletta M, Paolucci E, Stornaiuolo A, Cossu G, et al. Muscle regeneration by bone marrow-derived myogenic progenitors. Science 1998 Mar 6;279(5356):1528-1530.

36. Krause DS, Theise ND, Collector MI, Henegariu O, Hwang S, Gardner R, et al. Multi-organ, multi-lineage engraftment by a single bone marrow-derived stem cell. Cell 2001 May 4;105(3):369-377.

37. Wagers AJ, Sherwood RI, Christensen JL, Weissman IL. Little evidence for developmental plasticity of adult hematopoietic stem cells. Science 2002 Sep 27;297(5590):2256-2259.

38. Vassilopoulos G, Wang PR, Russell DW. Transplanted bone marrow regenerates liver by cell fusion. Nature 2003 Apr 24;422(6934):901-904.

39. Wang X, Willenbring H, Akkari Y, Torimaru Y, Foster M, Al-Dhalimy M, et al. Cell fusion is the principal source of bone-marrow-derived hepatocytes. Nature 2003 Apr 24;422(6934):897-901.

40. Chitteti BR, Cheng YH, Poteat B, Rodriguez-Rodriguez S, Goebel WS, Carlesso N, et al. Impact of interactions of cellular components of the bone marrow microenvironment on hematopoietic stem and progenitor cell function. Blood 2010 Apr 22;115(16):3239-3248.

41. Bhogal RH ASC. Immune cell communication and signaling systems in liver diseases In: Dufour J-F, Clavien PA, eds. Signaling in Liver Diseases. 2nd ed. New York: Springer. 2009.

42. Thurman RG. II. Alcoholic liver injury involves activation of Kupffer cells by endotoxin. Am J Physiol 1998 Oct;275(4 Pt 1):G605-G611.

43. Barth PJ, Westhoff CC. CD34+ fibrocytes: morphology, histogenesis and function. Curr Stem Cell Res Ther 2007 Sep;2(3):221-227.

44. Alpini G, McGill JM, Larusso NF. The pathobiology of biliary epithelia. Hepatology 2002 May;35(5):1256-1268.

45. Chan J, Vandeberg JL. Hepatobiliary transport in health and disease. Clin Lipidol 2012 Apr;7(2):189-202.

46. Nicolaou M, Andress EJ, Zolnerciks JK, Dixon PH, Williamson C, Linton KJ. Canalicular ABC transporters and liver disease. J Pathol 2012 Jan;226(2):300-315.

47. Hofmann AF. Bile Acids: The Good, the Bad, and the Ugly. News Physiol Sci 1999 Feb;14:24-29.

48. Oude Elferink RP, Paulusma CC. Function and pathophysiological importance of ABCB4 (MDR3 P-glycoprotein). Pflugers Arch 2007 Feb;453(5):601-610.

49. Thomas C, Pellicciari R, Pruzanski M, Auwerx J, Schoonjans K. Targeting bile-acid signalling for metabolic diseases. Nat Rev Drug Discov 2008 Aug;7(8):678-693.

50. Baghdasaryan A, Fickert P, Fuchsbichler A, Silbert D, Gumhold J, Horl G, et al. Role of hepatic phospholipids in development of liver injury in Mdr2 (Abcb4) knockout mice. Liver Int 2008 Aug;28(7):948-958.

51. Elferink RP, Tytgat GN, Groen AK. Hepatic canalicular membrane 1: The role of mdr2 P-glycoprotein in hepatobiliary lipid transport. FASEB J 1997 Jan;11(1):19-28.

52. Halilbasic E, Claudel T, Trauner M. Bile acid transporters and regulatory nuclear receptors in the liver and beyond. J Hepatol 2013 Jan;58(1):155-168.

53. Trauner M. Molecular alterations of canalicular transport systems in experimental models of cholestasis: possible functional correlations. Yale J Biol Med 1997 Jul;70(4):365-378.

54. Geier A, Wagner M, Dietrich CG, Trauner M. Principles of hepatic organic anion transporter regulation during cholestasis, inflammation and liver regeneration. Biochim Biophys Acta 2007 Mar;1773(3):283-308.

55. Dawson PA, Lan T, Rao A. Bile acid transporters. J Lipid Res 2009 Dec;50(12):2340-2357.

56. Trauner M, Boyer JL. Bile salt transporters: molecular characterization, function, and regulation. Physiol Rev 2003 Apr;83(2):633-671.

57. Geier A, Wagner M, Dietrich CG, Trauner M. Principles of hepatic organic anion transporter regulation during cholestasis, inflammation and liver regeneration. Biochim Biophys Acta 2007 Mar;1773(3):283-308.

58. Lew JL, Zhao A, Yu J, Huang L, De PN, Pelaez F, et al. The farnesoid X receptor controls gene expression in a ligand- and promoter-selective fashion. J Biol Chem 2004 Mar 5;279(10):8856-8861.

59. Yang Z, Wang L. Regulation of microRNA expression and function by nuclear receptor signaling. Cell Biosci 2011;1(1):31.

60. Makishima M, Okamoto AY, Repa JJ, Tu H, Learned RM, Luk A, et al. Identification of a nuclear receptor for bile acids. Science 1999 May 21;284(5418):1362-1365.

61. Ananthanarayanan M, Balasubramanian N, Makishima M, Mangelsdorf DJ, Suchy FJ. Human bile salt export pump promoter is transactivated by the farnesoid X receptor/bile acid receptor. J Biol Chem 2001 Aug 3;276(31):28857-28865.

62. Huang L, Zhao A, Lew JL, Zhang T, Hrywna Y, Thompson JR, et al. Farnesoid X receptor activates transcription of the phospholipid pump MDR3. J Biol Chem 2003 Dec 19;278(51):51085-51090.

63. Plass JR, Mol O, Heegsma J, Geuken M, Faber KN, Jansen PL, et al. Farnesoid X receptor and bile salts are involved in transcriptional regulation of the gene encoding the human bile salt export pump. Hepatology 2002 Mar;35(3):589-596.

64. Matsubara T, Li F, Gonzalez FJ. FXR signaling in the enterohepatic system. Mol Cell Endocrinol 2013 Apr 10;368(1-2):17-29.

65. Goodwin B, Jones SA, Price RR, Watson MA, McKee DD, Moore LB, et al. A regulatory cascade of the nuclear receptors FXR, SHP-1, and LRH-1 represses bile acid biosynthesis. Mol Cell 2000 Sep;6(3):517-526.

66. Lu TT, Makishima M, Repa JJ, Schoonjans K, Kerr TA, Auwerx J, et al. Molecular basis for feedback regulation of bile acid synthesis by nuclear receptors. Mol Cell 2000 Sep;6(3):507-515.

67. Liu Y, Binz J, Numerick MJ, Dennis S, Luo G, Desai B, et al. Hepatoprotection by the farnesoid X receptor agonist GW4064 in rat models of intra- and extrahepatic cholestasis. J Clin Invest 2003 Dec;112(11):1678-1687.

68. Modica S, Petruzzelli M, Bellafante E, Murzilli S, Salvatore L, Celli N, et al. Selective activation of nuclear bile acid receptor FXR in the intestine protects mice against cholestasis. Gastroenterology 2012 Feb;142(2):355-365.

69. Gadaleta RM, van Mil SW, Oldenburg B, Siersema PD, Klomp LW, van Erpecum KJ. Bile acids and their nuclear receptor FXR: Relevance for hepatobiliary and gastrointestinal disease. Biochim Biophys Acta 2010 Jul;1801(7):683-692.

70. Ozsolak F, Poling LL, Wang Z, Liu H, Liu XS, Roeder RG, et al. Chromatin structure analyses identify miRNA promoters. Genes Dev 2008 Nov 15;22(22):3172-3183.

71. Bartel DP. MicroRNAs: genomics, biogenesis, mechanism, and function. Cell 2004 Jan 23;116(2):281-297.

72. Yang Z, Wang L. Regulation of microRNA expression and function by nuclear receptor signaling. Cell Biosci 2011;1(1):31.

73. Boyer JL. Nuclear receptor ligands: rational and effective therapy for chronic cholestatic liver disease? Gastroenterology 2005 Aug;129(2):735-740.

74. Bauersachs J, Thum T. Biogenesis and regulation of cardiovascular microRNAs. Circ Res 2011 Jul 22;109(3):334-347.

75. Chen K, Rajewsky N. The evolution of gene regulation by transcription factors and microRNAs. Nat Rev Genet 2007 Feb;8(2):93-103.

76. Bartel DP. MicroRNAs: genomics, biogenesis, mechanism, and function. Cell 2004 Jan 23;116(2):281-297.

77. Bartel DP. MicroRNAs: target recognition and regulatory functions. Cell 2009 Jan 23;136(2):215-233.

78. Ambros V. The functions of animal microRNAs. Nature 2004 Sep 16;431(7006):350-355.

79. Bala S, Marcos M, Szabo G. Emerging role of microRNAs in liver diseases. World J Gastroenterol 2009 Dec 7;15(45):5633-5640.

80. Sato F, Tsuchiya S, Meltzer SJ, Shimizu K. MicroRNAs and epigenetics. FEBS J 2011 May;278(10):1598-1609.

81. Sinkkonen L, Hugenschmidt T, Berninger P, Gaidatzis D, Mohn F, rtus-Revel CG, et al. MicroRNAs control de novo DNA methylation through regulation of transcriptional repressors in mouse embryonic stem cells. Nat Struct Mol Biol 2008 Mar;15(3):259-267.

82. Krol J, Loedige I, Filipowicz W. The widespread regulation of microRNA biogenesis, function and decay. Nat Rev Genet 2010 Sep;11(9):597-610.

83. Pauli A, Rinn JL, Schier AF. Non-coding RNAs as regulators of embryogenesis. Nat Rev Genet 2011 Feb;12(2):136-149.

84. Lujambio A, Calin GA, Villanueva A, Ropero S, Sanchez-Cespedes M, Blanco D, et al. A microRNA DNA methylation signature for human cancer metastasis. Proc Natl Acad Sci U S A 2008 Sep 9;105(36):13556-13561.

85. Dews M, Homayouni A, Yu D, Murphy D, Sevignani C, Wentzel E, et al. Augmentation of tumor angiogenesis by a Myc-activated microRNA cluster. Nat Genet 2006 Sep;38(9):1060-1065.

86. Ji J, Wang XW. New kids on the block: diagnostic and prognostic microRNAs in hepatocellular carcinoma. Cancer Biol Ther 2009 Sep;8(18):1686-1693.

87. Qu KZ, Zhang K, Li H, Afdhal NH, Albitar M. Circulating microRNAs as biomarkers for hepatocellular carcinoma. J Clin Gastroenterol 2011 Apr;45(4):355-360.

88. Ura S, Honda M, Yamashita T, Ueda T, Takatori H, Nishino R, et al. Differential microRNA expression between hepatitis B and hepatitis C leading disease progression to hepatocellular carcinoma. Hepatology 2009 Apr;49(4):1098-1112.

89. Krutzfeldt J, Rajewsky N, Braich R, Rajeev KG, Tuschl T, Manoharan M, et al. Silencing of microRNAs in vivo with 'antagomirs'. Nature 2005 Dec 1;438(7068):685-689.

90. Jopling CL, Yi M, Lancaster AM, Lemon SM, Sarnow P. Modulation of hepatitis C virus RNA abundance by a liver-specific MicroRNA. Science 2005 Sep 2;309(5740):1577-1581.

91. Coulouarn C, Factor VM, Andersen JB, Durkin ME, Thorgeirsson SS. Loss of miR-122 expression in liver cancer correlates with suppression of the hepatic phenotype and gain of metastatic properties. Oncogene 2009 Oct 8;28(40):3526-3536.

92. Dai BH, Geng L, Wang Y, Sui CJ, Xie F, Shen RX, et al. microRNA-199a-5p protects hepatocytes from bile acid-induced sustained endoplasmic reticulum stress. Cell Death Dis 2013;4:e604.

93. Murakami Y, Toyoda H, Tanaka M, Kuroda M, Harada Y, Matsuda F, et al. The progression of liver fibrosis is related with overexpression of the miR-199 and 200 families. PLoS One 2011;6(1):e16081.

94. Shu J, Kren BT, Xia Z, Wong PY, Li L, Hanse EA, et al. Genomewide microRNA down-regulation as a negative feedback mechanism in the early phases of liver regeneration. Hepatology 2011 Aug;54(2):609-619.

95. Jacquemin E, De Vree JM, Cresteil D, Sokal EM, Sturm E, Dumont M, et al. The wide spectrum of multidrug resistance 3 deficiency: from neonatal cholestasis to cirrhosis of adulthood. Gastroenterology 2001 May;120(6):1448-1458.

96. Misawa R, Ise H, Takahashi M, Morimoto H, Kobayashi E, Miyagawa S, et al. Development of liver regenerative therapy using glycoside-modified bone marrow cells. Biochem Biophys Res Commun 2006 Apr 7;342(2):434-440.

97. Kallis YN, Forbes SJ. The bone marrow and liver fibrosis: friend or foe? Gastroenterology 2009 Oct;137(4):1218-1221.

98. Chan J, Vandeberg JL. Hepatobiliary transport in health and disease. Clin Lipidol 2012 Apr;7(2):189-202.

99. Dooley S, ten DP. TGF-beta in progression of liver disease. Cell Tissue Res 2012 Jan;347(1):245-256.

100. Dai BH, Geng L, Wang Y, Sui CJ, Xie F, Shen RX, et al. microRNA-199a-5p protects hepatocytes from bile acid-induced sustained endoplasmic reticulum stress. Cell Death Dis 2013;4:e604.

101. Trauner M, Fickert P, Baghdasaryan A, Claudel T, Halilbasic E, Moustafa T, et al. New insights into autoimmune cholangitis through animal models. Dig Dis 2010;28(1):99-104.

102. Smit JJ, Schinkel AH, Oude Elferink RP, Groen AK, Wagenaar E, van DL, et al. Homozygous disruption of the murine mdr2 P-glycoprotein gene leads to a complete absence of phospholipid from bile and to liver disease. Cell 1993 Nov 5;75(3):451-462.

103. Trauner M, Fickert P, Halilbasic E, Moustafa T. Lessons from the toxic bile concept for the pathogenesis and treatment of cholestatic liver diseases. Wien Med Wochenschr 2008;158(19-20):542-548.

104. Wynn TA. Fibrotic disease and the T(H)1/T(H)2 paradigm. Nat Rev Immunol 2004 Aug;4(8):583-594.

105. Brenner DA. Molecular pathogenesis of liver fibrosis. Trans Am Clin Climatol Assoc 2009;120:361-368.

106. Krohn N, Kapoor S, Enami Y, Follenzi A, Bandi S, Joseph B, et al. Hepatocyte transplantation-induced liver inflammation is driven by cytokines-chemokines associated with neutrophils and Kupffer cells. Gastroenterology 2009 May;136(5):1806-1817.

107. Safadi R, Friedman SL. Hepatic fibrosis--role of hepatic stellate cell activation. MedGenMed 2002 Jul 15;4(3):27.

108. Tarrats N, Moles A, Morales A, Garcia-Ruiz C, Fernandez-Checa JC, Mari M. Critical role of tumor necrosis factor receptor 1, but not 2, in hepatic stellate cell proliferation, extracellular matrix remodeling, and liver fibrogenesis. Hepatology 2011 Jul;54(1):319-327.

109. Tracey KJ, Cerami A. Tumor necrosis factor, other cytokines and disease. Annu Rev Cell Biol 1993;9:317-343.

110. Liu LY, Bates ME, Jarjour NN, Busse WW, Bertics PJ, Kelly EA. Generation of Th1 and Th2 chemokines by human eosinophils: evidence for a critical role of TNF-alpha. J Immunol 2007 Oct 1;179(7):4840-4848.

111. Napoli J, Bishop GA, McGuinness PH, Painter DM, McCaughan GW. Progressive liver injury in chronic hepatitis C infection correlates with increased intrahepatic expression of Th1-associated cytokines. Hepatology 1996 Oct;24(4):759-765.

112. Shi Z, Wakil AE, Rockey DC. Strain-specific differences in mouse hepatic wound healing are mediated by divergent T helper cytokine responses. Proc Natl Acad Sci U S A 1997 Sep 30;94(20):10663-10668.

113. Blakaj A, Bucala R. Fibrocytes in health and disease. Fibrogenesis Tissue Repair 2012;5(Suppl 1 Proceedings of Fibroproliferative disorders: from biochemical analysis to targeted therapiesPetro E Petrides and David Brenner):S6.

114. Chiaramonte MG, Donaldson DD, Cheever AW, Wynn TA. An IL-13 inhibitor blocks the development of hepatic fibrosis during a T-helper type 2-dominated inflammatory response. J Clin Invest 1999 Sep;104(6):777-785.

115. Louis H, Le MA, Quertinmont E, Peny MO, Geerts A, Goldman M, et al. Repeated concanavalin A challenge in mice induces an interleukin 10-producing phenotype and liver fibrosis. Hepatology 2000 Feb;31(2):381-390.

116. Tacke F. Functional role of intrahepatic monocyte subsets for the progression of liver inflammation and liver fibrosis in vivo. Fibrogenesis Tissue Repair 2012 Jun 6;5 Suppl 1:S27.

117. Xia S, Guo Z, Xu X, Yi H, Wang Q, Cao X. Hepatic microenvironment programs hematopoietic progenitor differentiation into regulatory dendritic cells, maintaining liver tolerance. Blood 2008 Oct 15;112(8):3175-3185.

118. Banchereau J, Briere F, Caux C, Davoust J, Lebecque S, Liu YJ, et al. Immunobiology of dendritic cells. Annu Rev Immunol 2000;18:767-811.

119. Connolly MK, Bedrosian AS, Mallen-St CJ, Mitchell AP, Ibrahim J, Stroud A, et al. In liver fibrosis, dendritic cells govern hepatic inflammation in mice via TNF-alpha. J Clin Invest 2009 Nov;119(11):3213-3225.

120. Braier J, Ciocca M, Latella A, de Davila MG, Drajer M, Imventarza O. Cholestasis, sclerosing cholangitis, and liver transplantation in Langerhans cell Histiocytosis. Med Pediatr Oncol 2002 Mar;38(3):178-182.

121. Geier A, Wagner M, Dietrich CG, Trauner M. Principles of hepatic organic anion transporter regulation during cholestasis, inflammation and liver regeneration. Biochim Biophys Acta 2007 Mar;1773(3):283-308.

122. Denson LA, Sturm E, Echevarria W, Zimmerman TL, Makishima M, Mangelsdorf DJ, et al. The orphan nuclear receptor, shp, mediates bile acid-induced inhibition of the rat bile acid transporter, ntcp. Gastroenterology 2001 Jul;121(1):140-147.

123. Zollner G, Fickert P, Fuchsbichler A, Silbert D, Wagner M, Arbeiter S, et al. Role of nuclear bile acid receptor, FXR, in adaptive ABC transporter regulation by cholic and ursodeoxycholic acid in mouse liver, kidney and intestine. J Hepatol 2003 Oct;39(4):480-488.

124. Donner MG, Keppler D. Up-regulation of basolateral multidrug resistance protein 3 (Mrp3) in cholestatic rat liver. Hepatology 2001 Aug;34(2):351-359.

125. Boyer JL, Trauner M, Mennone A, Soroka CJ, Cai SY, Moustafa T, et al. Upregulation of a basolateral FXR-dependent bile acid efflux transporter OSTalpha-OSTbeta in cholestasis in humans and rodents. Am J Physiol Gastrointest Liver Physiol 2006 Jun;290(6):G1124-G1130.

126. Zollner G, Wagner M, Moustafa T, Fickert P, Silbert D, Gumhold J, et al. Coordinated induction of bile acid detoxification and alternative elimination in mice: role of FXR-regulated organic solute transporter-alpha/beta in the adaptive response to bile acids. Am J Physiol Gastrointest Liver Physiol 2006 May;290(5):G923-G932.

127. Akita H, Suzuki H, Hirohashi T, Takikawa H, Sugiyama Y. Transport activity of human MRP3 expressed in Sf9 cells: comparative studies with rat MRP3. Pharm Res 2002 Jan;19(1):34-41.

128. Hirohashi T, Suzuki H, Sugiyama Y. Characterization of the transport properties of cloned rat multidrug resistance-associated protein 3 (MRP3). J Biol Chem 1999 May 21;274(21):15181-15185.

129. Hirohashi T, Suzuki H, Takikawa H, Sugiyama Y. ATP-dependent transport of bile salts by rat multidrug resistance-associated protein 3 (Mrp3). J Biol Chem 2000 Jan 28;275(4):2905-2910.

130. Soroka CJ, Lee JM, Azzaroli F, Boyer JL. Cellular localization and up-regulation of multidrug resistance-associated protein 3 in hepatocytes and cholangiocytes during obstructive cholestasis in rat liver. Hepatology 2001 Apr;33(4):783-791.

131. Kiuchi Y, Suzuki H, Hirohashi T, Tyson CA, Sugiyama Y. cDNA cloning and inducible expression of human multidrug resistance associated protein 3 (MRP3). FEBS Lett 1998 Aug 14;433(1-2):149-152.

132. Ogawa K, Suzuki H, Hirohashi T, Ishikawa T, Meier PJ, Hirose K, et al. Characterization of inducible nature of MRP3 in rat liver. Am J Physiol Gastrointest Liver Physiol 2000 Mar;278(3):G438-G446.

133. Mennone A, Soroka CJ, Cai SY, Harry K, Adachi M, Hagey L, et al. Mrp4-/- mice have an impaired cytoprotective response in obstructive cholestasis. Hepatology 2006 May;43(5):1013-1021.

134. Park YJ, Qatanani M, Chua SS, LaRey JL, Johnson SA, Watanabe M, et al. Loss of orphan receptor small heterodimer partner sensitizes mice to liver injury from obstructive cholestasis. Hepatology 2008 May;47(5):1578-1586.

135. Davis RA, Miyake JH, Hui TY, Spann NJ. Regulation of cholesterol-7alpha-hydroxylase: BAREly missing a SHP. J Lipid Res 2002 Apr;43(4):533-543.

136. Jung D, Kullak-Ublick GA. Hepatocyte nuclear factor 1 alpha: a key mediator of the effect of bile acids on gene expression. Hepatology 2003 Mar;37(3):622-631.

137. Eloranta JJ, Kullak-Ublick GA. Coordinate transcriptional regulation of bile acid homeostasis and drug metabolism. Arch Biochem Biophys 2005 Jan 15;433(2):397-412.

138. Jung D, Hagenbuch B, Fried M, Meier PJ, Kullak-Ublick GA. Role of liver-enriched transcription factors and nuclear receptors in regulating the human, mouse, and rat NTCP gene. Am J Physiol Gastrointest Liver Physiol 2004 May;286(5):G752-G761.

139. Hayhurst GP, Lee YH, Lambert G, Ward JM, Gonzalez FJ. Hepatocyte nuclear factor 4alpha (nuclear receptor 2A1) is essential for maintenance of hepatic gene expression and lipid homeostasis. Mol Cell Biol 2001 Feb;21(4):1393-1403.

140. Shih DQ, Bussen M, Sehayek E, Ananthanarayanan M, Shneider BL, Suchy FJ, et al. Hepatocyte nuclear factor-1alpha is an essential regulator of bile acid and plasma cholesterol metabolism. Nat Genet 2001 Apr;27(4):375-382.

141. Jung D, Hagenbuch B, Gresh L, Pontoglio M, Meier PJ, Kullak-Ublick GA. Characterization of the human OATP-C (SLC21A6) gene promoter and regulation of liver-specific OATP genes by hepatocyte nuclear factor 1 alpha. J Biol Chem 2001 Oct 5;276(40):37206-37214.

142. Ktistaki E, Talianidis I. Modulation of hepatic gene expression by hepatocyte nuclear factor 1. Science 1997 Jul 4;277(5322):109-112.

143. Kuo CJ, Conley PB, Chen L, Sladek FM, Darnell JE, Jr., Crabtree GR. A transcriptional hierarchy involved in mammalian cell-type specification. Nature 1992 Jan 30;355(6359):457-461.

144. Wang B, Cai SR, Gao C, Sladek FM, Ponder KP. Lipopolysaccharide results in a marked decrease in hepatocyte nuclear factor 4 alpha in rat liver. Hepatology 2001 Nov;34(5):979-989.

145. Wang X, Montini E, Al-Dhalimy M, Lagasse E, Finegold M, Grompe M. Kinetics of liver repopulation after bone marrow transplantation. Am J Pathol 2002 Aug;161(2):565-574.

146. Yoshida Y, Hirano T, Son G, Iimuro Y, Imado T, Iwasaki T, et al. Allogeneic bone marrow transplantation for hepatocellular carcinoma: hepatocyte growth factor suppresses graft-vs.-host disease. Am J Physiol Gastrointest Liver Physiol 2007 Dec;293(6):G1114-G1123.

147. Fanning SL, Appel MY, Berger SA, Korngold R, Friedman TM. The immunological impact of genetic drift in the B10.BR congenic inbred mouse strain. J Immunol 2009 Oct 1;183(7):4261-4272.

Acknowledgements

I would like to take this opportunity to express my deepest sense of gratitude and admiration to my supervisor, **Prof. Dr. Elke Roeb** who supported me throughout my PhD. Her courage and guidance gave me a lot of strength and inspiration to carry out this study. She is a wonderful lady and understands the situations very well and encouraged me all the time. When ever in need she is always kind hearted and helped me in several aspects during my time. My heartful thanks to her for making my dream come true.

I would like to thank my guide **PD Dr. Martin Roderfeld** for his constant encouragement and all his support during these years. I have been fortunate to work with him and have learnt a lot from him. I value his thinking; his sharp sense of observation and judgment.

I thank to the **Prof. Dr. Reinhard H. Damman** for being my co-supervisor.

Heartfelt thanks to **Dr. Yuri Churin** for invaluable support and maintaining an open and scientifically alive environment. It has been a pleasure to be his colleague.

I would like to thank to **Annette Tschuschner and Michaela Weiss,** who taught me how to isolate the bone marrow cells and other techniques.

I am grateful to know Arzu Koc, who helped me in several aspects in day to day life of Germany.

I thank all my lab members- Dr. T. Rath, Katharina Kopsch, Dr. T. Matono, Hannah Reinhard,, Lisa Hage and Dirk Schröder for being wonderful colleagues.

I am very much thankful to my parents and brother who supported and encouraged me throughout my education. Without their support I might not be here today.

I would like to extend my heartfelt thanks to my husband for his love, patience, constant encouragement and valuable discussions during the course of my study.

Erklärung

Hiermit erklare ich, dass ich die vorliegende Arbeit selbständig und ohne unzulässige Hilfe oder Benutzung anderer als der angegebenen Hilfsmittel angefertigt habe. Alle Textstellen, die wörtlich oder sinngemäß aus veröffentlichten oder nicht veröffentlichten Schriften entnommen sind, und alle Angaben, die auf mündlichen Auskünften beruhen, sind als solche kenntlich gemacht.

Bei den von mir durchgeführten und in der Dissertation erwähnten Untersuchungen habe ich die Grundsätze guter wissenschaftlicher Praxis, wie sie in der Satzung der Justus-Liebig-Universität Gießen zur Sicherung guter wissenschaftlicher Praxis niedergelegt sind, eingehalten.

Die vorgelegte Arbeit wurde weder im Inland noch im Ausland in gleicher oder ähnlicher Form einer anderen Prüfungsbehörde zum Zweck einer Promotion oder eines anderen Prüfungsverfahrens vorgelegt. Alles aus anderen Quellen und von anderen Personen übernommene Material, das in der Arbeit verwendet wurde oder auf das direkt Bezug genommen wird, wurde als solches kenntlich gemacht.

Place and date	Sravanthi Pasupuleti

8. Appendix

Publications

1) **Sravanthi Pasupuleti**, Yuri Churin, Andreas Geier, Hans-Joachim Mollenkopf, Martin Roderfeld, Elke Roeb. "Enterohepatic bile acid cycle is disturbed in BALB/c-Abcb4-knockout mouse model of intrahepatic cholestasis". (Manuscript is prepared)

2) Daniel Zahner, Hannah Reinhardt, Yuri Churin, **Sravanthi Pasupuleti**, Hans-Joachim Mollenkopf, Roberta Montalbano, Malvika Pompaiah, Kurt Reifenberg, Dirk Schröder, Dieter Glebe, Martin Roderfeld, and Elke Roeb."Liver damage, nutrient deprivation and oncogenic effects are aggravated by Hepatitis B Virus Surface Proteins in a murine cholangitis model". (Manuscript under preparation)

3) Roderfeld M, Rath T, **Sravanthi Pasupuleti**, Zimmermann M, Neumann C, Churin Y, Dierkes C, Voswinckel R, Barth PJ, Zahner D, Graf J, Roeb E (2012) Bone marrow transplantation improves hepatic fibrosis in Abcb4-/- mice via Th1 response and matrix metalloproteinase activity. Gut 61:907-916.

Posters & Abstracts

1) **Pasupuleti S**, Geier A, Churin Y, Roderfeld M, Roeb E. Intrahepatic bile acid retention in BALB/c-*Abcb4*$^{-/-}$ mice activates FXR-dependent rescue transporters at the basolateral and canalicular membrane. Z Gastroenterol 2013; 915: K-141 (Abstract/Talk, DGVS 2013)

2) **Pasupuleti S**, Roderfeld M, Roeb E. Bone marrow transplantation of CD117+ cells in *Abcb4*$^{-/-}$ mice. Z Gastroenterol 2013; 75:P1.38 (Abstract/Poster, GASL 2013)

3) Reinhard H, Roderfeld M, **Pasupuleti S**, Tschuschner A, Kopsch K, Kremer S, Churin Y, Roeb E. Etablierung und Charakterisierung einnes murinen second Hit-Modells für die virale medikamentös-toxische Leberscädigung.. Z Gastroenterol 2013; 76:P1.41 (Abstract/Poster, GASL 2013)

4) **Pasupuleti S**, Batra A, Koc A, Kremer S, Siegmund B, Roderfeld M, Roeb E. Transfer colitis in Rag1-/-- mice enhances the hepatic MMP-9 expression. Z Gastroenterol 2012; 85: P1.41 (Abstract/Poster,GASL 2012)

5) Roderfeld M, Rath T, **Pasupuleti S**, Roeb E, Th2→Th1 Switch improves hepatic fibrosis in *Abcb*$^{-/-}$-mice after bone marrow transplantation. HEPATOLOGY 54 (S1): 983A-984A (Abstract/Poster, AASLD 2011)

6) **Pasupuleti S**, Neumann C, Tschuschner A, Roeb E, Roderfeld M, Migration of hepatic CXCR4^{+} fibrocytes is directed by SDF-1 in *Abcb4*$^{-/-}$ mice. Z Gastroenterol 2011; 49: P442 (Abstract/Poster,DGVS-2011